2020

Development of Analytical Methods for Toxic Inhaled Hazards (TIH) and Their Metabolites

Obed Adu Gyamfi
South Dakota State University

DEVELOPMENT OF ANALYTICAL METHODS FOR TOXIC INHALED HAZARDS (TIH) AND THEIR METABOLITES

BY

OBED ADU GYAMFI

A dissertation submitted in partial fulfillment of the requirements for the

Doctor of Philosophy

Major in Chemistry

South Dakota State University

2020

DISSERTATION ACCEPTANCE PAGE

Obed Adu Gyamfi

This dissertation is approved as a creditable and independent investigation by a candidate for the Doctor of Philosophy degree and is acceptable for meeting the dissertation requirements for this degree. Acceptance of this does not imply that the conclusions reached by the candidate are necessarily the conclusions of the major department.

Brian Logue
Advisor Date

Douglas Raynie
Department Head Date

Dean, Graduate School Date

This dissertation is dedicated to my mom, Margaret Gyamfi.

ACKNOWLEDGEMENTS

I thank my dissertation advisor, Dr. Brian A. Logue, for his mentorship guidance and encouragement throughout my doctoral degree. I am grateful to the members of the Logue research group, the SDSU Department of Chemistry and Biochemistry, my committee members, and faculty and staff for their assistance and encouragement. I would also like to thank all the funding agencies that funded my research and made the completion of my degree possible. A special thanks to Boehringer Ingelheim NBRC, New Brunswick NJ (especially Drs. Wei Tong, and Berhane Tecle) for the internship opportunity. I am grateful to my parents, Margaret Gyamfi and Christopher Gyamfi, for their encouragement and support towards my personal and academic life. I gratefully acknowledge the support of my siblings, Justice, Josephine, Christiana, Evans, Deborah and Lois. I am forever indebted to you all. Lastly, I would also like to thank, Patience Pokuaa, Isaac Kyei, Seth Arhin-Donkor, Isaac Antwi, Maame Ama Amponsah, Salena Joseph, Hannah Kumi, Joseph Dzisam, Nesta Bortey-Sam and Shaquavia Herper for their encouragement and moral support throughout my study in SDSU.

TABLE OF CONTENT

ABBREVIATIONS

α-KgCN: α-ketoglutarate cyanohydrin

Å: Angstrom

A-967079: (1*E*,3*E*)-1-(4-Fluorophenyl)-2-methyl-1-pentene-3-one oxime

AP18: 4-(4-Chlorophenyl)-3-methyl-3-buten-2-one oxime

ATCA: 2-amino-2-thiazoline-4-carboxylic acid

ATOEA: 2-aminothiazoline-4-oxoaminoethanioc acid

ATP: Adenosine triphosphate

As: Peak asymmetry

ASIC: Acid-sensitive ion channels

AUC: Area under the curve

CE: Collision energy

C_{max}: Concentration maximum

CN: Cyanide as and HCN inclusively

CWA: Chemical warfare agent

DRG: Dorsal root ganglion

DP: Declustering potentials

EDTA: Ethylenediaminetetraacetic acid

ESI: Electrospray ionization

FDA: Food and Drug Authority

GSH: Reduced glutathione

GSSG: Oxidized glutathione

HC-030031:2-(1,3-Dimethyl-2,6-dioxo-1,2,3,6-tetrahydro-7*H*-purin-7-yl)-*N*-(4-isopropylphenyl) acetamide

HPLC: High performance liquid chromatography

HPLC-MS-MS: High performance liquid chromatography-tandem mass spectrometry

IACUC: Institutional Animal Care and Use Committee

ITCA: 2-iminothiazolidine-4-carboxylic acid

IV: Intravenous

JG: Jugular ganglia

K_{el}: Elimination constant

K_{dis}: Distribution constant

LLOQ: Lower limit of quantification

LRFFT: Live reef fish for food trade

LOD: Limit of detection

3-MST: 3-Mercaptopyruvate sulfurtransferase

μM: Micromolar

MAT: Marine aquarium trade

MRM: Multiple reaction monitoring

MIC: Methyl isocyanate

m/z: Mass-to-charge ratio

nM: Nanomolar

NDA: 2,3-naphthalenedialdehyde

PGA: Pyroglutamic acid

PRA: Percent residual accuracy

ppb: Parts per billion

ppm: Parts per million

Q1: First quadrupole mass analyzer

Q2: Collision cell

Q3: Third quadrupole mass analyzer

QC: Quality control

Rs: Resolution

RSD: Relative standard deviation

RT: Room temperature

SCN-: Thiocyanate

S/N: Signal-to-noise

SEM: Standard error of the mean

$t_{1/2,dis}$: distribution half-life

$t_{1/2,el}$: elimination half-life

Tmax: Time of maximum concentration

TIH: Toxic inhalation hazards

TRPA1: transient receptor potential ankyrin 1

TRP: Transient receptor potential

TG: Trigeminal ganglion

ULOQ: Upper limit of quantification

V: Volts

WDR: Wide dynamic range

WWI: World War I

WWII: World War II

LIST OF FIGURES

LIST OF TABLES

ABSTRACT

DEVELOPMENT OF ANALYTICAL METHODS FOR TOXIC INHALED HAZARDS (TIH) AND THEIR METABOLITES

OBED ADU GYAMFI

2020

Toxic inhalation hazards (TIHs), such as methyl isocyanate (MIC) and hydrogen cyanide (HCN), are noxious gases and vapors that are harmful, and often deadly, to humans. However, because of their low cost and high reactivity, they are extensively used for industrial productions, creating risk of exposure for both industrial workers (e.g., occupational exposure) and civilians (e.g., accidental release during transport). The illicit use of TIHs, including as terrorist agents, is also concerning. Considering the rapid toxicity of TIHs and the danger they pose to both human and animal lives, there is a critical need to develop of analytical methods for the analysis of TIH metabolites and therapeutic agents to verify their exposed and to help in further development of these therapeutics.

One therapeutic strategy for TIH exposure is inhibition of the transient receptor potential ankyrin 1 (TRPA1) ion channel, since some TIH toxic effects are triggered by activation of this channel. Antagonists of TRPA1 have shown near complete attenuation of the noxious effects from TIH exposure. One of the TRPA1 antagonists, A-967079, has shown impressive efficacy, high selectivity, high potency, and oral bioavailability. However, no method for its analysis from any matrix is currently available. Hence, a simple HPLC-MS/MS method was developed and validated to quantify A-967079 in plasma. The method features an excellent LOD of 25 nM, a wide linear range (0.05–200 μM), and good accuracy and precision. The method was successfully applied to determine A-967079 from

treated animals and it may facilitate the development of A-967079 as a therapeutic agent against the noxious effects of TIH exposure.

While there are a number of known metabolites of cyanide (CN), the interaction of CN with glutathione has not been explored. Therefore, we studied the interaction of CN and GSH to identify the novel CN metabolite, 2-aminothiazoline-4-oxoaminoethanioc acid (ATOEA). The production of ATOEA from cyanide exposure was confirmed by detection of both ATOEA and ATOEA-$^{13}C^{15}N$ in rabbit plasma (N = 11 animals) following administration of NaCN:K$^{13}C^{15}N$ (1:1), with a similar amount of ATOEA and ATOEA-$^{13}C^{15}N$ formed (R2 = 0.9924, $p < 0.05$). An HPLC–MS/MS method was developed and validated to analyze ATOEA from plasma, producing a linear range of 0.5–50 μM, a limit of detection of 200 nM, and excellent precision and accuracy. ATOEA concentrations were significantly elevated in the plasma of animals following cyanide exposure. Using this method, we showed that ATOEA is produced from interaction of CN and GSH and can serve as a biomarker of CN exposure.

A field portable detection method was developed to detect the CN metabolite, thiocyanate, from fish blood to verify CN-fishing (an illegal fishing technique practice in Southeast Asia that has detrimental effect on aquatic life). The cyanide sensor was adapted via oxidation of thiocyanate to cyanide using $KMnO_4$, microdiffusion, reaction of the cyanide with naphthalene dialdehyde and taurine, and fluorescence analysis of the resulting β-isoindole product. The method presented here features an excellent LOD (29 μg/L) and an acceptable linear range (59-590 μg/L), good accuracy (100±20%) and good precision (<20% relative standard deviation). The method was successfully applied to quantify thiocyanate from the blood of marine fish exposed to cyanide. The full development of the

proposed sensor would allow rapid field and laboratory analysis of suspected cyanide-caught fish by government, aquarium trade and food agencies to help enforce this illegal practice.

Chapter 1. Introduction

1.1. Overall Significance

Cyanide and other toxic inhalation hazards (i.e., methyl isocyanate (MIC), chlorine gas, chloroacetophenone, chloropicrin, etc.) have great importance for industries, including mining, agrochemicals, plastics, and pharmaceuticals. They have also been used for illicit activities like suicide, homicide, as chemical warfare agents and in illegal fishing activities (i.e., cyanide-fishing). Use of these chemicals poses severe risk to humans and the environment. Therefore, there is a critical need to improve ways to monitor the illicit use of these chemicals, to confirm human exposure to TIHs, and to develop effective therapeutics agents to battle their toxic effects.

1.2. Project Objectives

This dissertation is comprised of three main objectives: 1) Develop a simple and rapid analysis technique for the analysis of TRPA1 antagonist, A-967079, in plasma. 2) Identify novel metabolite of CN, produced by the interaction of CN with glutathione, 3) Develop a field portable analysis technique to determine SCN in fish blood, in order to monitor CN-fishing. Chapter 2 addresses the analysis of TRPA1 antagonist, A-967079; in plasma, using high-performance liquid chromatography tandem mass-spectrometry. Chapter 3 details the metabolism of CN by glutathione, to produce the novel CN metabolite, 2-aminothiazoline-4-oxoaminoethanoic acid. Chapter 4 describes the analysis of CN metabolite, SCN, in fish blood via modification of a field-portable CN sensor (i.e., the Cyanalyzer) to monitor CN fishing. Chapter 5 contains the conclusion and suggested future studies.

1.3. Toxic Inhalation Hazards

The increase in the world's population has caused a huge demand on modern industrial production. These demands have led to the use of easy and cost-effective manufacturing practices, including the use of small molecule precursor chemicals. Many of these chemicals are toxic inhalation hazards (TIHs), noxious gases which are toxic to humans and other organisms.[1-3] The ease of producing these compounds and their low-cost supply, in addition to their high reactivity makes them useful for synthesis of many industrially important products. They are also used themselves for a number of purposes including agriculture, mining, cleaning etc.[2, 4] For example, chlorine gas is used for water treatment, cleaning, antiseptics and chemical synthesis. Ammonia is used in the production of fertilizers.[4, 5] Methyl isocyanate (MIC), a reactive TIH, is widely use in the production of pesticides, fungicides and polymers.[6] The mining and the metallurgy industries employ sodium cyanide in the extraction previous metals and other minerals.[7]

The demand for TIHs poses risk of exposure to industrial workers, custodians, and farmers. Accidental leaks of TIHs in industries and highly populated areas during transportation have also injured and kill many.[7-12] TIHs, such as sulfur mustard, chlorine gas, cyanide, etc., have also been used as chemical warfare agents by many military and terrorist groups to kill and injure civilian population.[13-16]

Exposure to most of reactive TIHs compromises the respiratory system by causing severe damage of the airways and lung.[1, 17] Following trace level, reactive TIHs are perceived as irritating, and induce sneezing, coughing, mucus secretion, tearing, and upper airway inflammation.[1, 18] These responses help neutralize, and expel these toxins, limiting damage to alveolar sacs.[19, 20] At higher levels, the noxious responses advanced

to uncontrollable coughing, profuse lacrimation, resistance to airflow by bronchospasm, mucus hypersecretion, and upper and lower airway inflammation and compounds preexisting respiratory condition such as triggering attack on asthmatic individuals.[21, 22] In severe and prolong exposure, TIHs causes severe lung damage and also damages the delicate alveolar sacs by reacting with the lung tissues.[23, 24] These physiological behavioral responses from TIHs are as results of its detection by the olfactory and nociceptive sensory systems that triggers signals to the brain by activating transient receptor potential (TRP) and acid-sensitive ion channels.[3, 25, 26]

1.4. TRPA1 ion channel

Transient receptor potential ankyrin 1 (TRPA1) is a member of the superfamily of transient receptor potential (TRP) ion channel.[27] TRPA1 has a tetrameric structure with each subunit containing six transmembrane spanning segments (S1-S6), and an intercellular NH_2 and COOH termini domains.[28, 29] In between the S5 and the S6 transmembrane helices domain is a pore-forming loop.[30, 31] TRPA1 also has a large cysteine and lysine-rich N-terminus that contains 14-18 predicted ankyrin repeats, which distinguishes it from other TRP ion channels (Fig 1.1).[32-34] TRPA1 is abundantly expressed in nociceptive neuron of dorsal root ganglion (DRG), jugular ganglia (JG), and trigeminal ganglion (TG) neurons, which are the main receptors responsible for the noxious effect response of TIH exposure (Table 1.1).[1] TRPA1 channels expressed on nociceptors are consider important chemosensors.

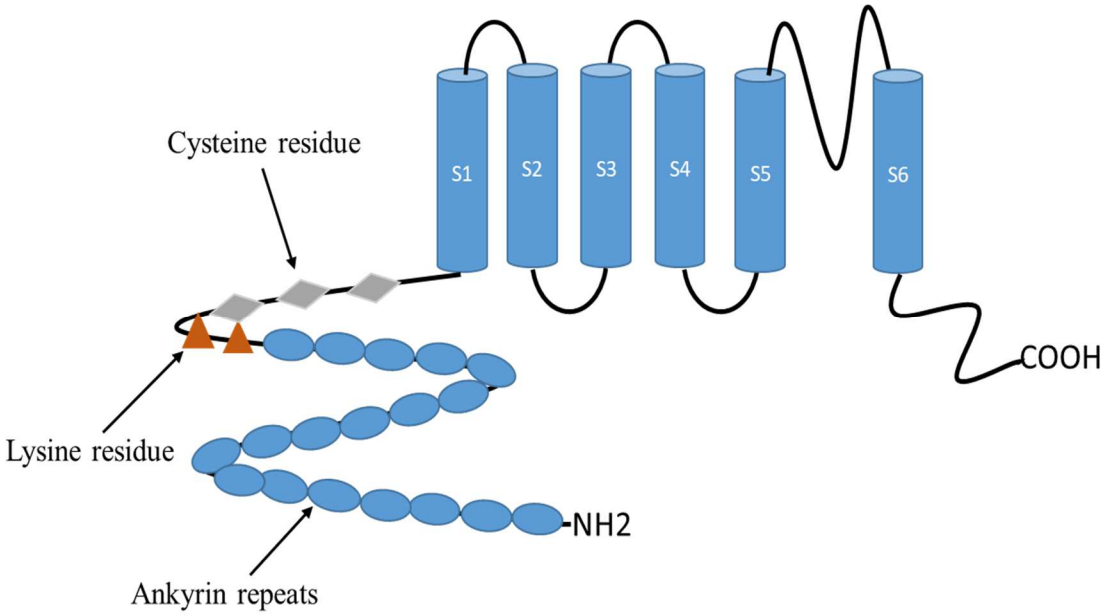

Figure 1.1. Diagram showing the structure of one subunit of TRPA1

Table 1.1. Toxic inhalation hazards and their activating TRPA1 sensory neurons

Type of Chemical	TIH (Toxicant)	Sensory Neuron
Electrophile	Trans-2-pentenal	TG[35]
Electrophile	Toluene diisocyanate	TG[36]
Electrophile	Methyl isocyanate	DRG[3]
Electrophile	Hexamethylene diisocyanate	DRG[3]
Electrophile	Benzyl bromide	DRG[3]
Electrophile	Bromoacetone	DRG[3]
Electrophile	Crotonaldehyde	JG[37]
Electrophile	Acrolein	JG, TG[37]

Electrophile	Allylisothiocyanate	TG[1]
Electrophile tear gas	Chloroacetophenone	DRG[3]
Electrophile tear gas	Chlorobenzalmalononitrile	DRG[38]
Electrophile tear gas	Dibenzoxazepine	DRG[38]
Electrophile air pollutant	Cigarette smoke extract	JG[37]
Aldehyde	Formalin	DRG[39]
Oxidant	Chlorine	DRG/TG[18]
Oxidant	Hydrogen peroxide	DRG/TG[18, 40]

DRG = dorsal root ganglia, JG = jugular ganglia, TG = trigeminal ganglia

Many types of chemical irritants and pharmacological agents activate TRPA1. Most especially, TRPA1 is activated many TIH including the reactive oxidizing and electrophilic chemical species (Table 1.1).[1, 41] TIH activation is initiated by covalent modification of the TRPA1 by electrophilic bonding (Michael's Addition) of the reactive TIH to either the cysteine or the lysine residue of the TRPA1.[32, 33] Reactive TIHs are detected by peripherals sensory neuron after activating of the TRPA1 ion channel (Table 1.1).[1, 29, 42] The activation of the ion channel following TIH exposure (i.e., electrophilic modification of TRPA1) induces neurogenic inflammatory and brain-mediated responses of the airways that lead to hypersensitivity of both the upper and lower airways causing noxious effects, including immediate unbearable irritation of the eye, nose, and throat, inducing sneezing, coughing, tearing, mucus secretion, upper airway inflammation, etc.[3, 34, 41, 43, 44]

The noxious effects cause by the activation of TRPA1 ion channel have led to scientists targeting this ion channel to develop therapeutics that could alleviate the acute effects of the lung diseases and disorders associated with reactive TIHs exposure.[17, 41] Evidence of the importance of this strategy was found when genetically deleted TRPA1 mice showed near complete no noxious effect from the exposure to TIHs. In addition, many antagonists of TRPA1 have been effective in blocking noxious behavior induced by neurogenic inflammation.[45, 46]

To date, a few promising TRPA1 antagonists have been reported, including AP18 (IC_{50} of 3.1 to 6.9 μM), HC-030031 (IC_{50} of 1 to 41.8 μM) and A-967079 (IC_{50} of 51 to 289 nM).[39, 47-49] AP18 is selective for TRPA1 over several other TRP channels; however, it has poor bioavailability through oral and intraperitoneal dosing.[50, 51] HC-030031 is bioavailable through various dosing and it is reported to be selective to other TRP ion channels, however, HC-030031 also inhibits other several pain-signaling proteins.[47, 52] A-967079 is potent, highly selective, and orally bioavailable TRPA1 antagonist. Unlike other TRP antagonists, A-967079 does not produce locomotor or cardiovascular side effects and does not have an effect on body temperature.[46, 49, 53]

1.5. History and Uses Cyanide

1.5.1. History and Ancient Use

Cyanide (HCN and CN^- are inclusively represented as CN) is known as highly toxic chemical that can cause death within minutes of exposure and has been used as a poison for thousands of years.[7, 54, 55] The use of CN dates back to the times of the ancient Egyptians and Romans, where CN containing plants (e.g., cassava, bitter almonds, cherry laurel leaves, peach pits, etc.) were used for poisonings and judicial executions.[56-58] In

1679, Wepfer first described CN poisoning by extraction it from almond.[59] Although CN containing plants have been used as poison for centuries, Carl Scheele first identified CN in 1782 by isolating it from Prussian blue dye and further described CN as an acidic water-soluble flammable gas and named it “prussic acid”.[58, 60] In 1815, Gay-Lussac definitively determined that the molecular formula of cyanide contained no oxygen, which disputed the theory that all acids must contain oxygen.[59] He further identified CN as a gas with an almond-like flavor, which is colorless and poisonous and name it cyanogen.[59, 61, 62]

1.5.2. Military Use

Military use of CN is dated back in the 1870s when Napoleon III ordered the use of CN as war weapon during the Franco-Prussian war (1870 war).[63] The use of CN as a chemical warfare agent (CWA) was officially documented during World War I (WWI), when the French used HCN in 1915. The use of HCN was discontinued by the French because HCN dispersed rapidly in open air.[58] In late 1916, the French and Austrians used cyanogen chloride and cyanogen bromide, respectively, to decrease diffusion in open air because they are less volatile and heavier than HCN.[14, 60] Later, the use of these derivatives of CN during the WWI was discontinue because they were unstable and corrosive.[14] During World War II (WWII) the Nazis used HCN (Zyklon B) to kill millions of civilians and soldiers in gas chambers. It was alleged that the Japans used CN on China during the WWII. In the 1980s, CN was used during the Iran-Iraq war to kill the Kurds of Iraq and Syria.[64-66]

1.5.3. Illicit Use (Cyanide Fishing)

For many centuries, different fishing techniques such as netting, angling, trapping hand gathering, and spearfishing have been used to harvest fish. Because of low harvesting yield per unit effort from many of fishing techniques, illegal techniques such as cyanide-fishing has been adopted in southeast Asia and many other regions.[67, 68] The use of CN to capture live fish for the marine aquarium trade was first reported in the Philippines at 1960s.[69, 70] Since then the practice has rapidly spread throughout many countries including Indonesia, Malaysia, Maldives, Papua New Guinea, Sri Lanka, Thailand, Vietnam,[71, 72] not only for aquarium trade but also for the live reef fish food trade which target large-sized groupers, wrasses and coral trout for human consumption.[73, 74] In the mid-1980s, it was estimated that more than 80% of all fish collected in Philippines for aquarium trade supply were harvested by CN and in the 1990s, almost 90% of fishing vessel in the eastern island of Indonesia had CN on board.[75, 76] CN fishing is illegal in most countries where the technique is practice. About 78% of the 18 main exporting countries have passed anti-cyanide fishing law to curb this practice. Although it is illegal, because of the nature of the trade chain involved in this practice, enforcement of these laws has not been successful and CN-fishing is still commonly practiced today. [74, 77]

CN fishing has led to population decline in moderately abundant target fish species, including *Cheilinus undulates*.[78, 79] Also, severe long-term effects on non-targeted species, including coral and other invertebrates, has been observed.[80] Exposure to very low concentration of CN causes reduction in respiration resulting in bleaching and eventual death of corals and anemones.[81, 82] Moreover, CN fishing endangers the fishers

involved in this practice due to their use of large quantities of cyanide and minimal protective measures used .[82]

1.6. Source of Cyanide

1.6.1. Natural Sources

CN is present in the environment in a number of forms. The major natural source of CN is edible plants that contain cyanide as cyanogenic glycosides, which release cyanide through hydrolysis.[83, 84] Several species (i.e., 800 species) of these edible plants and fruits have been identify to produce cyanide, including cassava, almonds, sweet potatoes, yams, peaches, apple, pears, sorghum, etc.[83, 85] Microorganisms (i.e., algae, bacteria and fungi) and several species of arthropod and insects such as centipedes, millipedes, moths, butterflies and beetles synthesize and excrete cyanide as a self-defense mechanism.[83, 86, 87] Volcanic eruptions can release HCN into the atmosphere by carried ash leading to the potential contamination of the air and nearby water.[88] The abundance of cyanogenic plants, insects, and microorganisms pose risk of cyanide exposure to people including survivalist, nature enthusiasts, farmers, and ranchers. Therefore, caution should be taken when choosing the type of plants and insects they eat, grow or touch to keep them from accidental cyanide exposure.

1.6.2. Anthropogenic Sources

Currently, anthropogenic exposure to CN occurs through industrial operations, metal extraction, fire/smoke inhalation, chemical synthesis, etc.[89, 90] About 1.4 million tons of CN is estimate to be produced annually.[89] HCN, the gaseous form of CN, is produced by three main processes, namely Andrussow, Degussa, and Shawinigan.[91-93] The Andrussow process utilizes reaction of methane and ammonia to produce HCN in the

presence of oxygen and a platinum catalyst.[92] The Degussa process of producing HCN also involves reaction of methane and ammonia to produce HCN using platinum as a catalyst, but does not utilize oxygen.[93] In the Shawinigan Process, HCN is produced by the reaction of ammonia and propane gas in the presence of coke.[94] CN salts (i.e., NaCN and KCN) are produce by reacting of HCN with the respective alkali metal. Extraction of precious metals such as gold, silver, zinc, etc. from their ore is one of the major uses of CN, due to CN strong binding capacity to these metals.[7, 61] In addition to its use to extract metals, CN is also used in the synthesis of pharmaceuticals, pesticides, dyes, fibers and polymers and pigments. Due to the large production CN and its extensive use in industry, there is an increased risk of occupational CN exposure.

Although occupation exposure to CN is alarming, smoke inhalation from household or industrial fires and cigarette smoke is the leading source of exposure.[95, 96] The production of HCN from cigarettes ranges from 10-400 μg/cigarette and the amount in secondhand smoke ranges from 0.006-0.27 μg/cigarette.[90] Another source of CN-containing smoke is the incomplete combustion of nitrogen-containing materials and compounds such as plastic, wool, silk, nylon, melamine and polyurethane.[96] Reports have shown that victims of fire accidents may have been exposure to both carbon monoxide (CO) and CN, and majority of the death resulting from these incidence are attributed to CN-poisoning.[55, 96]

1.7. Toxicity of Cyanide

The onset of CN exposure is rapid (i.e., symptoms can occur in as little as 15 seconds) and death may occur within minutes depending upon the level and route of exposure.[7, 59] A blood concentration of 19 μM is considered toxic, and it could be

considered fatal at blood concentrations greater than 115 μM.[97, 98] The primary effect of CN toxicity is the impairment of oxidative phosphorylation, a process whereby oxygen is utilized for production of ATP, an essential cellular energy source.[60, 99] This process involves the transfer of electrons from NADH to oxygen through a series of electron transfer steps. This process is catalyzed by cytochrome c oxidase enzyme, found in complex IV of the electron transport chain (Figure 1.2).[100-102] Upon exposure, CN inhibits cytochrome c oxidase by binding to Fe^{3+} found in the heme A3 moiety of the enzyme, resulting in loss of structure integrity and hence, the effectiveness of the enzyme.[103] Inhibition of cytochrome c oxidase prevents electron transfer, leading to impairment of cellular respiration.[96, 104] In addition, the disruption of H^{+} gradient ceases the production of ATP. In order to compensate for ATP loss, glucose is broken down via glycolysis, leading to the production of pyruvate that reduces to lactic acid.[58] As lactic acid concentration increases in blood, the body pH decreases leading to the impairment of several physiological processes, ultimately leading to cell death.[58, 89, 105]

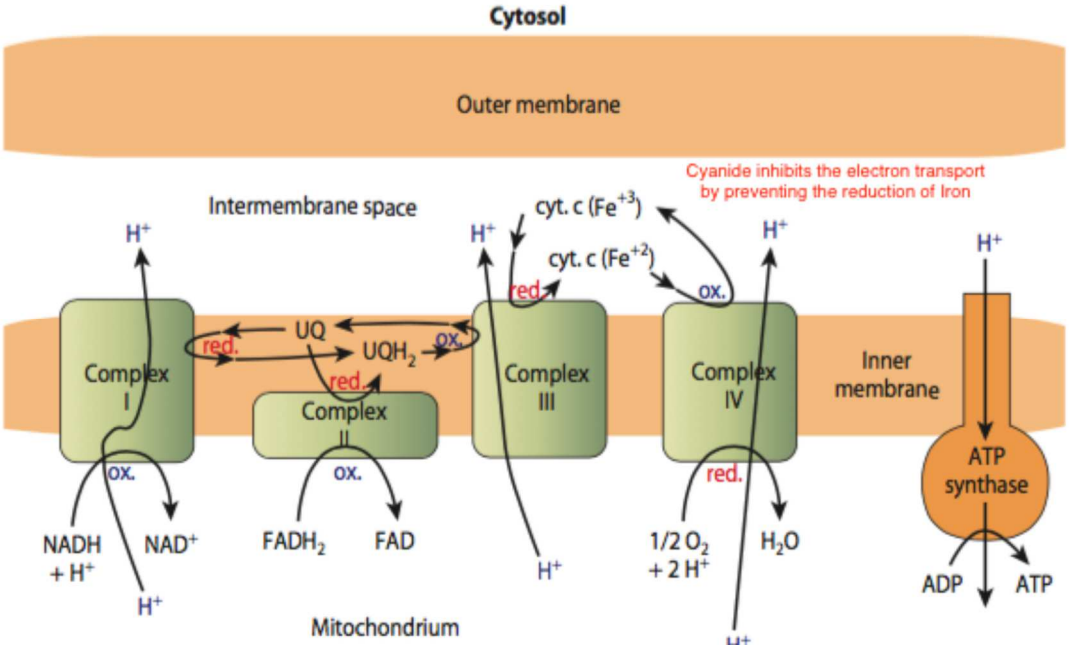

Figure 1.2. Diagram showing the inhibition of cytochrome c oxidase within the electron transport chain in the mitochondrial membrane.[102]

1.8. Metabolism of Cyanide

The strong reactivity and volatility of CN in biological environments leads to multiple metabolism pathways (Figure 1.3).[106] The most important naturally occurring CN metabolic pathway is the detoxification CN by a sulfur donor to form the much less toxic thiocyanate ion (SCN^-),[107] accounting for about 80% of the total CN metabolism.[60] The two major enzymes that catalyze this process are rhodanese and 3-mercaptopyruvate sulfurtransferase.[107-109] An alternative metabolism pathway for CN is its conversion to 2-amino-2-thiazoline-4-carboxylic acid (ATCA).[60] CN is metabolized into ATCA by its direct interaction with cysteine in the physiological environment.[110] This non-enzymatically catalyzed pathway accounts for about 0.10-9.19% of the total CN detoxification.[55, 111]

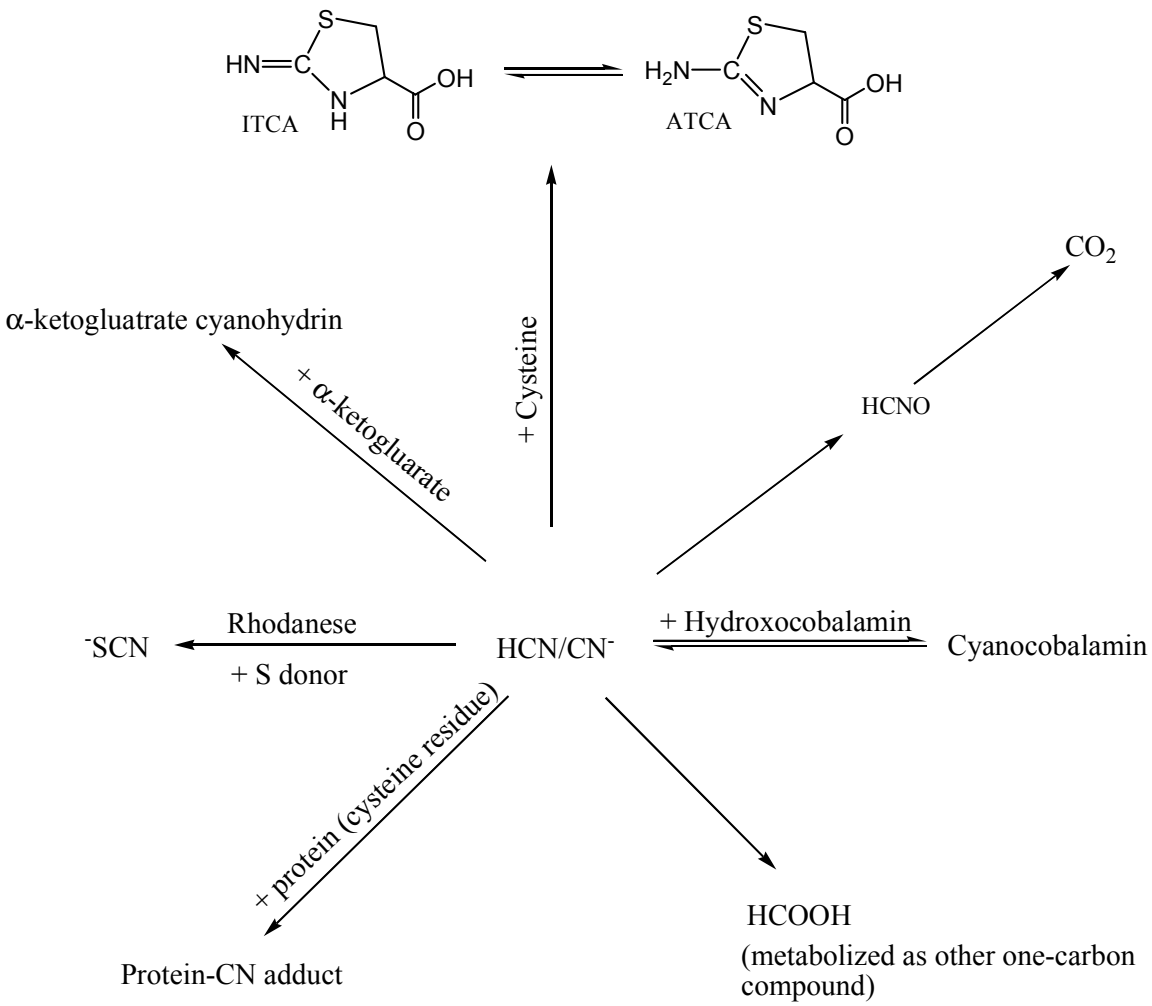

Figure 1.3. Metabolic pathway of cyanide and major ways of release. Diagram adapted from Logue et al.[111] Thiocyanate ion (SCN^-), 2-amino-2-thiazoline-4-carboxylic acid (ATCA), 2-iminothiazolidine-4-carboxylic acid (ITCA)

Other minor metabolites of CN exposure have been reported, but information about them is limited. One of these minor metabolites is α-ketoglutarate cyanohydrin (α-KgCN) which is formed from the reaction of CN with α-ketoglutarate (α-Kg) in biological environments.[112-114] The reversible reaction of cyanide with hydroxocobalamin to form cyanocobalamin is another minor metabolic pathway of CN.[115] CN-protein adducts, which are formed by the interaction of CN with disulfide bonds in human plasma proteins, has also been reported.[116]

Chapter 2. Analysis of Trpa1 Antagonist, A-967079, in Plasma Using High-Performance Liquid Chromatography Tandem Mass-Spectrometry

2.1. Introduction

Toxic inhalation hazards (TIHs) are noxious gases and vapors (methyl isocyanate (MIC), chlorine, chloroacetophenone, chloropicrin, etc.) that are harmful and often deadly when inhaled.**[1, 3, 13, 117]** However, because of their low cost and ease of manufacture along with their high toxicity and relatively short half-life, they are used for many purposes, including fumigation, fungicide, disinfection, pest control, and cleaning. Many TIHs are also important for metallurgy, plastics, pharmaceuticals, and semiconductors.[1, 2, 6] Therefore, industrial demand for TIHs, and their transport through highly populated areas, significantly increases the risk of exposure.[10, 118] The potential use of TIHs by terrorists to injure and kill civilians is also concerning.[13-16] The risk of TIH exposure is most infamously illustrated by the tragic accident in Bhopal, India (1984) where more than 8000 people died within few minutes of methyl isocyanate (MIC) exposure.[8, 9]

Many TIHs are detected by olfactory neurons and peripheral sensory neurons by activating transient receptor potential (TRP) cation channels,[29, 42, 119] and acid-sensitive ion channels (ASICs).[25, 26] The activation of these channels, following TIH exposure, triggers signaling to the brain which leads to immediate unbearable irritation of the eye, nose, and throat, and induces sneezing, coughing, mucus secretion, upper airway inflammation, and tearing.[3, 25, 34, 43] At prolonged or high-dose exposure, these responses progress to severe pain, intense coughing, profuse flow of tears, and resistance to airflow by bronchospasm, mucus hyper-secretion, and pneumonitis.[1, 41, 44] TRP ankyrin 1 (TRPA1), a member of the TRP ion channel family expressed on nociceptive primary afferent C-fibers, is a main receptor for the noxious effect response of TIH

exposure and is activated by about 40% of all TIHs, including all oxidizing and electrophilic TIHs (e.g., tear gas agents and MIC).[1, 3, 41, 43] The importance of TRPA1 in TIH response has been shown experimentally with both TRPA1-knockout (Trpa1−/−) mice and TRPA1 antagonist-treated mice showing complete cessation of the noxious effects of TIHs.[17, 41, 45, 46, 52]

To date, very few TRPA1 antagonists have entered into pre-clinical trials. The major setbacks of this therapeutic strategy is a lack of potency, selectivity, and bioavailability.[50, 120] For example, AP18 (4-(4-Chlorophenyl)-3-methyl-3-buten-2-one oxime, Fig 2.1) is potent and selective for TRPA1 over other TRP ion channels,[50, 51, 121] but shows poor bioavailability following intraperitoneal and oral administration. Similarly, HC-030031 (2-(1,3-Dimethyl-2,6-dioxo-1,2,3,6-tetrahydro-7*H*-purin-7-yl)-*N*-(4-isopropylphenyl)acetamide, Fig 2.1) is also selective for TRPA1 over other TRP channels, but it has been reported to also inhibit several non-TRP pain signaling proteins.[47, 52]

The limitations of TRPA1 agonist compounds have necessitated the continued search for more efficacious antagonists. Recently, (1*E*,3*E*)-1-(4-Fluorophenyl)-2-methyl-1-pentene-3-one oxime (A-967079, Fig 2.1) has shown impressive efficacy as an antagonist to TRPA1 and has multiple advantages over other compounds, including high selectivity, potency, and oral bioavailability.[46, 49] A-967079 has IC_{50} values of 67 and 289 nM for human and rat TRPA1 receptors, respectively. It displays 1000-fold selectivity for TRPA1 over other TRP channels, and greater than >150-fold selectivity over 75 other ion channels, enzymes and G-protein-coupled receptors.[46, 49, 53, 122] Other advantages of A-967079 including no locomotor or cardiovascular effects, a common side effect of

other TRP antagonists. Oral administration of A-967079 in rats produced robust bioavailability and analgesic efficacy for TIH-induced pain response (i.e., sneezing, tearing, coughing, etc.) and osteoarthritic pain.[49, 122] Intravenous injection of A-967079 has also shown to decrease the reactive gas response of wide dynamic range (WDR, i.e. to about 61% from baseline levels in rat) and pain specific-neurons.[46, 122]

In spite of the potential advantages of A-967079, there is no currently available validated analytical method for its quantification. Therefore, the objective of this study was to develop and validate a high-performance liquid chromatography tandem mass spectrometry (HPLC-MS/MS) method for the analysis of A-967079 in plasma, which can be used in further development of A-967079 as a countermeasure for TIH exposure.

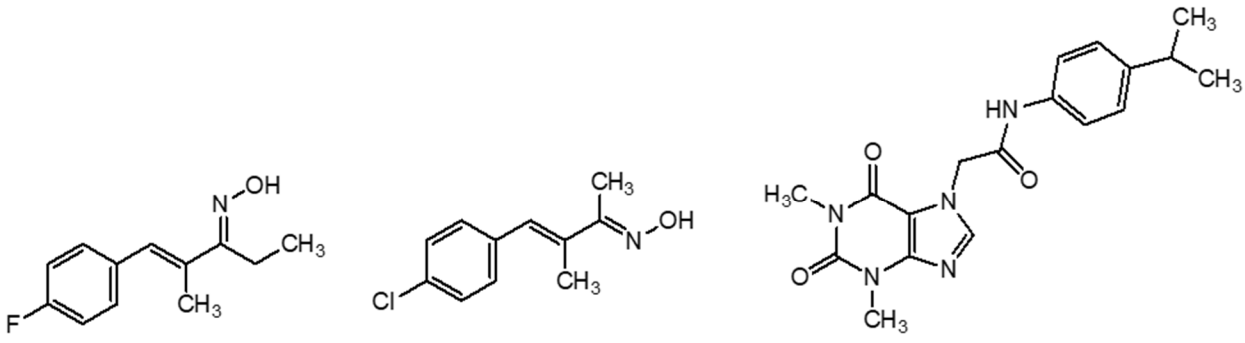

Figure 2.1. Chemical structures of TRPA1 antagonists with their respective identification.

2.2. Materials and Methods

2.2.1. Materials

All reagents and solvents were at least HPLC grade, unless otherwise specified. Ammonium formate was obtained from Sigma-Aldrich (St. Louis, MO, USA). Acetone, ethanol, and methanol (LC–MS grade) were purchased from Fisher Scientific (HanoverPark, IL, USA). A-967079 (>98% purity), supplied by Dr. Carl W. White (Pediatrics-Pulmonary Medicine, University of Colorado-Denver, Denver, CO, USA), was purchased from Med Chem 101 (Plymouth Meeting, PA, USA; 98% Purity; Lot X101075). Polymeric reversed phase column, PLRP-S 300Å (50 × 2.1 mm, 3.0 μm, part #:PL1912-1301) was purchased from Agilent (Santa Clara, CA 95051). Water was purified to 18.2 MΩ-cm by reverse osmosis using a Lab Pro polishing unit from Labconco (Kansas City, KS, USA). A-967079 was dissolved in ethanol:water (1:1) to make a stock solution of 10 mM concentration, which was further diluted to 5 mM in mobile phase A (pH~4), and stored at 4 °C. The stock solution of A-967079 (5 mM, in mobile phase A) was further diluted to 0.025–500 μM with either mobile phase A or plasma to produce working standard solutions.

2.2.2. Biological Samples

For analytical method development and validation, rabbit plasma (non-sterile with EDTA) was purchased from Pel-Freeze Biologicals and was stored at -80 °C until used. Rabbit plasma was used to develop the method presented here because we planned to utilize a rabbit model developed by our collaborators to prove the applicability of the analytical method for the analysis of A-967079 concentrations plasma. However, at the

time we were finalizing the method validation, efficacy studies of A-967079 were transitioned to a rat model. Plasma samples from A-967079-treated male Sprague-Dawley rats were obtained from the Pediatrics-Pulmonary Medicine, University of Colorado-Denver, Denver, CO, USA. Rats (250–350 g) were separated into eight groups (n=3 for each group) and each group was intraperitoneally administered 100 mg/kg A-967079 in 5% DMSO/sesame oil. Animals from groups 1–8 were euthanized at 0.25, 0.5, 1, 1.5, 2, 4, 8, and 24 h post-treatment, respectively, and blood was collected. Another group (n=3) was euthanized without A-967079 treatment and blood was collected as control (blank). Collected blood was placed in clean plastic tubes with EDTA anti-coagulant and centrifuged to separate the plasma from erythrocytes. Plasma was then transferred to a clean centrifuge tube, flash frozen, and shipped on dry ice (overnight) to South Dakota State University. Upon receipt, the plasma was stored at -80 °C until analysis was performed. All animals were cared for in compliance with the "Principles of Laboratory Animal Care'' formulated by National Society for Medical Research and the "Guide for the Care and Use of Laboratory Animals" prepared by the National Institutes of Health. The University of Colorado-Denver and Institutional Animal Care and Use Committee (IACUC) approved the animal study.

2.2.3. Sample preparation for HPLC-MS/MS analysis

Plasma (100 µL) was added to a 2-mL centrifuge tube. Acetone (300 µL) was added to the plasma to precipitate proteins. The sample was vortexed for about 3 min, and then cold centrifuged (8 °C) at 10,000 rpm (12,300 × g) for 5 minutes. An aliquot (300 µL) of the supernatant was transferred into a 4-mL glass screw-top vial and evaporated to dryness (at room temperature) using nitrogen. The contents of the glass vial were then reconstituted

with 100 µL of 0.1% ammonium formate in water (pH ~4). The solution was thoroughly mixed, filtered using a 0.22-µm tetrafluoropolyethylene membrane syringe filter, and transferred into an HPLC vial with glass insert (100 µL) for analysis.

2.2.4. HPLC-MS/MS Analysis

Liquid chromatography was performed on a Shimadzu HPLC (LC-20AD, Shimadzu Corp., Kyoto, Japan). The chromatographic separation was performed on an Agilent polymeric reversed phase column, PLRP-S 300Å (50 × 2.1 mm, 3.0 µm) protected by a guard cartridge with column temperature maintained at 40°C. Mobile phase A was 0.1% ammonium formate in water and mobile phase B was 0.1% ammonium formate in methanol, both with a pH of 4. The chromatographic separation was achieved using gradient elution at a flow rate of 0.35 mL/min as 20% B held constant for 2 minutes, increased linearly to 100% over another 2 minutes, held constant for 2 minutes, decreased to 20% B over 2 minutes, and held constant for 2 minutes to equilibrate between injections. A volume of 10 µL was injected for HPLC-MS/MS analysis.

A tandem mass spectrometer (AB Sciex Q-Trap 5500 MS) equipped with an electrospray ionization interface operating in the positive polarity was used to detect the A-967079. The mass spectrometric conditions were optimized by directly infusing A-967079 standard solution into mass spectrometer at a flow rate of 10 µL/min where A-967079 (m/z = 207), as an oxime, undergoes Beckmann rearrangement under acidic conditions to gain two protons to form its precursor A-967079 (m/z = 209).[123-125] Nitrogen (50 psi) was used as both the curtain and nebulization gas. The ion spray voltage and source temperature were 4,500 V and 500 °C, respectively with both nebulizer (GS1) and heater (GS2) gas pressures at 90 psi. The collision cell was operated with an entrance

potential of 10.0 V and a collision cell exit potential of 11.0 V at a medium collision gas flow rate. A-967079 was analyzed in multiple reactions monitoring mode (MRM) and the chromatograms were acquired with the Analyst software program. The MS/MS operating parameters and MRM transitions are listed in Table 2.1.

Table 2.1. MRM transitions, optimized collision energies (CEs), and declustering potentials (DPs) for the detecting of A-967079 by MS–MS analysis.

Compounds	Q1 (m/z)	Q3 (m/z)	Time (ms)	CE (V)	DP (V)
A-967079 (identification)	209	191	100	13.37	116.93
A-967079 (quantification)	209	162	100	46.97	46.97

2.2.5. Calibration, quantification, and limit of detection

The developed analytical method was validated using the Food and Drug Administration (FDA) bioanalytical method validation guidelines.[126, 127] To determine the limit of detection (LOD), multiple concentrations of A-967079 were prepared in plasma and analyzed by HPLC-MS/MS. The LOD was defined as the lowest concentration of A-967079 that reproducibly produced a signal-to-noise (S/N) of 3. The noise was determined as peak-to-peak noise in the blank samples over the elution time of A-967079.

For the calibrators, a working standard of A-967079 was prepared in rabbit plasma. From the working solution, calibration standards of A-967079 with concentration range of 0.025–500 μM (0.025, 0.05, 0.1, 0.2, 0.3, 0.5, 1, 3, 5, 10, 30, 50, 100, 200 and 500 μM) were prepared in rabbit plasma. All calibration standards were analyze in triplicate. The average peak areas were plotted as a function of A-967079 concentration in plasma to obtain the linearity, accuracy, and precision of the calibration standards. Both non-

weighted and weighted (1/x and $1/x^2$) calibration curves were constructed using linear least squares and calibrator accuracy was used to determine the best model for quantification. The lower limit of quantification (LLOQ) and upper limit of quantification (ULOQ) were defined as satisfying the inclusion criteria of <15% relative standard deviation (RSD, as a measure of precision), and a percent error (as a measure of accuracy) of 100±20% back-calculated from the nominal concentration for all calibration standards within the linear range. The goodness-of-fit of the calibration curves was determined using percent residual accuracy (PRA) (i.e., PRA values ≥ 90% are indicative of a good fit).[128, 129]

The accuracy and precision of the method were evaluated by analyzing three different quality control (QC) standards, 2 μM (low QC), 20 μM (medium QC), and 60 μM (high QC), not included in the calibration curve. QCs were analyzed in quintuplicate over three days (within 7 calendar days). *Intraassay* precision and accuracy were calculated for each individual day, and *interassay* precision and accuracy were calculated from comparison of the data gathered over three separate days.

2.2.6. Recovery, matrix effect and stability

The assay recovery of A-967079 was determined by the analysis of low, medium and high QC standards from spiked plasma as a ratio of the same concentration of QCs spiked in water. Recovery (i.e., signal recovery) was determined as a percentage of the ratio of the analyte peak areas from spiked plasma which underwent the sample preparation procedure listed above to the peak areas of dried aqueous QC standards reconstituted in Mobile Phase A which contained the amount of A-967079 corresponding to 100% recovery. The matrix effect was determined by creating calibration curves in both aqueous and plasma matrices, and comparing their slopes. A slope ratio (plasma slope/aqueous

slope) from the calibration curves greater than one indicates enhancement of the analyte in plasma, whereas slope ratio less than one indicates suppression of the analyte signal by plasma matrix.

The short- and long-term storage stability of A-967079 was evaluated by analyzing plasma spiked with high and low QCs stored at different temperatures at multiple storage times. The stability (i.e., signal stability) of A-967079 was determined as a percentage of the initial signal. A-967079 was considered stable in plasma at a specific temperature if the signal was within 15% of the initial signal. Short-term stability of the QCs was assessed for 24-h both in the autosampler (at 15 °C) and on the benchtop (at room temperature). Freeze-thaw stability was evaluated over three freeze-thaw cycles where four different sets of both low and high QCs were prepared. One set of both QCs was analyzed in triplicate on the same day, while the other sets were stored at -80 °C. For each cycle, all QC standards were thawed unassisted at room temperature. One set of the thawed QCs was analyzed in triplicate as first cycle. The remaining two sets of QCs were again stored at -80 °C. This procedure was repeated twice more to evaluate the remaining two freeze-thaw cycles. For the long-term stability studies, QC standards were stored at various storage conditions (-80, -30, and 4 °C) and analyzed over 30 days (0, 1, 3, 5 10, 20, and 30 days).

2.2.7. Pharmacokinetic Analysis

Pharmacokinetics parameters were determined using the plasma concentration data. The first order rate constants (k) associated with both distribution phase (k_{dis}), and elimination phase (k_{el}) of the curve were estimated via linear regression of the log plasma A-967079 concentration-time curve. The plasma distribution half-life ($t_{1/2,dis}$) and

elimination half-life ($t_{1/2,el}$) were calculated using natural logarithm (2)/k. The area under the plasma A-967079 concentration-time curve was calculated by trapezoidal rule.

2.3. Results and Discussion

2.3.1. HPLC-MS-MS Analysis of A-967079

The analytical method for A-967079 from plasma reported here features a rapid and simple one-pot sample preparation method, consisting of protein precipitation, centrifugation, and transfer and drying of the supernatant and subsequent reconstitution in aqueous mobile phase for HPLC-MS/MS analysis. The overall sample preparation time was less than 20 min, with the total chromatographic analysis time of 10 min (including equilibration following sample analysis). The ESI(+)-MS of A-967079 ($[M^{\cdot}]^{+}$ = 209 m/z), with corresponding proposed assignments of fragments is shown Figure 2.2. Transitions 209→162 and 209→191 m/z were used for quantification and identification of A-967079, respectively. The optimized DPs and CEs for quantification and identification of A-967079 are shown in Table 2.1.

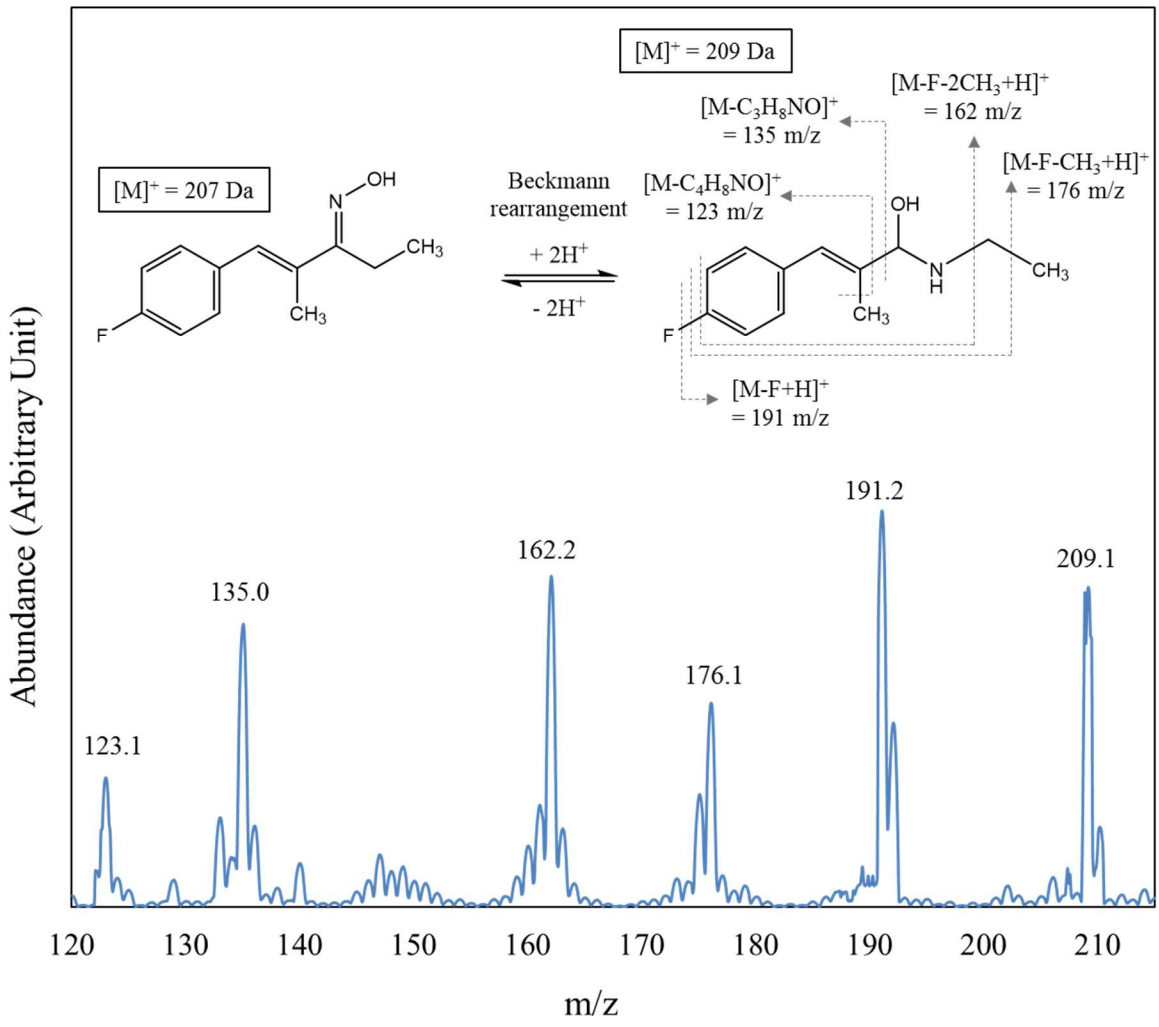

Figure 2.2. Representative ESI(+) mass spectra of A-967079 and identification of the abundant ions. A-967079 (207 Da) undergoes Beckmann rearrangement to produce a 209 Da product.

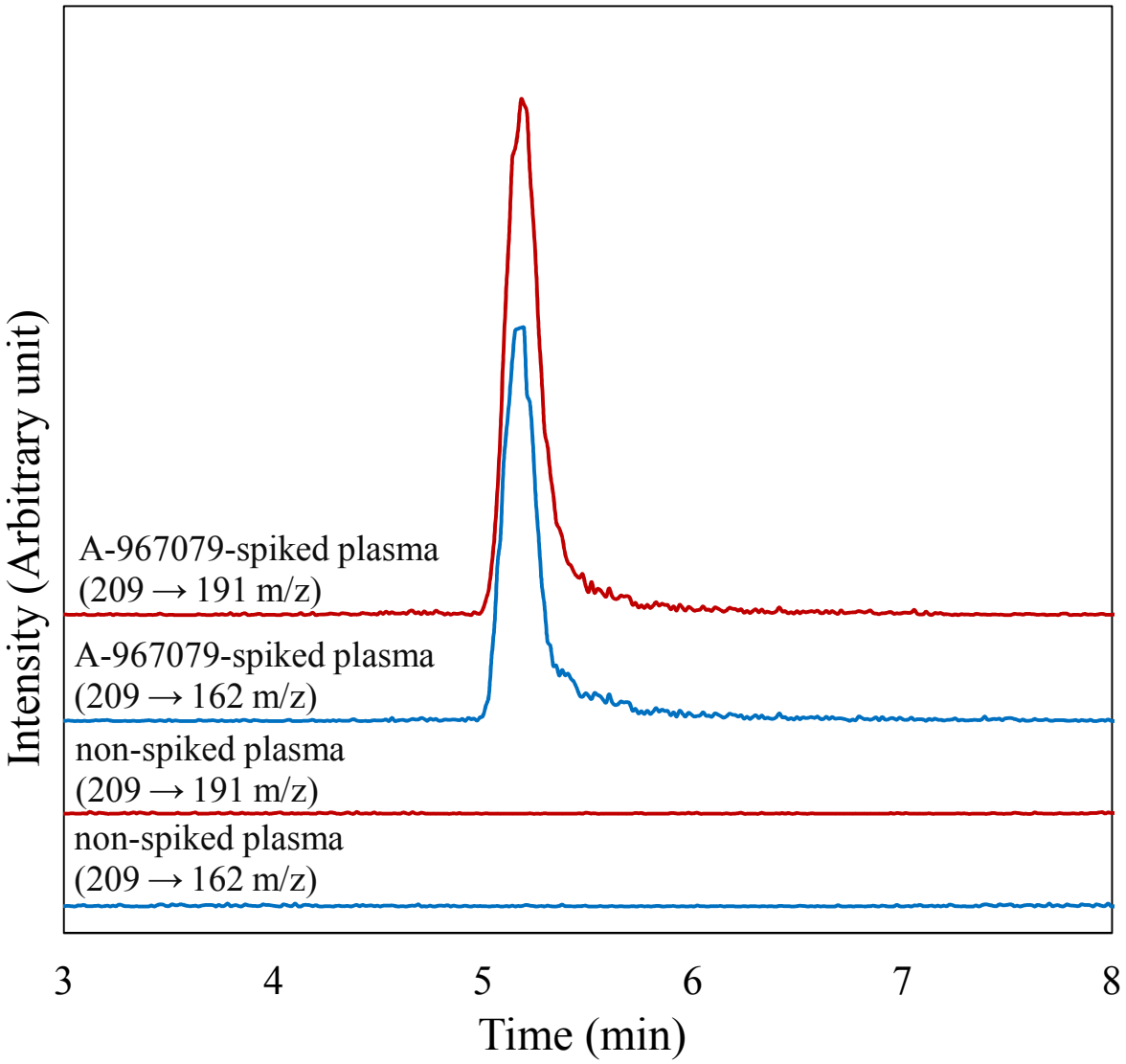

Figure 2.3. Representative HPLC-MS/MS chromatograms of spiked (5 μM) and non-spiked A-967079 in rabbit plasma. The chromatograms represent signal response to the MRM transitions of A-967079 (209 → 191 and 209 → 162 m/z).

Representative HPLC-MS/MS chromatograms of the A-967079 analyzed from spiked plasma are shown in Figure 2.3. Although the sample preparation protocol was simple, the method produced excellent selectivity. The A-967079 showed a sharp peak eluting at approximately 5.2 min, which was completely resolved from other components

in the matrix. Although the A-967079 peak tailed slightly (A_s= 1.80), the tailing did not affect quantification of A-967079.

2.3.2. Linear range, calibration and limit of detection

Standard curves were constructed over the concentration range of 0.025–500 μM A-967079 in rabbit plasma. The 0.025 and 500 μM calibrators were outside the linear range based on the accuracy and precision criteria. Therefore, the linear range of the method was 0.5 μM (LLOQ) to 200 μM (ULOQ) as best described by $1/x^2$ weighted linear regression. The linear range of the method was large, spanning over three orders of magnitude, which is excellent for bioanalytical HPLC-MS/MS methods[127, 130] and should be very useful for studies were analysis of a wide range of A-967079 concentrations is necessary. The calibration curves were found to be stable over three days as determined by consistency of the calculated slopes and the excellent fit of the data over the entire linear range for each day, as defined by the PRA (Table 2.2). Moreover, the method showed an excellent LOD of 25 nM in plasma as validated by analysis of multiple A-967079-spiked samples below the LLOQ over a 3-day period.

Table 2.2. Linear equations, coefficients of determination (R^2), and percent residual accuracy (PRA) for calibration curves created over 3 days.

Day	Equation	R^2	PRA(%)
1	y = 1.24e5x – 926	0.9867	95
2	y = 1.24e5x – 1021	0.9974	94
3	y = 1.24e5x – 1296	0.9962	92

2.3.3. Accuracy and precision

The accuracy and precision of the method were estimated by quintuplicate analysis of low, medium and high QCs on three different days (Table 2.3). The intraassay and interassay accuracies were both 100±10.5% of the nominal QC concentrations, respectively. The precision of the method was good, with all QCs producing %RSDs <15%. The accuracy and the precision of the method were within the FDA-acceptable range for method validation from a biological matrix.[127, 129, 130]

Table 2.3. The intra- and interassay accuracies and precisions of A-967079 analysis from spiked rabbit plasma by HPLC-MS/MS.

	Intraassay						Interassay	
Conc	Accuracy (%)			Precision (%RSD)			Accuracy	Precision
(μM)	Day 1	Day 2	Day 3	Day 1	Day 2	Day 3	(%)[a]	(%RSD)[a]
0.75	100±7.8	100±6.2	100±3.8	14.2	4.3	11.3	100±7.8	<14.2
7.5	100±6.2	100±3.5	100±10.5	10.8	5.1	9.5	100±10.5	<10.5
35	100±8.2	100±1.8	100±8.3	7.5	6.3	6.8	100±8.3	<7.5

[a]Aggregate of three days of QC method validation (n = 15)

2.3.4. Matrix effect, recovery and stability

To determine the effect of the plasma matrix on the analysis of A-967079, the slopes of standard curves of A-967079 spiked in aqueous and plasma solutions were

compared. The plasma to aqueous standard curve slope ratio was approximately 0.24, showing about 76% of suppression of A-967079 signals via the current method. The recoveries for low, medium, and high QCs of A-967079 from plasma were 22%, 23%, and 26% respectively. Since the % recovery value is the combination of matrix effect and recovery, the 24% average recovery is likely due exclusively to the 76% matrix effect suppression of A-967079 signals in rabbit plasma. Although there is a strong matrix effect, it was extremely consistent, and therefore, did not affect quantification of the A-967079. If desired, the signal suppression could be corrected via an internal standard, but over the course of method development, the consistency and accuracy of quantification of A-967079 via the method allowed for external standardization.

For the benchtop stability, A-967079 was stable for 10 h in plasma and started degrading below 85% of the control. Furthermore, A-967079 showed excellent stability, with not more than 15% deviation from the control, in plasma (-80 °C) over three freeze-thaw cycles evaluated. Moreover, the prepared A-967079 plasma samples were stable for 24 h in the autosampler, with each signal at least 85% of the initial signal. The long-term stability of A-967079 was evaluated at multiple temperatures. It was stable for 10 days at 4 °C and showed excellent stability (i.e., not more than 15% deviation from the control) in plasma at both -30 °C and -80 °C for 30 days. From the results of the stability studies, we recommend that when storage is necessary, plasma samples should be stored at either -30 °C or -80 °C, and can be thawed and refrozen 3 times for analysis. If samples are to be analyzed within 10 days, they can be stored at 4 °C.

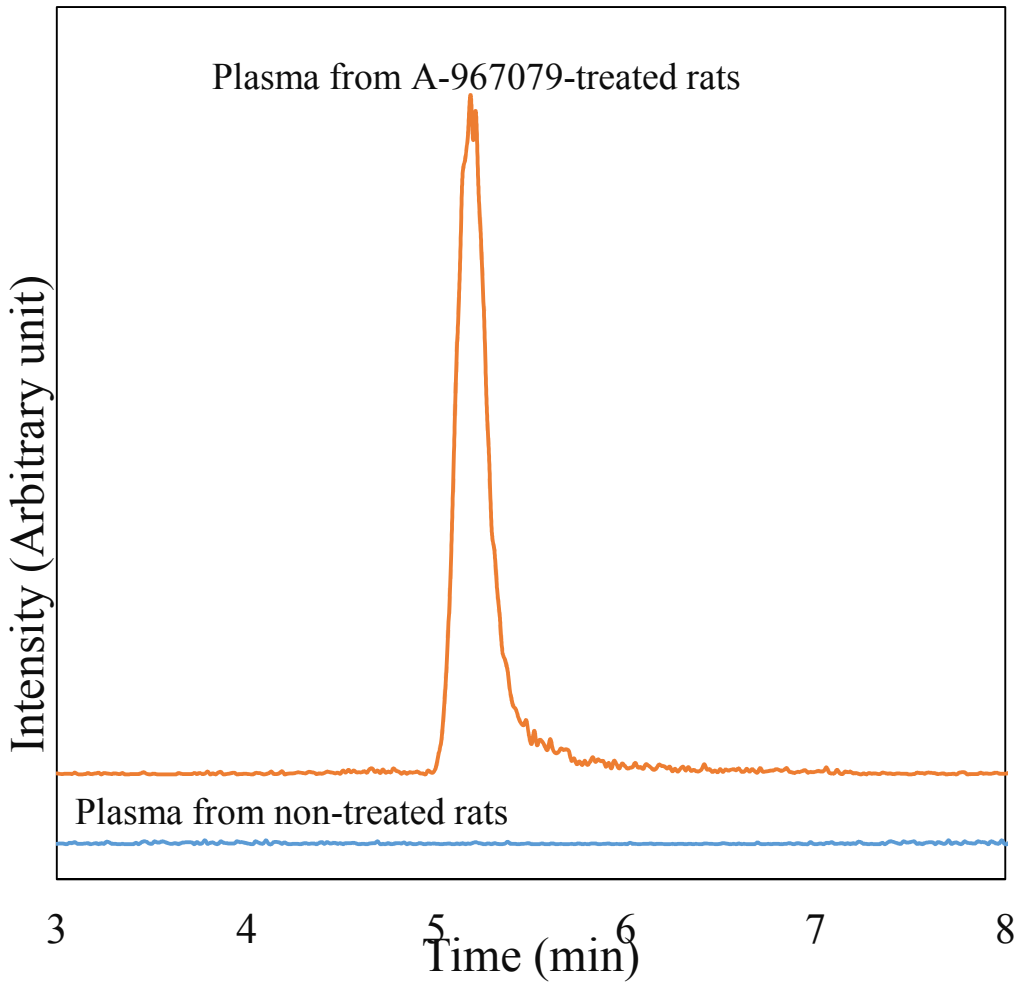

Figure 2.4. HPLC-MS/MS chromatogram from the plasma of A-967079-treated rats and rat plasma obtained prior to A-967079 treatment. The chromatograms represent signal response to MRM quantification transition of A-967079 (209 → 162 m/z).

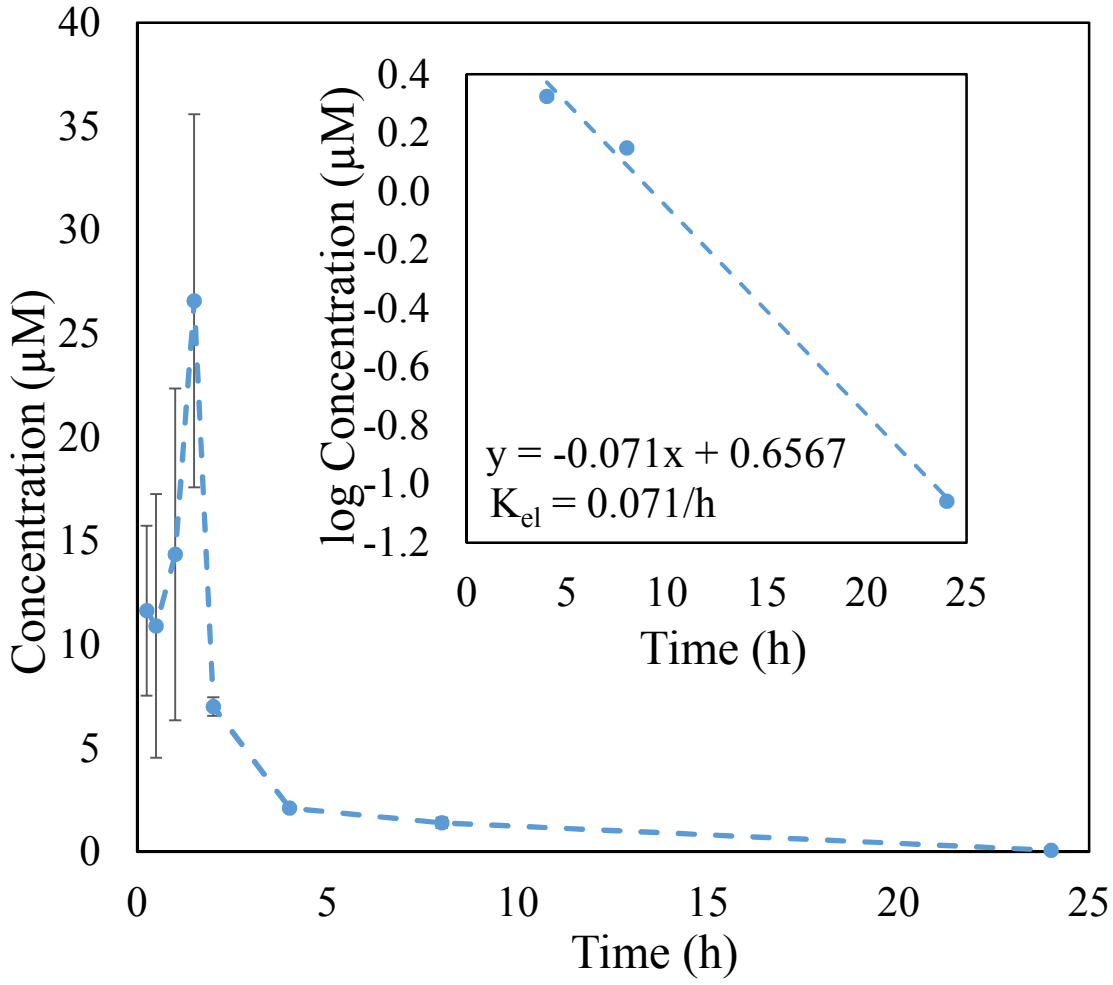

Figure 2.5. Plasma concentration-time pharmacokinetic profile of A-967079 following intravenous administration of A-967079 to rats. Error bars represent standard error of the mean (SEM, n=3). Inset: Representation of elimination constant (K_{el}) of A-967079 by log concentration-time graph.

2.3.5. Method application and pharmacokinetics

The validated method was applied to the analysis of plasma from rats treated with A-967079. Chromatograms from HPLC-MS/MS analysis of plasma of rats treated with A-967079 and rat plasma obtained prior to treatment are shown in Figure 2.4. In the plasma of treated rats, A-967079 was elevated as a prominent peak eluting at 5.20 min, whereas no peak was present in the plasma obtained from rats prior to A-967079 treatment. This

result confirmed the applicability of the method to analyze A-967079-treated animals, and further verified the selectivity of the method.

The pharmacokinetic profile of A-967079 for a single dose in rats is shown in Figure 2.5 with pharmacokinetic parameters listed in Table 2.4. The profile shows a rapid increase and subsequent quick decrease in A-967079 concentration, with a C_{max} and t_{max} of 26.6 μM and 1.50 h, respectively. The distribution half-life ($t_{1/2,dis}$) and distribution constant (K_{dis}) were 1.8 h and 0.3943 h^{-1}, respectively. These results show that A-967079 is quickly absorbed and distributed in the rat. Elimination was slower, with a $t_{1/2,el}$ of 9.76 h. The large area under the curve (i.e., AUC=56.3 μM*h) along with relatively slow elimination of A-967079 indicate the relatively slow clearance. This suggests that A-967079 may have the ability to treat victims of TIH exposure for extended periods following treatment.

Table 2.4. Pharmacokinetic parameters of A-967079 in a rat.

C_{max} (μM)	$t_{1/2,dis}$ (h)	$t_{1/2,el}$ (h)	K_{dis} (h^{-1})	K_{el} (h^{-1})	AUC (μM*h)
26.60	1.757	9.76	0.3943	0.0710	56.30

2.4. Conclusion

A simple and sensitive HPLC-MS/MS method for the determination of A-967079 in plasma was developed. The method presented here is the first validated method for the detection of A-967079 in any matrix. The method features simple sample preparation, rapid analysis, an excellent detection limit, and a wide linear range of 0.05–200 μM (i.e., covered over 3 orders of magnitude). The method presented has the ability to analyze A-967079

from plasma of treated animals, which will allow further drug development of A-967079 as therapy for pain and other noxious effects from TIH exposure.

Acknowledgements

We gratefully acknowledge support from the CounterACT Program, National Institutes of Health Office of the Director, and the National Institute of Environmental Health Sciences (NIEHS), Grant number U54 ES027698 (CWW). The opinions or assertions contained herein are the private views of the authors and are not to be construed as official or as reflecting the views of the National Institutes of Health or the CounterACT Program.

Chapter 3. Metabolism of Cyanide by Glutathione To Produce The Novel Cyanide Metabolite, 2-Aminothiazoline-4-Oxoaminoethanoic Acid

3.1. Introduction

Exposure to cyanide (HCN or CN^-, inclusively represented as CN) can occur by the consumption of foods that contain cyanogenic glycosides (e.g., almonds),[131, 132] and from the use of CN in electroplating, plastic production, synthesis of pesticides, and mining (extraction of gold and silver).[55] Other sources of exposure include smoke from cigarettes, fires, vehicles, and the use of CN in homicides, suicides or terrorist activities.[95, 133-135] The toxic effects of CN are rapid and can lead to death. Therefore, the confirmation of CN exposure is important for forensic and diagnostic applications.[136] Confirmation of cyanide exposure can be accomplished by detection of either protonated (HCN, pKa = 9.2) or non-protonated (CN^-) forms of CN,[137] where HCN is highly volatile and CN^- is a strong nucleophile.[55, 138] Although direct analysis is the most straightforward way to verify CN exposure, CN is relatively quickly eliminated

from biological fluids ($t_{1/2}$ = 0.34-1.0 h in biological fluids) due to its volatility and reactivity. Therefore, confirmation of CN exposure through direct analysis is unreliable in many circumstances, especially after a relatively long period of time has elapsed.[111] These limitations have led to the exploration of more stable markers to confirm CN exposure.

Free thiocyanate (SCN^-) is the major metabolite of cyanide, formed from the reaction of cyanide with sulfur donors in the presence of rhodanese (Figure 3.1.).[107] Due to its longer half-life in biological fluids,[55, 113] thiocyanate is a longer-lived marker for cyanide exposure. However, thiocyanate has limitations as a marker to confirm cyanide exposure.[106, 138] Ballantyne reported a low recovery of thiocyanate and concentration instability during various storage conditions in whole blood.[139] Furthermore, edibles like broccoli, cauliflower and cabbage are known to contain significant amounts of thiocyanate.[140, 141] Thiocyanate can also be formed by metabolism of other compounds beside cyanide.[132] These issues contribute to the large and variable background thiocyanate concentrations in biological fluids (i.e., average SCN^- concentrations are approximately 30.9 ± 13 μM, 130.2 ± 55 μM, and 568.0 ± 128 μM, for blood, urine, and saliva, respectively),[55, 136] rendering the analysis of free thiocyanate to confirm CN exposure inconsistent.

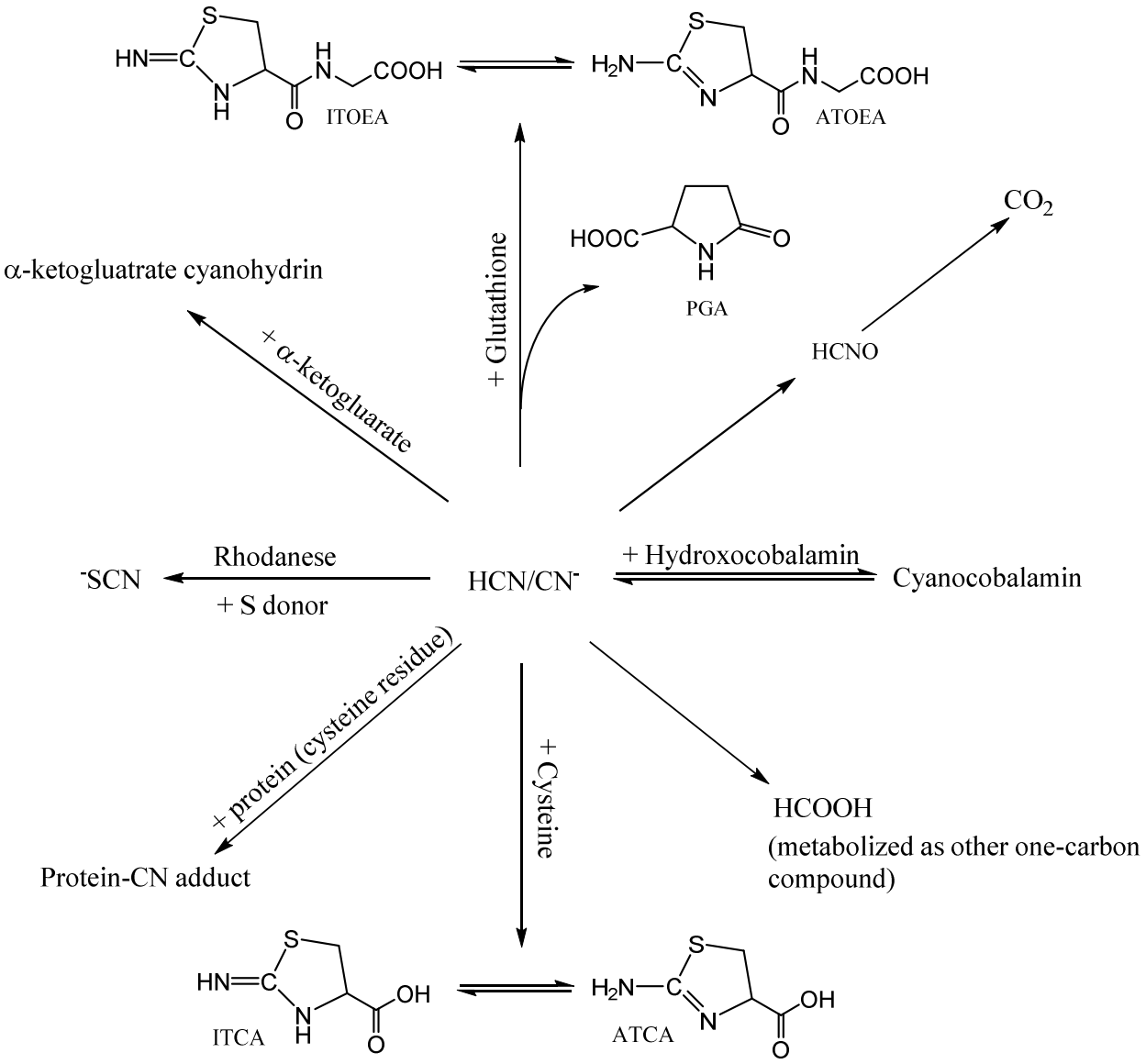

Figure 3.1. Current metabolic pathway of cyanide and major ways of release. Diagram adapted from Logue et al.[111] Pyroglutamic acid (PGA), 2-amino-2-thiazoline-4-carboxylic acid (ATCA), 2-iminothiazolidine-4-carboxylic acid (ITCA), 2-aminothiazoline-4-oxoaminoethanoic acid (ATOEA), 2-iminothiazolidine-4-oxoaminoethanoic acid (ITOEA), and glutathione (GSH).

The conversion of CN to 2-amino-2-thiazoline-4-carboxylic acid (ATCA) by the reaction of cyanide with cysteine, as shown in Figure 3.1, is an alternative metabolism pathway for CN.[77, 138] The reaction of CN with cysteine leads to the formation of ATCA, and its tautomeric form, 2-iminothiazolidine-4-carboxylic acid (ITCA) (Figure 3.1).[110] ATCA (ITCA and ATCA are referred to inclusively as ATCA) is formed in the physiological environment by direct interaction of cyanide with cysteine. Moreover, ATCA is not formed from other known processes,[136] does not metabolize further after its formation,[77, 138, 142] and it is highly stable in biological samples (i.e., ATCA has been shown to be stable for months under various storage conditions).[110, 111] However, Petrikovics et al.[143] reported that, at sublethal doses of CN, the concentration of ATCA in plasma does not increase significantly, suggesting that ATCA might not be a good biomarker for sublethal cyanide exposure. Conversely, Bhandari et al,[89] reported that ATCA concentrations generally followed CN concentrations (i.e., quick elimination in three animal species and that only a very small amount of ATCA was formed) for sublethal doses of ATCA. While ATCA may not be a good marker for diagnosis because of its low abundance and relatively short half-life, its stability makes it extremely promising for forensic purposes (i.e., post-mortem verification of cyanide exposure).[144, 145]A number of other markers of CN exposure have been discovered, but information is limited for these markers. CN reacts with α-ketoglutarate (α-Kg) in biological environments to form α-ketoglutarate cyanohydrin (α-KgCN).[113, 114] The studies by Mitchell et al.[112, 146] reported α-KgCN absorption and elimination kinetics were similar to CN and ATCA. Also, low recovery and poor stability of α-KgCN was demonstrated at various storage conditions except for −80°C, where it was stable for 30 days. The reversible reaction of cyanide with

hydroxocobalamin to form cyanocobalamin is another important metabolic pathway of CN.[115] Although cyanocobalamin is a promising marker, hydroxocobalamin, a precursor of cyanocobalamin, is an antidote for cyanide poisoning which would convolute detection when this antidote is delivered.[147, 148] Also equilibrium between hydroxocobalamin and cyanocobalamin causing concentration instability and the photo-degradability of cyanocobalamin[149, 150] limits its use as a marker to confirm cyanide exposure. In 2007, Fasco et al.[116] discovered cyanide-protein adducts (formed by the interaction of CN with disulfide bonds in proteins) in human plasma proteins. Others also confirmed the presence of these markers following CN exposure.[151, 152] Because many proteins have long half-lives (e.g., 25 days for albumin and 55 days for hemoglobin),[16, 153] the analysis of cyanide protein adducts may be an excellent forensic marker for confirming cyanide exposure, but little information is currently available on the usefulness of these adducts. Because of the limitations of each marker of CN exposure, other markers of CN exposure may address the disadvantages of the currently known markers.

The affinity of CN for biological thiols, as observed with the production of SCN^-, ATCA, and protein-adducts, likely indicates CN also reacts with other sulfur containing molecules such as glutathione. Glutathione (GSH; (2S)-2-amino-4-[[(1R)-[(carboxymethyl) carbamoyl]-2-sulfanylethyl] carbamonyl] butanoic acid) is a ubiquitous tripeptide in mammals and is an excellent antioxidant. GSH molecules are kept in a reduced state in animal cells, where its intracellular concentration can be as high as 10 mM. GSH reduces any disulfide bond formed within cytoplasmic proteins to cysteine by acting as an electron donor. In the process, GSH is converted to its oxidized form, glutathione disulfide (GSSG).[154, 155] The detoxification of cyanide with GSH or GSSG may be a first-line

defense against cyanide intoxication, as studies have demonstrated a reduced toxicity of cyanide in glutathione and glutathione-disulfide-pretreated mice.[156] Although the mechanism of reduced toxicity is unknown, it is likely that CN is converted to a less-toxic compound based on its interaction with GSH. Supporting this hypothesis is a study by Okafor et al.[157, 158] who studied the effects of CN generated by cassava (i.e., cyanogenic glycosides in cassava can produce a large concentration of CN) on endogenous GSH in rats, and reported a reduction in glutathione concentration in rats fed with cassava.

The objective of this study was to investigate the interaction of cyanide with glutathione with structural identification of biomarkers of cyanide exposure. A secondary objective was to develop an analytical method to quantify this biomarker. A tertiary objective was to evaluate the toxicokinetics of this marker.

3.2. Materials and Methods

3.2.1. Materials

All reagents were high-performance liquid-chromatography (HPLC) grade. Acetone and methanol were obtained from Fisher Scientific (Hanover Park, IL, USA). Reduced glutathione, oxidized glutathione, pyroglutamic acid, and ammonium formate were supplied by Sigma-Aldrich (St. Louis, MO, USA). Cyanamide (NH_2CN) was purchased from Acros Organic (Morris Plains, NJ, USA). Isotopically-labeled cyanamide ($^{15}NH_2{}^{13}C^{15}N$) was obtained from Cambridge Isotope Laboratories (Andover, MA, USA). Water was purified to 18 MΩ-cm using a Water PRO PS polisher (Labconco, Kansas City, KS, USA). All stock solutions were stored at 4 $^{\circ}$C. Working ATOEA solutions were obtained from stock solutions of ATOEA (2 mM) or ATOEA-$^{13}C^{15}N$ (1 mM) via serial dilutions to the desired concentration.

3.2.2. Synthesis of ATOEA and ATOEA-$^{13}C^{15}N$

The proposed reaction scheme for the synthesis of ATOEA is shown in Figure 3.1. The synthesis of ATOEA was achieved by the modification of Nagasawa et al.[60] method for the synthesis of ATCA. Cyanamide (NH_2CN, 1.77 g, 41.2 mmol) was added to L-glutathione (GSH) (dissolved in 100 mL of H_2O, 12.70 g, 41.3 mmol) with stirring. The resulting clear solution was heated by refluxing under a continuous stream of nitrogen gas until the pH of the entrained gas dropped from 11 to about 8 (as measured by wetted pH indicator paper). The reaction mixture was stirred overnight at room temperature, and then concentrated on a rotary evaporator until a white sticky product formed. Following overnight refrigeration, the solid was collected, recrystallized from ethanol/H_2O (5:1), and the product was dried in a vacuum desiccator over phosphorus pentoxide (P_4O_{10}) to yield approximately 43% ATOEA. Characterization was achieved by ^{1}H-NMR Spectroscopy along with ESI-MS operated in positive polarity mode.^{1}H-NMR (D_2O, 400 MHz) δ 1.1 (td, 2H) 3.5-3.6 (m, 2H) 3.7 (s, 2H) 3.85 (t, 1H). ESI (+)-MS: *m/z* 158.0, 101.0, 74.2, 59.0. An isotopically labeled standard, ATOEA-$^{13}C^{15}N$ was synthesized as described above for ATOEA, with NH_2CN replaced with $^{15}NH_2{}^{13}C^{15}N$. ESI (+)-MS: *m/z* 160.1, 103.0, 74.1, 59.0.

3.2.3. Biological Samples

Rabbit plasma (ethylenediaminetetraacetic acid anti-coagulant) for analytical method development was purchased from Pel-Freeze Biologicals and stored at -80 °C until used. Plasma from CN-exposed, New Zealand White rabbits was obtained from the University of California, Irvine. In one experiment rabbits (N = 8) were infused intravenously with 20 mg of NaCN in 60 mL of 0.9% NaCl at continuous rate of 1 mL/min

until apnea. Blood samples were drawn prior to infusion to establish a baseline. Blood samples were also drawn at 15, 25, 35 min following initiation of CN exposure, apnea, and 5, 7.5, 10, 15, 30 min post-apnea (without administration of antidote). In another experiment, stable isotope labeled CN was used to confirm the production of ATOEA from CN. Rabbits (N = 11) were administered lethal doses of 10 mg NaCN (50%) and 13.7 mg $K^{13}C^{15}N$ (50%) in 60 mL of 0.9% NaCl (1 mL/min continuous intravenous infusion) and blood samples were drawn prior to exposure (baseline), and 15, 25, and 35 min following initiation of cyanide infusion. A blood sample was also drawn at apnea. Glyoxylate (200 mg in 2 mL of 0.9% NaCl) was administered as an antidote and blood samples were drawn at 5, 7.5, 10, 15, 25, 30, 60, and 90 min post-administration of antidote.

After blood was drawn from rabbit, it was placed in EDTA tubes, and centrifuged to separate the plasma. Plasma was then transferred to a clean centrifuge tube, flash frozen, and shipped on dry ice (overnight) to South Dakota State University for analysis of ATOEA and ATOEA-$^{13}C^{15}N$. Upon receipt, the plasma was stored at -80 °C until analysis was performed. All animals were cared for in compliance with the "Principles of Laboratory Animal Care'' formulated by National Society for Medical Research and the "Guide for the Care and Use of Laboratory Animals" prepared by the National Institutes of Health. The CN exposure study was approved by UCIs and Institutional Animal Care and Use Committee (IACUC).

Table 3.1. MRM transitions, optimized declustering potentials (DPs), and collision energies (CEs) for the detection of ATOEA, ATOEA-$^{13}C^{15}N$, and PGA by MS–MS analysis

Compounds	Q1 (m/z)	Q3 (m/z)	Time (ms)	DP (V)	CE (V)
ATOEA (quantitation)	204	101	100	90	26
ATOEA (identification)	204	158	100	116	21.7
ATOEA-$^{13}C^{15}N$ (quantitation)	206	103	100	95.6	22
ATOEA-$^{13}C^{15}N$ (identification)	206	160	100	94	29.6
PGA (identification)	130	84	100	56.4	18.3

3.2.4. Sample preparation for HPLC-MS-MS analysis

Plasma samples (100 µL) were analyzed in triplicate. Initially, acetone (400 µL) was added to precipitate the proteins. The contents were allowed to stand for 5 minutes at room temperature. The sample was vortexed briefly (<10 s), then cold centrifuged (8 ^{0}C) at 13,200 rpm (16,200 × g) for 10 minutes. An aliquot (300 µL) of the supernatant was transferred into a 4-mL glass screw-top vial, and nitrogen dried for 10 min at room temperature. The dried samples were then reconstituted with 200 µL of 1 mM aqueous ammonium formate, and mixed thoroughly, filtered with a 0.22-µm tetrafluoropolyethylene membrane syringe filter, and analyzed using HPLC-MS-MS.

3.2.5. HPLC-MS-MS Analysis

HPLC tandem mass spectrometry (HPLC-MS-MS) was conducted on a Shimadzu HPLC (LC-20AD, Shimadzu Corp., Kyoto, Japan) coupled to an AB Sciex Q-Trap 5500

MS. The chromatographic separation was achieved using an Agilent Poroshell 120 C18 (150 × 3.0 mm, 2.7 μm) column. The chromatographic separation was carried out with mobile phase components of aqueous 1 mM ammonium formate as solvent A and 1 mM ammonium formate in methanol as solvent B. The sample was stored in a cooled autosampler (15 ^{o}C) and 10 μL was injected. Separation was achieved using gradient elution at a flow rate of 0.35 mL/min with 20% B held constant for 2 minutes, increased linearly to 100% over 2 minutes, held constant for 2 minutes, decreased to 20% B over 2 minutes, and held constant for 2 minutes to equilibrate between injections.

ATOEA and PGA were detected using positive polarity electron spray ionization (ESI)-MS-MS. Standard solutions of ATOEA, ATOEA-$^{13}C^{15}N$, and PGA were directly infused (10 μL/min) to determine optimum MRM transitions. After infusion of ATOEA, ATOEA-$^{13}C^{15}N$ and PGA standard solutions into the ESI, molecular ions of m/z 204 ($[M+1]^+$), m/z 206 ($[M+1]^+$), and m/z 130 ($[M+1]^+$) respectively, were identified. The most abundant product ions of ATOEA, ATOEA-$^{13}C^{15}N$, and PGA are listed in Table 3.1. Nitrogen gas (50 psi) was used as the curtain and nebulization gas. The ion spray voltage and temperature source were 4,500 V and 500 °C with both nebulizer (GS1) and heater (GS2) gas pressures at 90 psi. The collision cell was operated with an entrance potential of 10.0 V and a collision potential of 11.0 V at a medium collision gas flow rate. The total mass spectrometry acquisition time was 5 min. ATOEA, ATOEA-$^{13}C^{15}N$, and PGA were analyzed in multiple reaction monitoring (MRM) mode via the parameters outlined in Table 3.1.

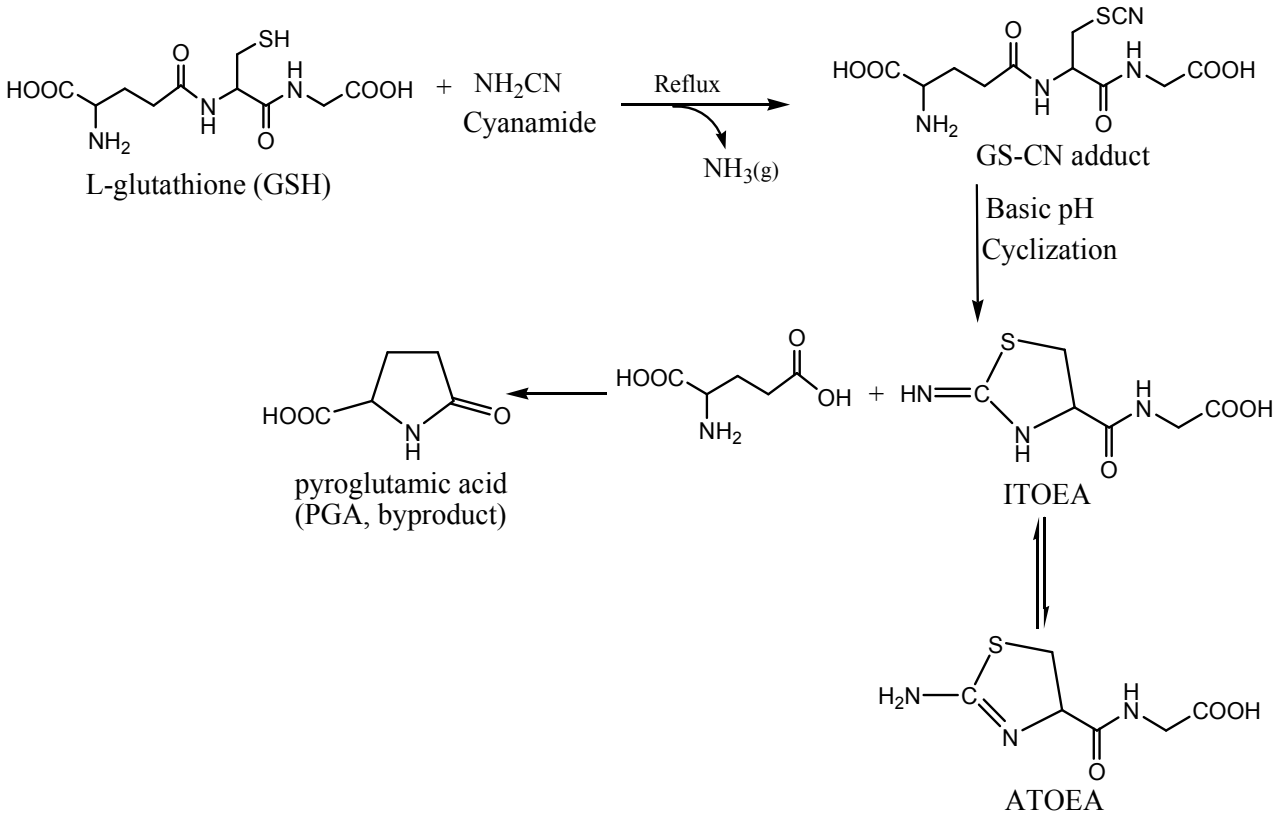

Figure 3.2. Proposed scheme for the synthesis of ATOEA (with pyroglutamic acid as a byproduct) from the reaction of GSH with NH_2CN. GSH is proposed to react with NH_2CN to form a GS-CN[116, 159] adduct which likely cyclizes to form ITOEA and glutamic acid.[116, 160] ITOEA then interconverts to form ATOEA.[60] Glutamic acid then cyclizes to produce pyroglutamic acid (PGA).[160, 161]

3.2.6. Calibration, quantification, and limit of detection

The validation of the analytical method was achieved by generally following the FDA bioanalytical method validation guidelines.[126, 130] The lower limit of quantification (LLOQ) and upper limit of quantification (ULOQ) were defined as satisfying the inclusion criteria of <15% relative standard deviation (RSD, as a measure of precision), and a percent deviation within ±20% back-calculated from the nominal concentration (as a measure of accuracy) for all calibration standards within the linear

range. The limit of detection (LOD) was determined by analyzing multiple concentrations of ATOEA below the LLOQ and determining the lowest concentration which reproducibly produced a signal-to-noise ratio of at least 3. The percent residual accuracy (PRA) was used to determine the goodness-of-fit of the calibration curves (i.e., PRA values ≥ 90% are indicative of a good fit).[128]

From the ATOEA stock solution, calibration standards for ATOEA (0.2, 0.5, 1, 3, 5, 10, 20, 35, 50, 100, 200 and 300 μM) were prepared in rabbit plasma. Following analysis of the calibration standards, calibration curves were plotted using the peak area of the analyte (ATOEA) as a function of the ATOEA concentration in plasma. Both weighted ($1/x$ and $1/x^2$) and unweighted calibration curves were created using linear least squares. A weighted $1/x^2$ fit was chosen as the best model to fit the calibration data.

QC standards ($N = 5$) were prepared in rabbit plasma at three different concentrations: 0.75 (low QC), 4 (medium QC), and 30 μM (high QC) for ATOEA. The QC standards were analyzed in quintuplicate each day for 3 days and were run in parallel with the calibration standards. *Intraassay* precision and accuracy were calculated from each day's analysis, and *interassay* precision and accuracy were calculated from comparison of the data gathered over three separate days.

3.2.7. Recovery, matrix effect and stability

The recovery of ATOEA was determined by the analysis of five QC replicates (low, medium and high concentrations) prepared in aqueous solution compared with equivalent QCs in plasma. Recovery (i.e., signal recovery) was determined as a percentage by dividing the analyte signal peak area from spiked plasma by the peak area of the equivalent aqueous QC standard. Calibration curve equations for calibrators prepared in DI water and plasma

were compared to evaluate matrix effects. A slope ratio (plasma slope/aqueous slope) from the calibration curves <1 indicates suppression effect, whereas slope ratio >1 indicates an enhancement effect.

The stability of ATOEA in plasma was evaluated by analyzing low and high QCs stored at various temperatures at multiple storage times. The stability (i.e., signal stability) of ATOEA was calculated as a percentage of the initial signal, with ATOEA considered stable at a particular temperature if the signal was within 15% of the initial signal. Short-term stability was assessed in the autosampler for 24-hrs, on the bench top (at room temperature) for 24 hr, and over multiple (3) freeze-thaw cycles. Long-term stability experiments were conducted under various storage conditions (-80, -20, and 4 ^{0}C) for 0, 2, 4, 6 10, 20, and 30 days.

3.2.8. Toxicokinetic Analysis

The toxicokinetic behavior of ATOEA after intravenous administration of CN at different time points was modeled with a two-compartment model.[162] The maximum concentration (C_{max}) of ATOEA in plasma, time taken to reach maximum concentration (T_{max}), distribution constants (K_{dis}), elimination constants (K_{el}), distribution half-life ($t_{1/2,dis}$) and elimination half-life ($t_{1/2,el}$) were obtained from the concentration-time curve. Area under curve (AUC) after apnea was also obtained from the concentration-time curve using trapezoidal rule. The correlation between the concentrations of ATOEA and ATOEA-$^{13}C^{15}N$ after intravenous administration of CN and $^{13}C^{15}N$ (1:1) was determined by student t-test

3.3. Results and Discussion

3.3.1. Mechanism of glutathione-cyanide interaction

Previous studies on the cyanylation of sulfhydryl groups of peptides and proteins have demonstrated that CN reacts with thiol of the cysteine residue in a peptide/protein to form a covalently bonded peptide/protein-CN adduct at pH values slightly above neutral.[116, 159, 160] In 1974, Dagani[160] demonstrated that at pH 8-10, the adduct cyclizes at the N-terminus of the cysteine residue, which then cleaves to form a 2-iminothiazolidine derivative. In this study we modelled the interaction of CN with sulfhydryl groups of peptides/proteins[116, 159, 160] using glutathione (GSH) as the peptide. Figure 3.1 shows the proposed reaction scheme for the reaction of GSH with NH_2CN. In summary, the thiol group of GSH is proposed to react with the CN of NH_2-CN to form a glutathione-CN adduct (GS-CN),[116, 159] releasing ammonia gas (NH_3) in the process.[60] This reaction is supported by a number of studies.[60, 116, 159, 160] As the reaction proceeds, more NH_3 gas is released into the reaction contents, increasing their basicity (pH=11).[60] Subsequently, the NH_3 gas escapes the reaction contents and the pH of the contents decrease.[60] Once the pH of the reaction contents decreases to between 8-10, the GS-CN adduct likely undergoes intramolecular cyclization between the N-terminus of the cysteine residue and the C≡N bond,[160] which cleaves the glutamate-cysteine peptide bond to produce 2-iminothiazolidine (i.e., ITOEA, which tautomerizes to 2-aminothiazoline derivative (ATOEA))[60, 116, 160] similar to ATCA.[159] The cyclization also produces glutamic acid,[159] which cyclizes to produce pyroglutamic acid (PGA) as a byproduct.[161]

3.3.2. ATOEA and PGA as biomarkers

To confirm the formation of ATOEA from CN exposure, analytical methods were developed to quantify pyroglutamic acid and ATOEA in plasma of cyanide-exposed rabbit. The mass spectra of ATOEA and ATOEA-$^{13}C^{15}N$ are shown in Figure 3.2. Figure 3.2a shows the mass spectrum of ATOEA produced by ESI(+)-MS with the molecular ion structure ($(M+H)^+$, m/z = 204) inset. The mass spectrum of ATOEA-$^{13}C^{15}N$ ($(M+H)^+$, m/z = 206) with its abundant ions identified as produced by ESI(+)-MS is shown Figure 3.2b. For ATOEA, transitions 204→101 and 204→158 were used for quantification and identification, respectively. The quantification and identification transitions for ATOEA-$^{13}C^{15}N$ were 206→103 and 206→160, respectively. The optimized MS-MS parameters for the detection of both ATOEA, ATOEA-$^{13}C^{15}N$ and PGA are shown in Table 3.1.

Figure 3.0 shows the HPLC-MS-MS chromatograms of ATOEA (Fig 3.3a) and PGA (Fig 3.3b) analyzed from spiked rabbit plasma, and plasma from pre- and post-cyanide exposed rabbits. The representative HPLC-MS-MS chromatograms of the MRM transitions of ATOEA analyzed from spiked water are also depicted in Figure 3.3c. The ATOEA eluted at approximately 3.1 min with only small endogenous ATOEA signal visible in the pre-exposed samples. PGA eluted at approximately 2.4 min with large endogenous concentrations of PGA in pre-CN exposed samples. Therefore, although we were able to consistently verify increasing concentrations of PGA following CN exposure, the relatively large endogenous concentration of PGA in non-exposed animals limits the usefulness of PGA as cyanide biomarker. Therefore, ATOEA was the focus of the rest of the study. Although ATOEA was the focus of the study, the increase in both ATOEA and

PGA in the plasma of CN-exposed animals supports the reaction scheme shown in Figure 3.1 as the biological process responsible for the production of ATOEA.

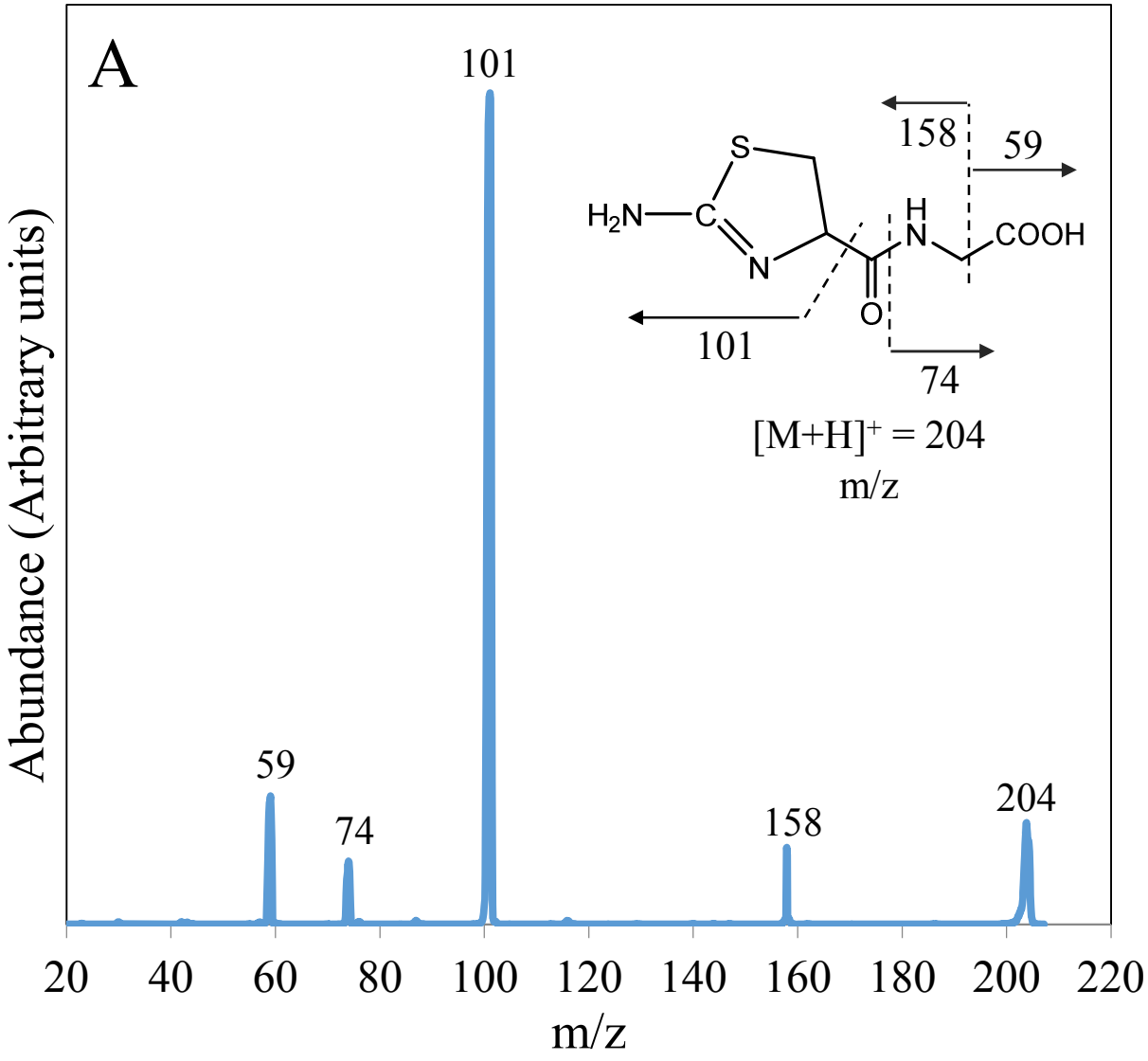

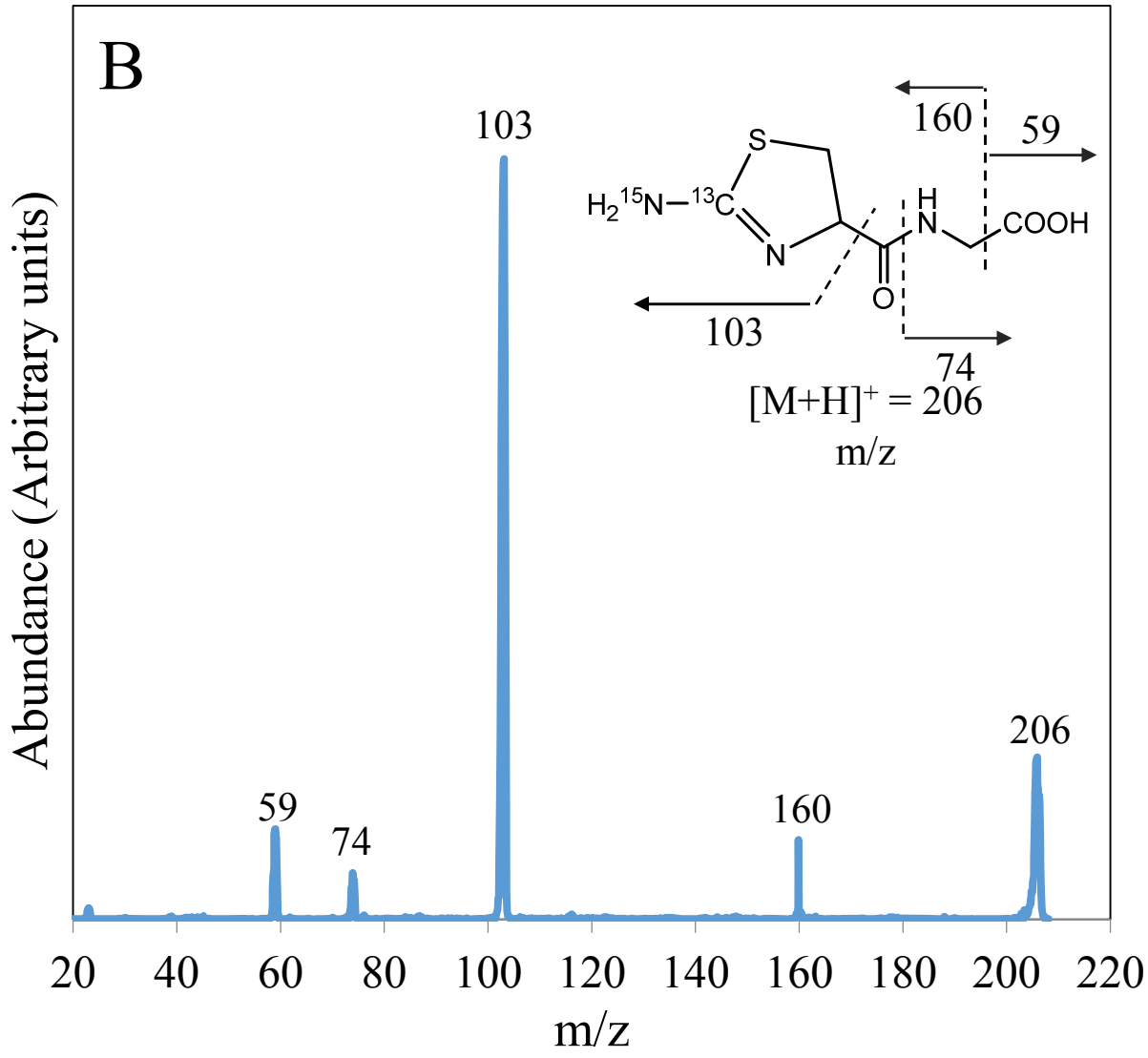

Figure 3.3. ESI(+) mass spectra of ATOEA (A), and ATOEA-$^{13}C^{15}N$ (B) with identification of the abundant ions. Insets: Structures of ATOEA (A), and ATOEA-$^{13}C^{15}N$ (B) with abundant fragments indicated.

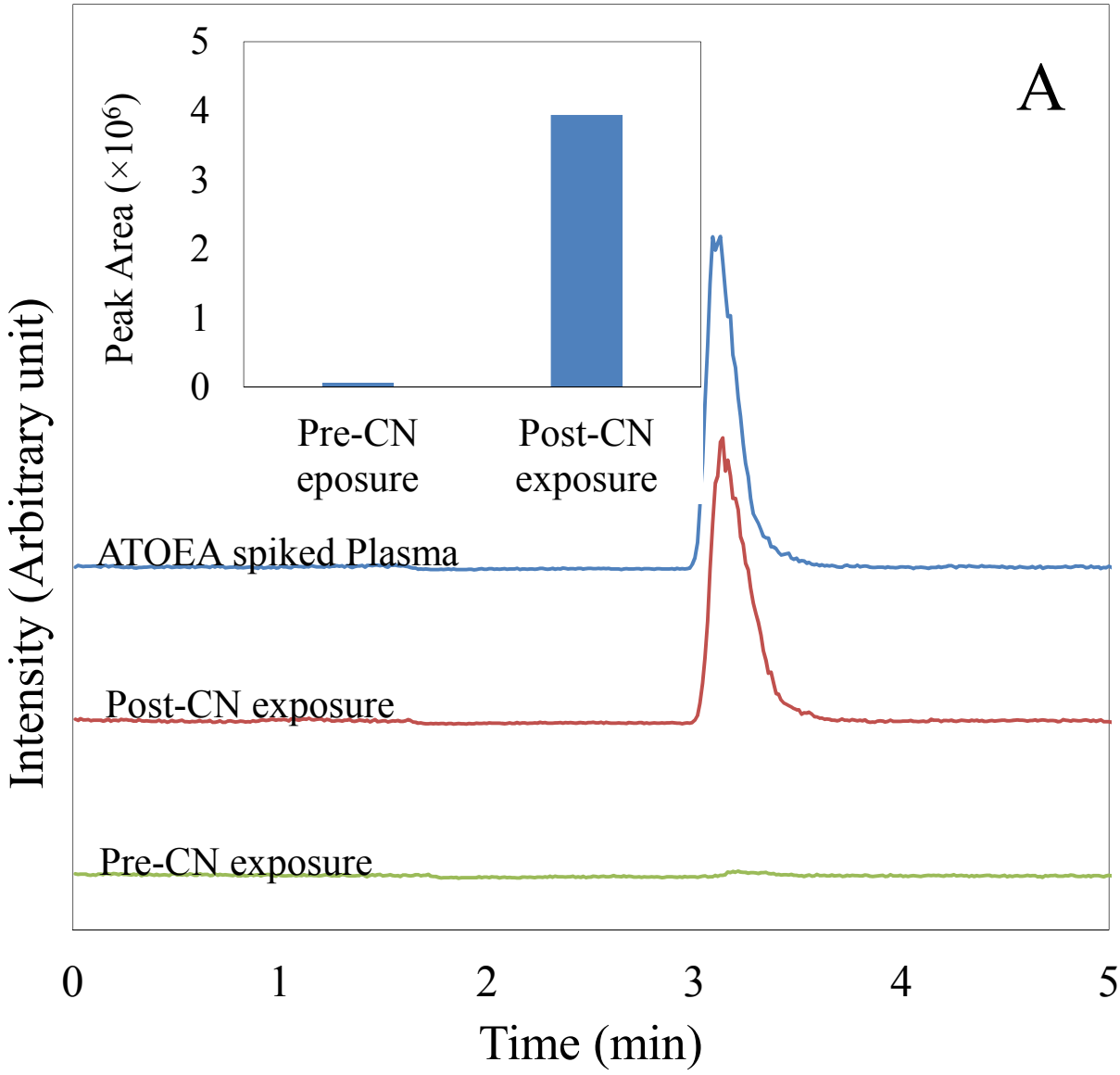
A
Peak Area (×10^6)
5
4
3
2
1
0
Pre-CN eposure
Post-CN exposure
ATOEA spiked Plasma
Post-CN exposure
Pre-CN exposure
Intensity (Arbitrary unit)
0
1
2
3
4
5
Time (min)

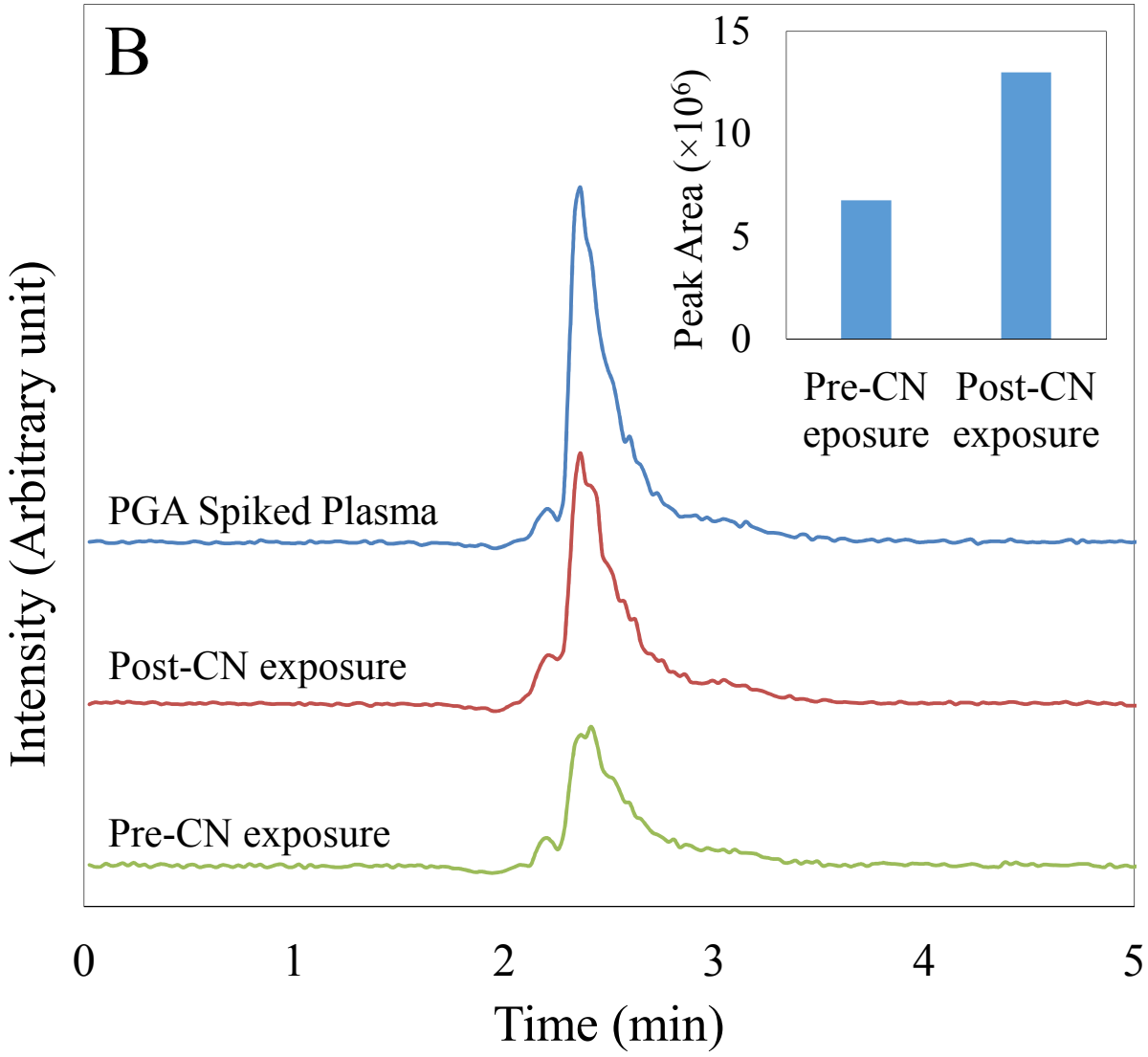
B
Peak Area (×10^6)
15
10
5
0
Pre-CN eposure
Post-CN exposure
PGA Spiked Plasma
Post-CN exposure
Pre-CN exposure
Intensity (Arbitrary unit)
0
1
2
3
4
5
Time (min)

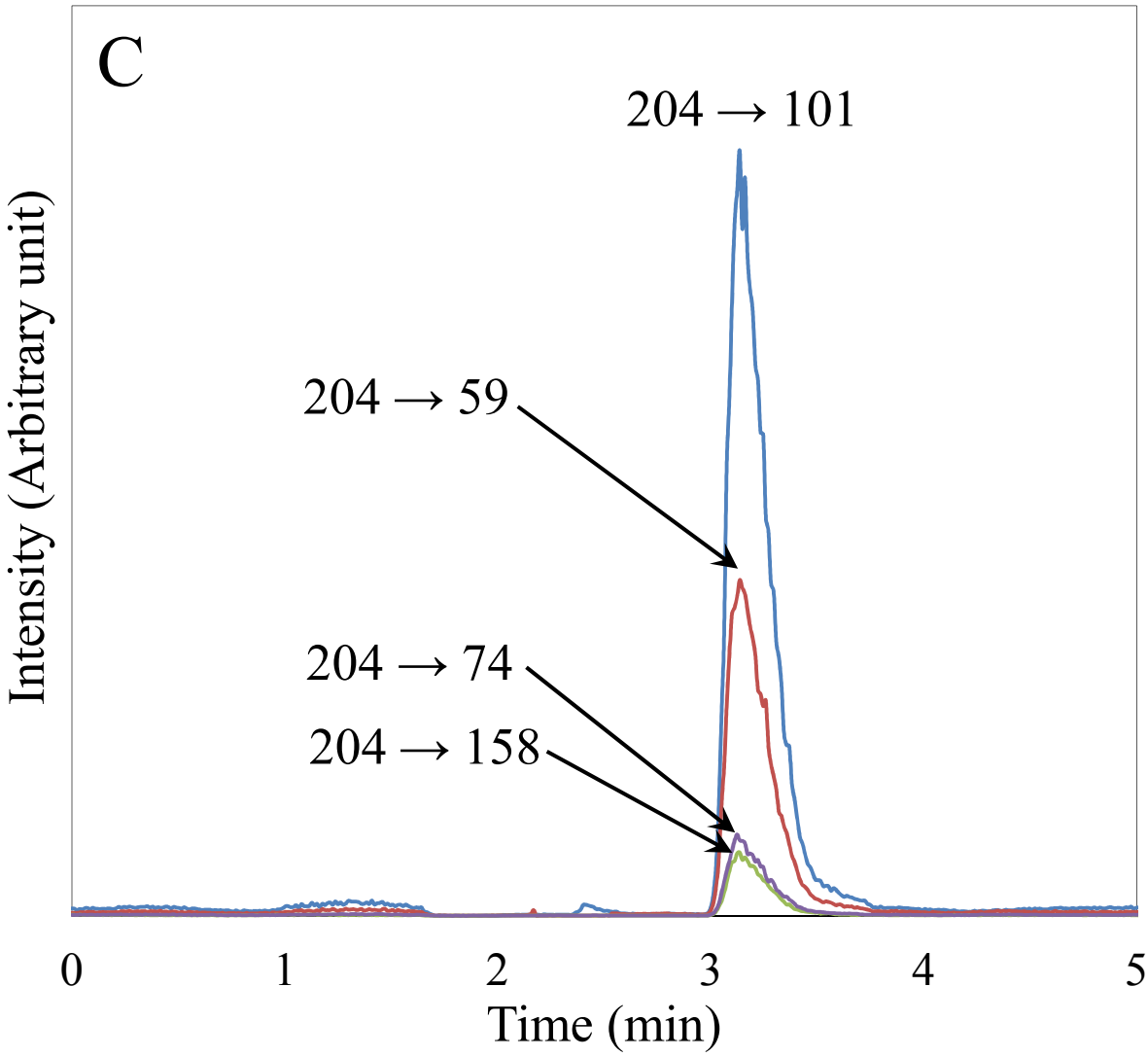

Figure 3.4. HPLC-MS-MS chromatograms of ATOEA (A), PGA (B) and ATOEA MRM transitions (C). A: ATOEA-spiked rabbit plasma and the plasma of a cyanide-exposed rabbit, pre-exposure, and post-exposure. B: PGA-spiked rabbit plasma and the plasma of a cyanide-exposed rabbit, pre-exposure, and post-exposure. C: Signal response to the MRM transition of ATOEA (10 µM) spiked aqueous standards (204→101, 204→59.0, 204→74.1, and 204→158.0). The chromatograms represent the signal response of the MRM transition 204.0→101, and 130.0→84 m/z for ATOEA (A) and PGA (A), respectively. Inserts: Peak areas of pre-CN exposure and post-CN exposure (25 min infusion) plasma sample for ATOEA (A) and PGA (B).

3.3.3. HPLC-MS-MS Analysis of ATOEA

The analytical method for ATOEA involved quick and simple sample preparation, consisting of protein precipitation, centrifugation, transfer of supernatant, drying, and reconstitution in aqueous ammonium formate, for HPLC-MS-MS analysis. Even with this simple sample preparation protocol an internal standard was not necessary to correct for matrix effects or incomplete recovery. The sample preparation time was approximately 20 min and the HPLC-MS-MS analysis time was 10 min. Despite the quick and simple sample preparation and analysis, the ATOEA was completely resolved from other components in the matrix and showed a sharp peak eluting at approximately 3.1 min, but considerable tailing (As= 2.31).

ATOEA calibration curves were constructed in rabbit plasma within the concentration range of 0.2-300 μM. The 0.2, 100, 200 and 300 μM calibrators fell outside the entire linear range based on the accuracy and precision criteria, producing a linear range of 0.5 to 50 μM, which was best described by a $1/x^2$ weighted linear regression. The percent residual accuracy (PRA) values of all the calibration curves analyzed were ≥ 95%, indicating excellent fit of the data over the entire linear range (i.e., PRA values ≥ 90% are indicative of a good fit).[128]

The accuracy and precision of the method were determined by quintuplicate analysis of three different QC standards (0.75, 4, and 30 μM) on three different days (Table 3.2). The precision of the method was excellent, with both the *intraassay* and *interassay* analysis producing percent relative standard deviation (%RSD) values of <6%. The accuracy for *intraassay* and *interassay* analyses was also excellent (100±8% of nominal

QC concentration). The LOD was 0.2 μM ATOEA in plasma as validated by analysis of multiple ATOEA-spiked samples over a 3-day period.

Table 3.2. The accuracy and precision of ATOEA analysis from spiked rabbit plasma by HPLC-MS-MS.

Conc (μM)	Intraassay		Interassay	
	Accuracy (%)[a]	Precision (%RSD)[a]	Accuracy (%)[b]	Precision (%RSD)[b]
0.75	100±2.4	4.19	100±7.8	5.63
4	100±7.6	3.75	100±5.0	3.71
30	100±7.4	4.08	100±6.9	3.49

[a]QC method validation ($N = 5$) for day 3

[b]Mean of three different days of QC method validation ($N = 15$)

The matrix effect was assessed by comparing the slopes of standard curves of ATOEA in aqueous calibrators (deionized (DI) water) and plasma. The slope of the aqueous curve was approximately 2 times the slope of plasma calibration curve. Therefore, a significant matrix effect exists for the analysis of ATOEA from plasma via the current method. Recovery for low, medium, and high QCs were 59%, 45%, and 55% respectively. Because the % recovery value is the combination of matrix effect and recovery, the recovery values can be attributed to the matrix effect suppression of the ATOEA signal instead of low recovery.

The long-term stability of ATOEA was evaluated for 30 days at -80, -20, and 4 ^{0}C. ATOEA was stable at -80 ^{0}C for 30 days, at -20 ^{0}C for 4 days, but degraded rapidly at 4

^{0}C (i.e., stable for only 2 days). For short-term stability, prepared samples of ATOEA were stable for at least 20 h on the autosampler but were only stable for 6 h on the bench-top, showing that ATOEA degraded relatively quickly in plasma at room temperature. Additionally, ATOEA was stable in plasma for 3 freeze-thaw cycles. From the results of the stability studies, we recommend that when storage is necessary, that plasma samples are stored at -80 ^{0}C and can be thawed and refrozen 3 times for analysis. If samples are to be analyzed within 4 days, they can be stored at -20 ^{0}C.

3.3.4. Toxicokinetics of ATOEA in rabbits following cyanide exposure

To definitively confirm the direct relationship between cyanide exposure and the production of ATOEA, rabbits were exposed to a 1:1 mixture of labeled ($^{13}C^{15}N^{-}$) and unlabeled (CN^{-}) cyanide. The concentrations of ATOEA and ATOEA-$^{13}C^{15}N$ in plasma of cyanide-exposed rabbits mirror each other, as shown in Figure 3.4. ATOEA was below the LOD in pre-exposed rabbit plasma. The concentration of both ATOEA and ATOEA-$^{13}C^{15}N$ increased rapidly during the infusion of CN^{-} and $^{13}C^{15}N^{-}$, and then decreased quickly after apnea (at C_{max}) following stopping CN administration and the administration of antidote. The decrease of ATOEA concentration when the cyanide infusion was stopped (after apnea), and after glyoxylate was administered may be due the ability of carbonyl group of glyoxylate to bind with free cyanide to form cyanohydrin or the rapid distribution and elimination of CN.[163] There was excellent agreement ($R^2 = 0.9924$, $p < 0.05$) between the concentrations of ATOEA and ATOEA-$^{13}C^{15}N$ from plasma of cyanide exposed rabbits.

The identification of ATOEA-$^{13}C^{15}N$ in rabbit plasma after $^{13}C^{15}N$ was the administered, confirms that ATOEA is produced during the metabolism of CN. The

percentage of cyanide converted to ATOEA was estimated at about 1.25-4.10%. This estimation was based on the measured ATOEA and cyanide concentration after factoring in the estimated percentage of cyanide that detoxified to ATCA and thiocyanate as reported by Bhandari et al,[89] and the percent distribution of cyanide between plasma and RBCs (i.e., 70-96% of the blood cyanide is found in RBCs).[106]

Table 3.3. Toxicokinetic parameters of ATOEA in rabbits following intravenous infusion of CN. These parameters are likely a combination of ATOEA elimination and sequestration of CN by glyoxylate.

C_{max} (µM)	$t_{1/2dis}$ (min)	$t_{1/2el}$ (min)	K_{dis}	K_{el}	AUC (µM*min)
3.79	14.87	92.20	0.0466	0.0075	55.60

Table 3.3 shows the toxicokinetic parameters for ATOEA. The formation of ATOEA in rabbits was rapid and it mirrored the cyanide dose. Once the cyanide infusion was stopped, the ATOEA was distributed and eliminated. A two-compartment model best described the toxicokinetic behavior of ATOEA, with a calculated elimination half-life ($t_{1/2,el}$) of 92.2 min ($K_{el} = 7.5 \times 10^{-3}$ min^{-1}).

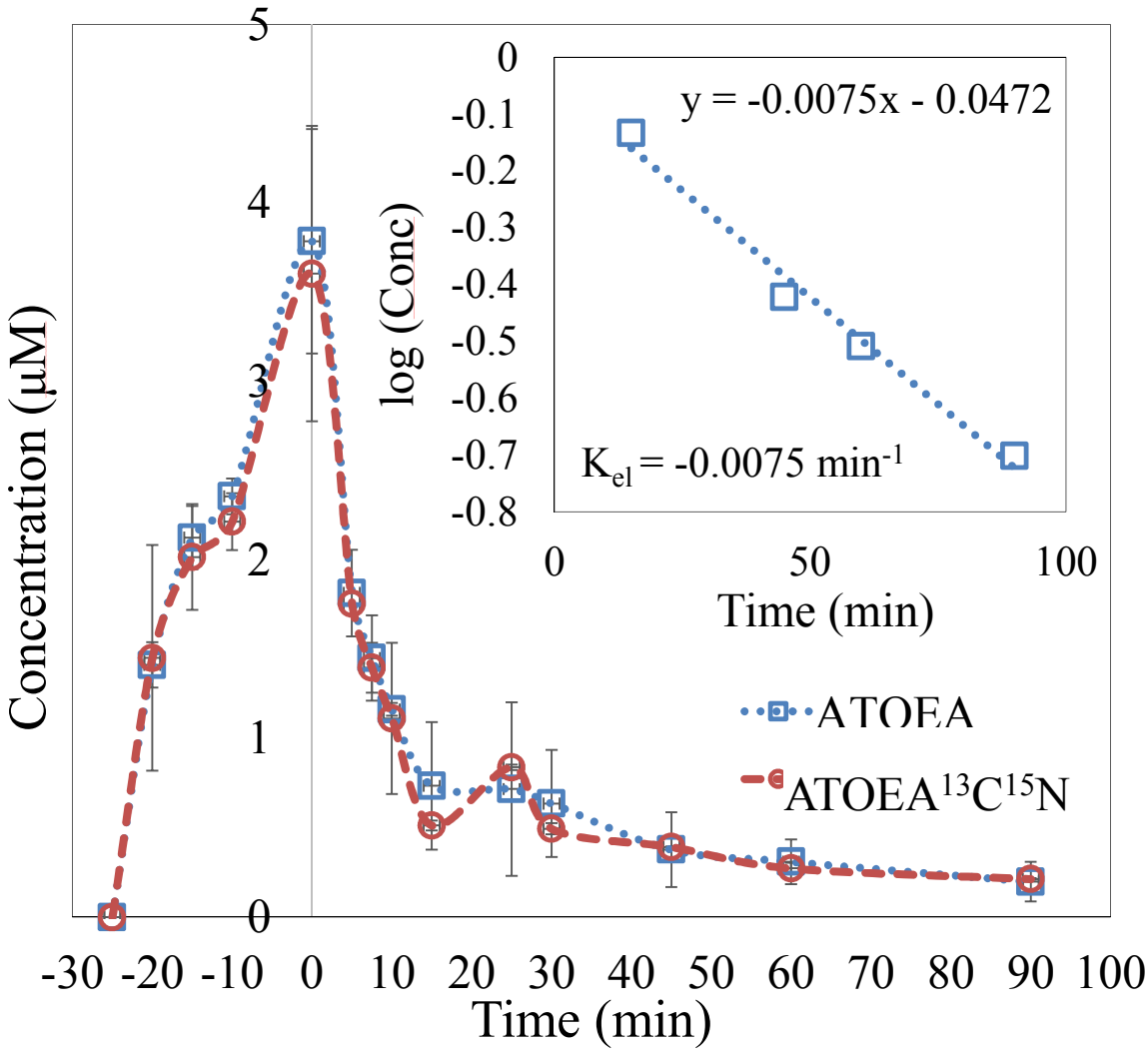

Figure 3.5. Plasma concentrations of ATOEA and ATOEA-$^{13}C^{15}N$ following exposure of rabbits to equal amounts of CN^- and $^{13}C^{15}N$. Pre-exposure, 15 min, 25 min, and 35 min, following cyanide exposure are designated as time -25, -20, -15, and -10 respectively. Apnea is represented by time zero. Error bars represent standard error of the mean (SEM). Inset: Representation of elimination constant (K_{el}) of ATOEA by log concentration-time graph.

3.3.5. ATOEA as a biomarker of cyanide exposure

ATOEA may be a better long-term biomarker for cyanide exposure than cyanide itself because of its slower elimination half-life ($t_{1/2,el}$), and large area under the curve (55.6 µM*min). The low concentrations of ATOEA in pre-exposure plasma samples, and the

early detection of ATOEA, within a few minutes of CN exposure, suggest that ATOEA can also be used as a diagnostic biomarker for both acute and high-dose CN poisoning. Although ATOEA has many advantages as a marker of cyanide poisoning, its limitation is its poor stability in plasma at temperatures above -80 ^{0}C. Future work should identify the degradation product of ATOEA in biological samples and the stability of this product.

3.4. Conclusions

A novel cyanide metabolite, ATOEA was found based on the interaction of glutathione and cyanide. A rapid and simple HPLC-MS-MS with excellent accuracy and precision was successfully developed to quantify ATOEA in plasma and applied to analyze plasma of rabbits exposed to cyanide. The toxicokinetics of ATOEA from rabbits exposed to cyanide confirms that it is a promising biomarker that can serve as both a diagnostic and potentially forensic biomarker for cyanide exposure.

Acknowledgement

The research described was supported by interagency agreements (AOD16026-001-00000/A120-B.P2016-01 and AOD18015-001-00000/MRICD-IAA-18-0129-00) between the NIH Office of the Director (OD) and the U.S. Army Medical Research Institute of Chemical Defense under the oversight of the Chemical Countermeasures Research Program (CCRP) within the Office of Biodefense Research (OBRS) at the National Institute of Allergy and Infectious Diseases (NIAID/NIH). Any opinions, findings and conclusions or recommendations expressed in this material are solely those of the authors and do not necessarily represent the official views of the CCRP, NIAID, NIH, HHS, USAMRAA, USAMRICD or DoD.

.

Chapter 4. Verification of Cyanide-Poisoned Fish By Field Portable Detection of The Cyanide Metabolite, Thiocyanate From Fish Blood

4.1. Introduction

Since the 1930s, live reef fish have been legally harvested for the marine aquarium trade (MAT) and live reef fish for food trade (LRFFT) industries.[69] The demand for live reef fish in these industries increased in the middle of the 20th century, resulting in the integration of illegal methods, such as cyanide fishing, to meet this demand.[164] The use of cyanide fishing first originated in the Philippines in the early 1960s,[69, 70] and the practice has spread throughout many regions including China, Indonesia, Malaysia, the Maldives, Papua New Guinea, Sri Lanka, Thailand and Vietnam.[71-74] Cyanide fishing involves the use of cyanide (abbreviated as CN, representing both hydrogen cyanide and cyanide ion) to stun and disorient valuable fish hiding in coral reefs, making them easier to collect. Cyanide fishing is accomplished via two main techniques: 1) the manual spraying of a saturated solution of CN salt from a squirt bottle at a fish hiding in a coral reef, and 2) pumping large volumes (about 200 L) of saturated CN solution from a fishing boat into a coral reef area and collecting stunned fish by hand netting.[76, 165, 166] Because CN fishing is much more immediately profitable compared to legal fishing methods (2.5-10 times),[67, 68, 167] it has become so popular that an estimated 150-640 metric tons of CN are used for CN-fishing annually.[75] Although it is more profitable in the near term, it is a major threat to the health of coral reefs, marine life which depend on these reefs, the coastal and ocean environments, and the future fishing industry in the West Pacific Ocean.[168]

CN has many deleterious effects on the marine ecosystem and the fish trade. Firstly, CN can damage targeted fish, which can ultimately result in death.[72] Studies have shown

that 5-75% of the targeted fish collected by CN for aquarium trade die a few hours post-harvest, with more than 90% mortality rate recorded from collection to consumer.[72, 80] Additionally, many targeted species, such *Cheilinus undulates*, are on the verge of extinction as result of the effectiveness of CN fishing.[78, 79] CN fishing also affects non-targeted species.[81] One of the most concerning effects of CN-fishing is its impact on coral reefs. CN interrupts coral-algal symbiosis, a process that provides nutrients to the coral, resulting in a process called "bleaching," where colored coral becomes white and pale.[82, 169, 170]

The damage to marine ecosystems produced by CN fishing has led to about 80% of fish exporting countries banning the practice.[74, 171] Although CN fishing is banned in most exporting countries, the technique is still commonly practiced[67, 68] because enforcement of anti-CN fishing laws is difficult, partially due to the lack of a reliable test to determine if fish were CN caught.[172] The availability of a reliable testing technology to detect CN exposure post-harvest would not only help in the enforcement of the anti-cyanide fishing laws by government authorities, but may also allow testing by wholesalers and retailers.[172, 173]

While the direct analysis of CN from biological fluids can be used to confirm CN exposure immediately following an exposure event, it is increasingly unreliable as the time post-exposure increases.[111] This is because CN is reactive and volatile, leading to a very short half-life in most animals (e.g., 0.34–1.00 hr in humans; see Table 1) and instability in biological matrices.[55, 60, 137] Therefore, indirect analysis of stable markers of CN has been proposed as a means to confirm CN exposure, especially at times greater than a few hours post-exposure. Thiocyanate (SCN^-; represented as SCN herein) is the major

metabolite of CN, accounting for about 80% of the total CN metabolism.[55, 89, 137] SCN is a longer-lived marker of CN exposure (Table 1), with half-lives ranging from 4.95-192 hr in mammals and 2.4-144 hr in fish.[55, 107, 113, 174] The main drawback of using SCN as a marker for CN exposure in most animals is that SCN is consumed or produced via diet. This leads to large and highly variable background concentrations of SCN in mammalian blood (474-32900 μg/L) resulting from sources other than CN exposure (Table 1). Therefore, the use of SCN to confirm CN exposure in mammals is highly questionable.[55, 136] Similarly, while data is limited and inconsistent, previous studies have suggested that some freshwater fish have high levels of SCN in their blood (not detected-5100 μg/L) from sources other than CN exposure.[175-178] Conversely, marine fish have much lower endogenous SCN concentrations (<50 μg/L) than mammals, likely because they have diets low in SCN-containing and SCN-producing foods.[174, 179] Therefore, acute CN exposure should lead to highly elevated SCN concentrations in fish. Additionally, since SCN has a long half-life relative to CN in both fish and mammals, elevated levels of SCN should persist for relatively long periods of time following CN exposure.[178, 180, 181] Breen et al. (2019) demonstrated both greatly elevated SCN levels following CN exposure and long-lived elevation of SCN concentrations (i.e., 41 days post-exposure) in CN-exposed fish.[179] A recent study also reported high elevation of SCN concentration in blood plasma of marine fish following CN.[174] Therefore, the properties of SCN in fish appear to be ideal for the use of SCN as a promising marker for determination of CN-caught fish.[178]

In recent years, researchers have proposed two potential matrices for the analysis of SCN to determine CN-caught fish: holding seawater or blood.[178-180, 182, 183]

Holding seawater is fresh seawater to which CN-caught fish are transferred in order to revive the fish and hold them for transport. It is suggested that SCN is excreted in the urine of CN-caught fish into the holding seawater. In fact, analysis of excreted SCN in seawater to confirm CN-fishing has been previously reported,[180, 181, 184] but several attempts to replicate these findings by other scientist have failed.[185, 186] Bonanno et al. (2020) reported that marine fish (*A. clarkii*) do not excrete SCN after CN exposure and can absorb low concentrations of SCN from water refuting these studies.[174] Although this approach has advantages of being non-invasive, non-destructive, and easy,[180] this approach has not be reproducibly verified. Moreover, fishers could easily replace or adulterate the holding seawater (e.g., by using masking agents) to avoid being caught by authorities. The analysis of SCN from fish blood is very difficult to adulterate and long-term elevation of SCN in fish blood following CN exposure has been shown.[179] While both the analysis of holding seawater and blood have advantages, blood SCN is the most definitive way to monitor CN-fishing.

Scientists have developed and suggested multiple analytical SCN testing methods to monitor CN fishing.[71, 180, 181] In the late 1990s, Barber and Pratt developed an ion selective electrode technique to monitor CN-fishing, but the method produced low sensitivity, accuracy, and recovery.[71, 182, 187] More recently, Vaz et al. (2012 and 2017) reported two analytical techniques (i.e., HPLC-optic fiber and HPLC-UV) to analyzed SCN from sea water, with the purpose of detecting SCN excreted from CN-caught fish into the sea water used to hold fish.[180, 181] Though the Vas et al. methods feature rapid sample preparation and are non-invasive, they require sophisticated instrumentation, are not portable, and the results were not reproducible.[185, 186] Breen et al.[185] also

used the Bhandari et al.[137] LC-MS/MS method for analysis of SCN from seawater to verify concentration found from the HPLC-UV technique. This method provided featured quick and easy sample preparation, very good accuracy, linearity, and sensitivity, but it required expensive and sophisticated instrumentation and was not rapid or field portable. Breen et al.[179] reported an HPLC-UV method to analyze SCN in fish plasma for toxicokinetic studies of SCN in CN-exposed fish. The method was featured excellent sensitivity and simple sample preparation, but required sophisticated instrumentation, somewhat difficult preparation of chromatographic media, utilized plasma as opposed to whole blood (i.e., creating the additional requirement of blood component separation, adding time and complexity to the analysis), and was not field-portable. While these methods proved useful for research studies, each has its drawbacks for monitoring CN-fishing, including the fact that none of the methods are truly rapid (i.e., as defined as sample preparation and analysis times of less than about 5 min), field-portable or simple, which may be essential for monitoring CN-fishing.[179-181, 184]

Recently, our lab developed and validated an automated field-portable fluorescence-based sensor for the analysis of CN in blood to confirm exposure.[7, 54, 188] The technology features a short analysis time (60 s), a small sample volume (25 μL), field portability (approximate dimensions of 24.2 × 16.7 × 10.8 cm (L × W × H) and a mass <0.1 kg), and user-friendly operation that does not require special expertise. The sensor was successfully used to analyze CN from the blood of CN-exposed mammals (i.e., rabbits (N = 205)). While the sensor was excellent for measuring CN, it was not designed to analyze SCN.

Considering the effect of CN-fishing on marine ecosystems and economies, there is a critical need to develop a reliable, field-portable, and easy to operate technology to confirm CN exposure in fish caught from countries where CN-fishing is practiced. Therefore, the objectives of this study were to extend the CN sensor technology developed in our lab for the analysis of blood SCN, to validate the analytical characteristics of the sensor, and to confirm its ability to accurately quantify elevated SCN levels from the blood of marine fish exposed to CN.

Table 4.1. Endogenous blood concentrations and half-lives of cyanide and thiocyanate from acute exposures of cyanide for multiple animal models. Adapted and updated from Logue et al.[55]

Animal	Marker of CN Exposure	Species	Half-life (hr)	Endogenous Concentration Range (µg/L)
Mammals	CN	Human	0.34-1.0[55, 189]	0.52-2.10[110, 191]
		Pig	0.54[190]	229.3[89, 192]
		Rat	0.64[190]	5.0-280[193]
		Goat	1.28[190]	ND
		Rabbit	2.95[89]	99.8-145.9[89, 192]
	SCN	Human	96-192[189]	1792-32944[55, 117, 194]
		Pig	4.95[190]	473.9-2384[89, 190, 195]
		Rat	5.8-50[89, 190]	1160-3074[190, 196]
		Goat	13.9[190]	ND
		Rabbit	ND	501[192]
Fish	SCN	Rainbow Trout[a]	48.5[178]	ND-5100[175-177][e]
		Salmon[b]	ND	58
		Clownfish[c]	144[178, 179]	<50[179][f]
		Clownfish[d]	2.4-28.8[174]	34[174]

ND = Not determined. [a]*Oncorhynchus mykiss*. [b]*Salmo salar,* Current study. [c]Clownfish (*A. ocellaris*). [d]Clownfish (*A. clarkii*). [e]Multiple Rainbow Trout studies were conducted with SCN not detected in two groups with N= 6 and 10, respectively, and mean concentrations of 360, 820, and 5100 ppb for groups of N= 9, 6, and 6, respectively. [f]Endogenous concentration was below the LOQ (50ppb) of the method.

4.2. Materials and Methods

4.2.1. Materials

All reagents and solvents were at least HPLC grade. Sodium cyanide (NaCN), sodium hydroxide (NaOH), sulfuric acid (H_2SO_4), ethanol, methanol, potassium dihydrogen phosphate (KH_2PO_4), and dibasic potassium phosphate (K_2HPO_4) were purchased from Fisher Scientific (Hanover Park, IL). Taurine (2-aminoethane sulfonic acid) and sodium metaboratetetrahydrate ($NaBO_2 \cdot 4H_2O$) were purchased from Alfa Aesar (Ward Hill, MA). Sodium thiocyanate (NaSCN) was obtained from Acros Organics (Morris Plains, NJ). Potassium permanganate ($KMnO_4$) was purchased from Science Company (Lakewood, CO) NDA (2,3-Naphthalene dialdehyde) was obtained from TCI America (Portland, OR). Tricaine methanesulfonate was obtained from Western Chemical Inc. (Ferndale, WA). Water was purified to 18.2 MΩ-cm by reverse osmosis using a Lab Pro polishing unit from Labconco (Kansas City, KS, USA).

A stock solution of NaOH (1 M) and phosphate/borate buffer (0.1 M:0.05 M; pH 8.5) were prepared in DI water. Stock solutions of NaCN (2 mM) and NaSCN (1 mM) were prepared in 10 mM NaOH. H_2SO_4 (2 M) was prepared as 50:50 v/v aqueous and ethanol. Taurine (0.1 M) solution was prepared in phosphate borate buffer. A stock solution of NDA (2 mM) was prepared in phosphate borate buffer and 40% methanol. A saturated solution of $KMnO_4$ was prepared in DI and its concentration (0.6 M) was determined by titrating it against 0.2 M oxalic acid.

Caution: CN is highly toxic to humans and animals. Therefore, CN solids and solutions must be handled with care. All CN solutions were handled in a hood and prepared as basic aqueous solutions (10 mM NaOH) to ensure CN remained as non-volatile CN^-.

4.2.2. Fish Blood for SCN Analysis

Salmon whole blood (EDTA anti-coagulant) used for analytical method development was purchased from EastCoast Bio (North Berwick, ME) and stored at -80 °C until used. Salmon whole blood was used instead of blood from a marine fish because we were unable to identify a source of large quantities of marine fish whole blood.

Fish blood from CN-exposed and control marine fish was obtained from Department of Chemistry and Physics, Roger Williams University, Bristol, RI, USA. Marine fish (5.1-21 g), *A. clarkii*, approximately 6-12 months of age, were split into three groups, each group having 10-12 fish. Each group was placed in a basket and immersed in a CN solution (at 50 ppm) or control for 45 s. After exposure, the fish were transferred into a seawater bath free of CN for rinsing. After rinsing, fish were housed in 20 L polycarbonate tanks containing CN-free filtered seawater with light aeration. After 72 hr, fish were removed from the holding tanks for blood collection. Firstly, fish were anesthetized with tricaine methanesulfonate at a concentration of 200 ppm, buffered 2:1 with sodium bicarbonate in seawater, and then dried and weighed. Upon severance of the caudal peduncle with a #21 surgical blade, blood was collected in 125 µL heparinized microcapillary blood collection tubes. Blood was similarly collected from a control group, which was not exposed to CN. Collected blood was placed in clean plastic centrifuge tubes, flash frozen, and shipped on dry ice (overnight) to South Dakota State University. Upon receipt, the blood was stored at -80 °C until analysis was performed.

The Roger Williams University Institute of Animal Use and Care Committee (Approval #R180820) approved all fish experiments. Fish were cultured in captivity at Roger Williams University or Sea & Reef Aquaculture, Franklin, ME, thereby ensuring

they were not collected with cyanide. For all experiments, the water temperature was maintained by housing fish in a temperature-controlled room or placing buckets containing fish in a warm water bath both held at 25 ^{o}C. All fish were fed pelletized food (Skretting Green Granule 1 mm) once per day unless otherwise noted. Water quality was maintained through daily water changes (100%) at a salinity of 30 with light aeration.

4.2.3. Sensor Analysis of SCN

The analysis of fish blood was performed using a previously developed sensor prototype (Figure 4.1) which consists of a self-contained sample preparation cartridge (Figures 4.1A and B) and a detection system (Figures 4.1C and D). The CN sensor chemistry was modified for the analysis of SCN by adding $KMnO_4$ to oxidize SCN to CN, with the resulting CN analyzed as described in Bortey-Sam et al.[188] Briefly, a saturated aqueous solution of $KMnO_4$ (80 µL of a 94 mg/mL solution) was added to the sample chamber of the cartridge (Figure 4.1A & 4.1B) and the water was completely dried. Fish whole blood (25 µL of non-spiked, SCN-spiked, or CN-spiked salmon blood or blood from CN-exposed or non-CN-exposed marine fish) was carefully added to the sample chamber, avoiding contact with the dried $KMnO_4$, water (80 µL) was then added to dissolve the $KMnO_4$. The cartridge was capped, placed into the fluorometric reader, and the analysis was started. H_2SO_4 (2 M, 200 µL) was automatically added to the sample chamber and 200 µL each of NDA, taurine, and base solutions were automatically added to the capture chamber. In the sample chamber, the $KMnO_4$ was dissolved via addition of the H_2SO_4 solution and SCN was oxidized into CN by $KMnO_4$. The CN was then liberated from the blood matrix in the sample chamber by acidification with H_2SO_4 to form HCN gas. Ambient air (approximately 200 mL/min for 34 s) was used as carrier gas to transfer the

HCN from the sample chamber into the capture chamber (Figure 4.1A), where it was captured by the NaOH solution, forming CN^-. Taurine and NDA reacted with the captured CN^- in a linear fashion to form a fluorescent β-isoindole product. Throughout this process, the capture solution was mixed by bubbling air via a specific protocol, aiding the β-isoindole formation. A high-powered LED was directed into the capture solution through a focusing lens to illuminate the mixture and the fluorescence of the β-isoindole product was measured at 400-650 nm (Figure 4.1D) to quantify the SCN concentration. Most of the steps described above are automated (i.e., initiated by the user by pushing a single button).

4.2.4. $KMnO_4$ Oxidation of SCN to CN

The ability of $KMnO_4$ to completely oxidize SCN to CN was evaluated by analyzing CN-spiked blood without $KMnO_4$ (5 μM, as a positive control), and the same concentration of SCN-spiked blood with $KMnO_4$ (as a sample) and without $KMnO_4$ (as a negative control). Non-spiked blood samples with $KMnO_4$ and without $KMnO_4$ oxidation were also analyzed as a sample blank and negative control blank, respectively. The blank subtracted average signals of the positive and negative control samples were compared to the blank subtracted average signal of SCN-spiked blood to evaluate the ability of $KMnO_4$ to oxidize the SCN to CN.

4.2.5. Analysis of Total CN

To evaluate if the sensor was measuring total CN (CN + SCN) in the blood matrix or SCN only, the same concentrations (1-10 μM, 58-580 μg/L) of CN and SCN were prepared separately in salmon blood. The sensor was used to analyze the concentrations of both CN and SCN in these samples. In addition, standards of both CN and SCN were

spiked in the same fish blood to create mixed standards of 1-10 µM (58-580 µg/L) each for CN and SCN (i.e., CN + SCN concentrations of 2-20 µM, 116-1160 µg/L). Blank signals were evaluated using non-spiked and $KMnO_4$ oxidized salmon blood. The blank-corrected sum of signals of the individually spiked CN and SCN samples was compared to the signal of the sample containing both CN and SCN.

4.2.6. Background Concentration of SCN in Salmon Blood

The background concentration of SCN in salmon blood was determined using standard addition. Briefly, different concentrations of SCN working standard were spiked into the same volume of salmon blood to produce final spiked concentrations of 0, 0.5, 1, 3, and 5 µM (0, 29, 58, 174, and 290 µg/L). These samples were analyzed in triplicate using the sensor and the mean signals were plotted as a function of the nominal spiked concentration to obtain a linear curve with a non-zero Y-intercept. The curve was extrapolated to the concentration axis (x-axis) to find the background concentration of SCN in salmon blood. This experiment was repeated 3 times and the mean background SCN concentration, along with its confidence level, was calculated. The confidence level was calculated at the 95% confidence interval. Enough marine fish blood could not be collected to perform the standard addition method.

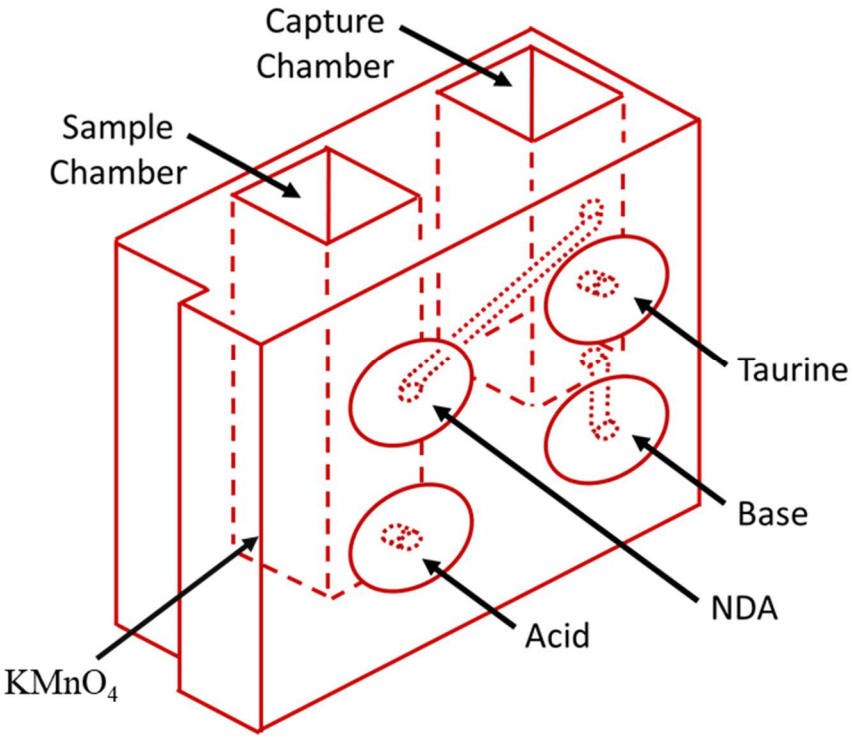

FIGURE 1A

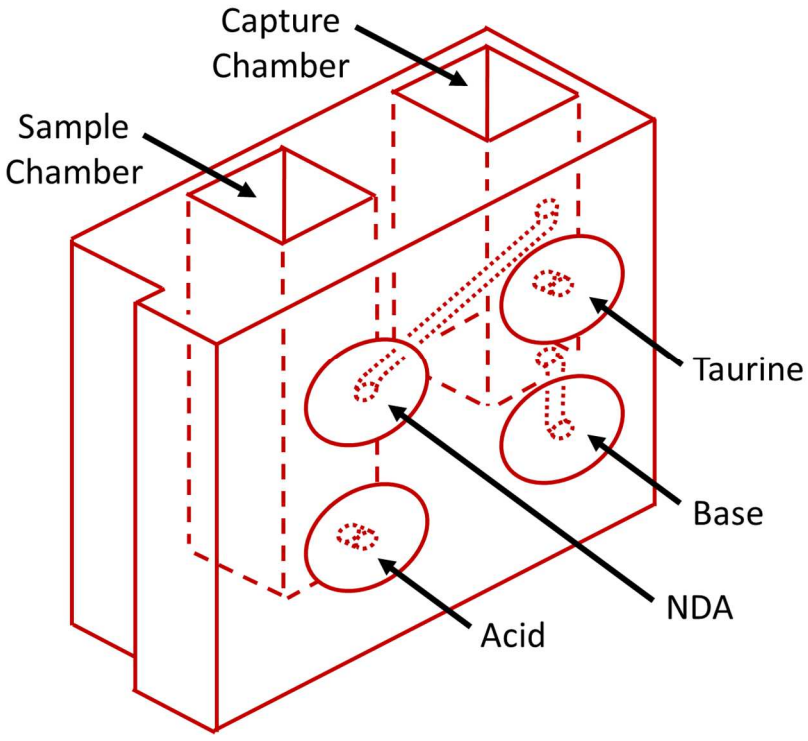

FIGURE 1B

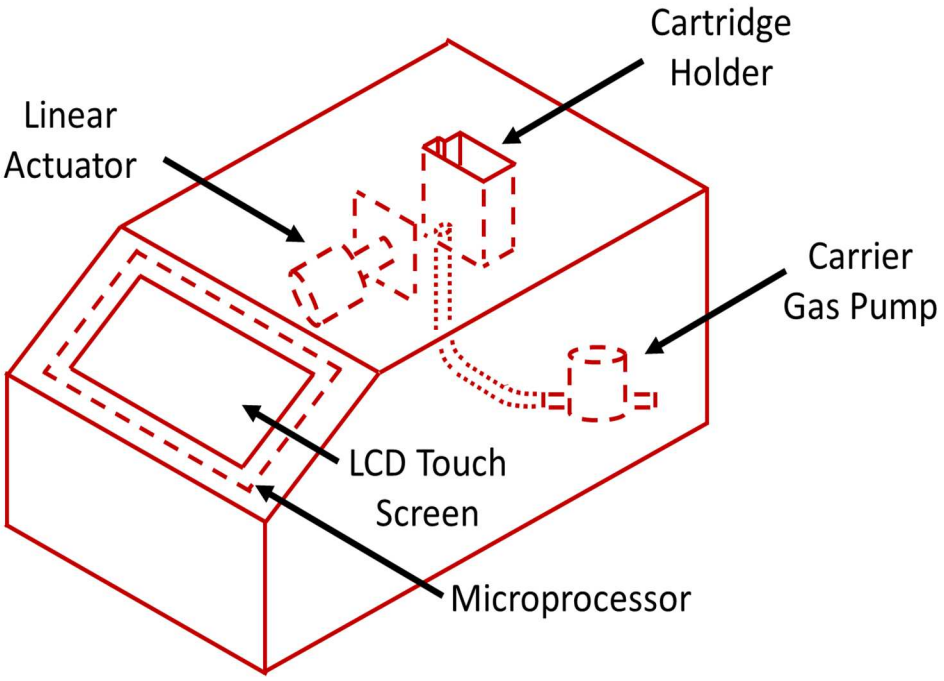
Cartridge
Holder
Linear
Actuator
Carrier
Gas Pump
LCD Touch
Screen
Microprocessor

FIGURE 1C

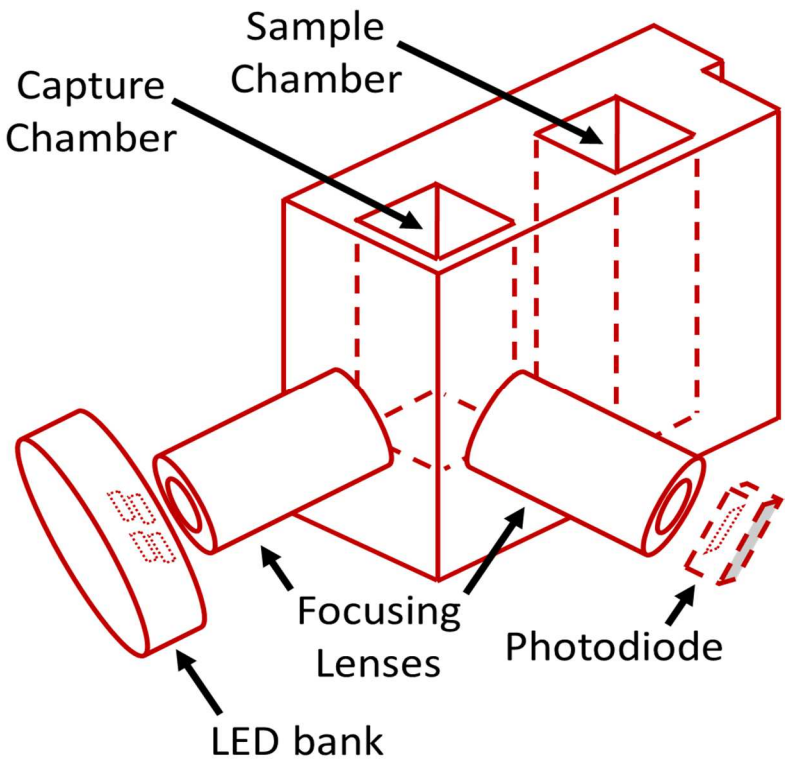

FIGURE 1D

Figure 4.1. Schematics of the sample preparation cartridge and fluorescence detection system for the analysis of SCN in fish blood adopted from Bortey-Sam et. al.[188] A) The sample preparation cartridge "front" view highlighting carrier gas channels, the sample chamber and the capture chamber. B) The sample preparation cartridge "back" view highlighting the reagent storage "bubbles," the reagent flow channels, the sample chamber and the capture chamber. C) The fluorescence detection system highlighting the sample preparation cartridge holder, the carrier gas pump, the linear actuator for depression of the reagent bubbles, the touch screen, and the microprocessor. D) The sample preparation cartridge showing the position of the optical components for fluorometric analysis of the CN-NDA-taurine complex.

4.2.7. Analytical Method Development and Validation

The analytical method for the analysis of SCN in salmon blood via the sensor was validated following the FDA bioanalytical method validation guidelines.[126] From the SCN stock solution, a working standard of SCN was prepared from dilution with salmon blood. From the working standard, calibration standards of SCN, blank, 0.3, 0.5, 1, 3, 5, 8, 10, and 20 μM (blank, 17.4, 29, 58, 174, 290, 464, 580, and 1160 μg/L) were prepared via dilution with fish blood and analyzed in triplicate by the sensor. Following analysis, the average signals measured by the sensor were plotted as a function of the concentration of SCN spiked in blood to obtain the linearity, accuracy, and precision of the calibration standards. Calibration curves were created using non-weighted linear least squares to obtain the equation of the line. The lower limit of quantification (LLOQ) and upper limit of quantification (ULOQ) were defined as satisfying the inclusion criteria of a precision of ≤20% relative standard deviation (RSD), and accuracy of a percent deviation within ±20% of the nominal concentration for all calibration standards within the linear range. The goodness-of-fit of the calibration curves was determined using both Percent Residual Accuracy (PRA)[128] and the coefficient of determination (R^2). The limit of detection (LOD) was defined as the lowest concentration of SCN that produced a signal equal to the summation of the mean blank signal and 3 times the standard deviation of the blank.

The accuracy and precision of the method were determined by analyzing three QC standard concentrations of SCN prepared in fish blood with concentrations of 2 μM (116 μg/L, low QC), 4 μM (232 μg/L, medium QC), and 7 μM (406 μg/L, high QC). All the QCs were within the calibration range but not included in the calibration curve and analyzed in quintuplicate each day for 3 days. *Intraassay* precision and accuracy were

evaluated from each day's analysis, and *interassay* precision and accuracy were calculated from comparison of the data gathered over three separate days.

4.3. Results and Discussion

4.3.1. Sensor Analysis of SCN and CN

A CN sensor previously developed in our lab proved to be excellent for the rapid, simple and field-portable analysis of CN from blood.[188] Considering the excellent performance of the sensor for CN, we hypothesized that incorporation of $KMnO_4$ to oxidize SCN to CN would allow conversion of the CN sensor to an SCN sensor. While the practical implementation of $KMnO_4$ into the sensor was challenging, the overall hypothesis was confirmed, with $KMnO_4$ converting SCN to CN and subsequent analysis of CN via the previous CN analysis method. Because the CN sensor was modified to allow SCN analysis, the SCN sensor features all the advantages of the CN sensor. Most importantly for monitoring CN fishing, the overall sample preparation and analysis time is only 60 s, it requires a very small volume of blood (i.e., allowing monitoring of CN fishing without requiring the sacrifice of the fish tested and allowing testing of even very small fish), it is portable, and it is easy to use. Additionally, the reagents are stable, with the dry $KMnO_4$ evaluated as stable in the cartridge for at least 30 days (longest period tested). In addition, the simplicity of the analysis should allow all stakeholders to monitor CN-fishing, i.e., operation does not require special expertise and all sample preparation steps are automated. It should be noted that obtaining blood from live fish would require special expertise, but once the blood is obtained, analysis of SCN via the sensor is rapid and simple.

The fundamental difference in the SCN and CN sensors was the use of $KMnO_4$ to initially oxidize SCN to CN, with analysis of the CN produced as previously

described.[188] Therefore, the analysis of SCN via the current sensor relied on consistent conversion of SCN to CN via oxidation by $KMnO_4$. Consistent oxidation of SCN was evaluated by repeated comparison of the blank-corrected signals produced from fish blood spiked with the same concentrations (5 µM/290 µg/L) of CN (no $KMnO_4$ oxidation), SCN (no $KMnO_4$ oxidation), and SCN with $KMnO_4$ oxidation over three days (N = 3). Signals produced from non-spiked, fish blood (no $KMnO_4$ oxidation) were comparable to signals produced from SCN-spiked fish blood (no $KMnO_4$ oxidation). Equivalent signals from these two samples confirmed that oxidation is necessary for the analysis of SCN via the sensor. The signal produced from SCN-spiked $KMnO_4$-oxidized fish blood was significantly above the non-oxidized blood samples, but equivalent to the signals from CN-spiked fish blood. This indicates that the oxidation of SCN to CN was efficient, likely converting essentially all the spiked SCN to CN, and that $KMnO_4$ did not create significant matrix effects for the analysis of SCN, although it did produce slightly larger background signals.

Directly following CN exposure, the majority of CN in an organism has yet to be converted to SCN. Therefore, the detection of both CN and SCN from biological fluids using the same technology would be advantageous, allowing the determination of CN-caught fish in both the early stages of exposure and long after the exposure occurred. The current sensor technology was evaluated for the potential of analyzing both CN and SCN as "total CN". To evaluate the ability of the sensor to measure total CN, the sum of signals of the separately spiked CN and SCN blood was compared to the signal of the blood sample containing both CN and SCN, as shown in Figure 4.2. Overall, the sum of the signals produced from the individually spiked fish blood are not significantly different from the

signal produced by CN and SCN spiked blood for each concentration above 58 µg/L. These higher concentrations produced signal recoveries of ~92-99% of the "total CN", generally confirming the efficiency and consistency of the $KMnO_4$ oxidation of SCN to CN. The disparity between the sum of signals of the individually spiked blood and the CN/SCN spiked blood at 58 µg/L is because the signal produced from analysis of the lowest concentration CN-spiked blood standard (58 µg/L/1 µM) was similar to signals produced from non-spiked (i.e., blank) blood. The minimal signal produced from the smallest concentration of CN was likely due to reaction of CN^- with electrophilic centers in the blood. CN^- is a strong nucleophile and will bind to many components of blood. These binding sites are relatively plentiful for lower concentrations of CN but become less available as the amount of CN increases. Even though total CN was not measured over the entire concentration range tested, the sensor was capable of analyzing total CN when high concentrations of cyanide were present, which is likely to occur in the early stages following CN exposure. Considering the results in Figure 2, the sensor is able to detect both CN and SCN such that at times immediately following CN exposure, where high blood CN concentration and low SCN concentrations are present, the sensor will still allow verification of cyanide-caught fish. After some time, when some of the CN has been converted to SCN, the sensor will detect both these analytes. At longer times following exposure, CN concentrations will be low and likely undetectable by the sensor, but SCN concentrations will be elevated, allowing verification of CN-caught fish. Therefore, the sensor should be able to determine CN-caught fish soon after capture and during later time periods following CN exposure, until SCN concentrations fall below the LOD of the sensor.

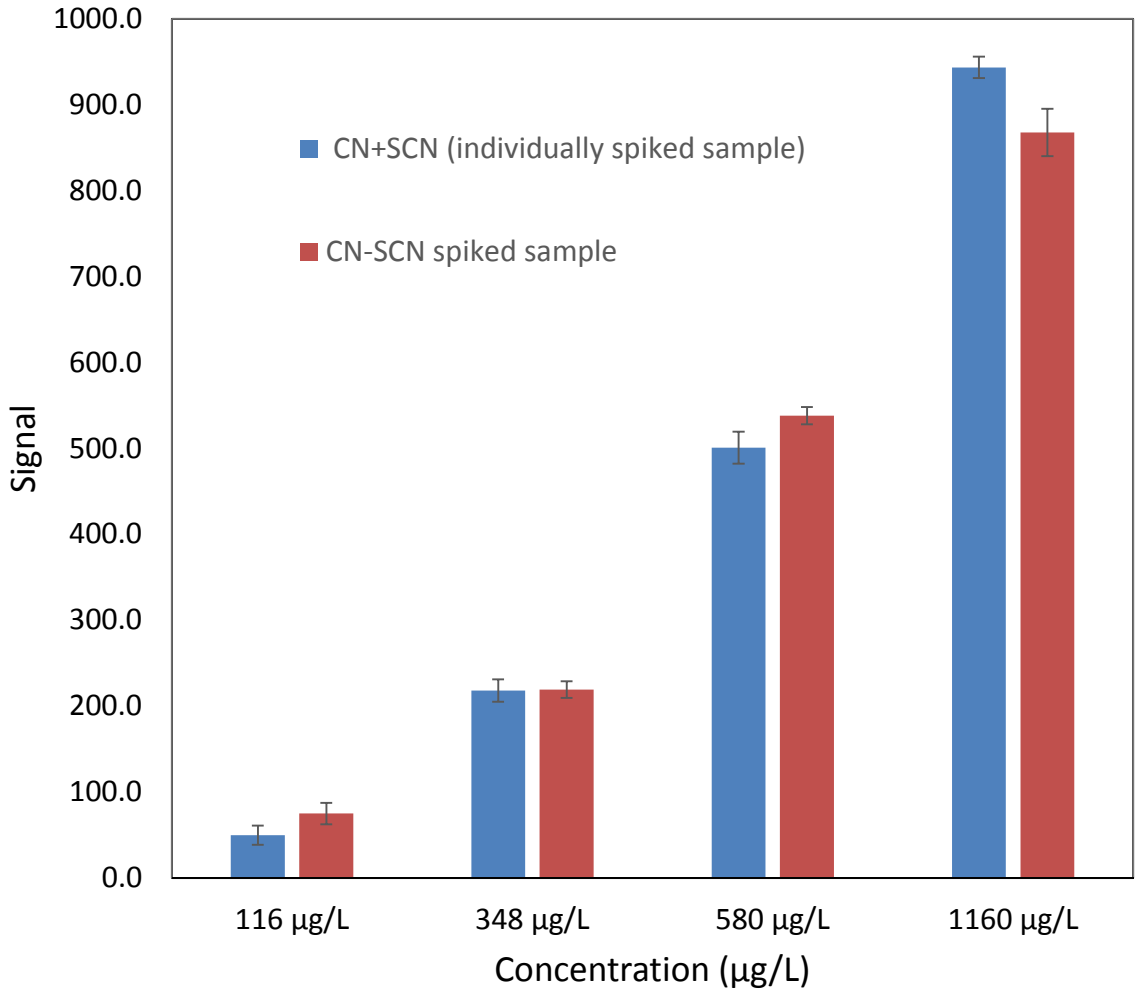

Figure 4.2. Bar graph showing the comparison of the sum of blank-corrected signals of the individually spiked CN and SCN samples (CN+SCN (individually spiked sample), in blue) to the signal of the sample containing both CN and SCN spiked together (CN-SCN spiked sample, in orange).

4.3.2. Background Concentration of SCN in Salmon Blood

Endogenous concentrations of SCN have been previously found in fish blood (Table 1.1). When performing preliminary evaluation of calibration curves in salmon blood for the current study, non-zero intercepts, indicative of the presence of SCN in non-spiked

blood, were observed. In order to quantify the endogenous SCN in the salmon blood used in this study, standard addition was carried out. Endogenous SCN concentrations were analyzed over three days, producing concentrations ranging from 0.5-1.5 μM (29-87 μg/L) with a mean of 1 μM (58±29 μg/L).

4.3.3. SCN Sensor Method Validation

Calibration curves were initially constructed within the concentration range of 0.3-20 μM (17.4-1160 μg/L). Based on the accuracy and precision criteria, the calibrators 0.3, 0.5, and 20 μM (17.4, 29, and 1160 μg/L) fell outside the entire linear range. Therefore, the linear range of the method was 58 μg/L (LLOQ) to 580 μg/L (ULOQ) as best described by non-weighted linear regression. All the calibration curves were stable over three days of validation, as determined by consistency of their slopes (Table 3), producing an excellent fit of the calibrators over the entire linear range with PRA values ≥ 93% and an average R^2 value of 0.9846. The LOD of the current method was 0.5 μM (29 μg/L) in fish blood as defined by the lowest concentration of SCN that produced a signal equal to the summation of the mean blank signal and 3 times the standard deviation of the blank.

Table 4.2. Linear equations, coe□cients of determination (R^2), and percent residual accuracy (PRA) for calibration curves created over 3 separate days.

Day	Equation	R^2	PRA (%)
1	y = 1.291x + 216	0.9865	94
2	y = 1.297x + 156	0.9797	93
3	y = 1.301x + 163	0.9885	95

Table 4 shows the accuracy and precision of the method as evaluated by quintuplicate analysis of low, medium and high QCs on three different days. The precision and accuracy determined from each day's analysis (*intraassay) ranged from 4.7 to 15.1%* RSD *and* 100±19.7% for precision and accuracy, respectively. The precision and accuracy calculated from comparison of the data gathered over 3 separate days (*interassay)* were 17.9% RSD and 100±6.9% for precision and accuracy, respectively. Both the intraassay and interassay accuracy and precision of the sensor found from the 3-day validation meet the accuracy and precision inclusion criteria of 100±20% and ≤ 20% RSD.

Table 4.3. The intra- and inter-assay accuracy and precision of SCN analysis from spiked fish blood

Conc (μM)	Intraassay						Interassay	
	Accuracy (%)			Precision (%RSD)			Accuracy (%)[a]	Precision (%RSD)[a]
	Day 1	Day 2	Day 3	Day 1	Day 2	Day 3		
2.0	100±3.2	100±8.2	100±2.1	15.1	11.8	14.6	100±1.0	<17.9
4.0	100±2.8	100±19.7	100±0.9	8.6	5.5	5.5	100±6.9	<9.5
7.0	100±0.9	100±3.4	100±3.1	10.5	9.6	4.7	100±3.1	<9.0

[a]Aggregate of three days of QC method validation (N = 15)

4.3.4. Application of the Method

The validated method was used to analyze SCN from the blood of marine fish (*A. clarkii*, commonly known as clownfish) exposed to CN. The concentrations of SCN obtained from the blood of CN-exposed fish (N = 3) were each well above the LLOQ (159.1, 176.4 and 183.2 μg/L; average = 172.9±14.0 μg/L). The endogenous SCN concentration was above the LOD but below the LLOQ, so it could not be quantified, but appeared to be near the LOD (29 μg/L). The amount of blood available precluded the use of standard addition to quantify the concentration of SCN in the non-CN-exposed fish. The ability of the sensor to differentiate between CN-exposed and non-exposed fish supports the capability of the SCN sensor to determine CN-caught fish.

4.4. Conclusions

Considering the danger CN-fishing poses to aquatic ecosystems, a rapid and field portable sensor was developed to analyze the major CN metabolite, SCN, in fish blood. This method features simple sample preparation, short analysis time (<60 s), small sample volume requirements (25 μL), minimal required expertise to operate and is fully field portable. The accuracy and precision of the method were acceptable, and the method produced an LOD of 29 μg/L, below endogenous SCN concentrations found for most fish species studied. The method was found to detect both CN and SCN in fish blood and was successfully applied to quantitate SCN from the blood of fish exposed to CN. The current method is a promising technology that could be used by various stakeholders involve in fighting the practice of CN-fishing to monitor the practice in the field.

Chapter 5. Conclusions, Broader Impacts, and Future Work

5.1 Conclusions

A simple, direct, and rapid novel HPLC-MS/MS method was developed for analysis of TRPA1 antagonist A-967079 from plasma. The method was successfully applied to evaluate the pharmacokinetics in A-967079 from plasma of treated animals. A novel cyanide metabolite ATOEA, was discovered based on the metabolism of cyanide by glutathione. The kinetics of ATOEA in CN-exposed animals confirms that it is a promising biomarker to confirm cyanide exposure. A field portable fluorescent detection method was developed to determine the CN metabolite thiocyanate, from fish blood. The method features a short analysis time, an excellent accuracy and precision and was successfully applied to analyze SCN from fish exposed to CN to verify CN-fishing.

5.2 Broader Impacts

Toxic inhaled hazards are useful in industrial manufacturing but pose major global threat to humanity. Researching to better understand the toxicological behavior of these hazards, development of technologies to determine their exposure, and development of effective therapeutic agents are crucial to defend against the effects of TIHs exposure. The novel method for the analysis of A-967079 presented here will allow for further development of A-967079 as a promising therapeutic agent against the noxious effect of TIHs exposure. In addition, the discovery of a novel cyanide metabolite ATOEA, has provided additional insight into the metabolism of cyanide and can serve as a potential marker to confirm CN exposure. Furthermore, rapid, easy and field portable method developed for SCN analysis in fish blood will allow government, aquarium trade and food agencies to monitor the CN-fishing and enforce laws to curb this illegal practice. Overall,

the work presented here will contribute to the development methods to confirm exposure to TIH and the development of therapeutic agents for TIH.

5.3 Future Work

Future work should include the application of the A967079 developed method to expand the pharmacokinetic studies of A967079 in many animal models before extending to human studies for full development of A967079 as therapeutics. The toxicokinetics of ATOEA in other animal models should be evaluated to better understand the kinetics of ATOEA, and also future work should identify degradation product(s) of ATOEA in biological samples and evaluate the stability of the product(s). Lastly, the thiocyanate method should be apply to analyze fish blood samples from areas where CN-fishing is practice to further evaluate the technology.

References

1. Bessac, B.F. and S.-E. Jordt, *Sensory detection and responses to toxic gases: mechanisms, health effects, and countermeasures.* Proceedings of the American Thoracic Society, 2010. **7**(4): p. 269-277.
2. Evans, R.B., *Chlorine: state of the art.* Lung, 2005. **183**(3): p. 151-167.
3. Bessac, B.F., et al., *Transient receptor potential ankyrin 1 antagonists block the noxious effects of toxic industrial isocyanates and tear gases.* The FASEB Journal, 2009. **23**(4): p. 1102-1114.
4. Brown, J., *An internet database for the classification and dissemination of information about hazardous chemicals and occupational diseases.* American journal of industrial medicine, 2008. **51**(6): p. 428-435.
5. Dotson, A., P. Westerhoff, and S.W. Krasner, *Nitrogen enriched dissolved organic matter (DOM) isolates and their affinity to form emerging disinfection by-products.* Water Science and Technology, 2009. **60**(1): p. 135-143.
6. Logue, B.A., et al., *Determination of methyl isopropyl hydantoin from rat erythrocytes by gas-chromatography mass-spectrometry to determine methyl isocyanate dose following inhalation exposure.* Journal of Chromatography B, 2018. **1093**: p. 119-127.
7. Jackson, R., et al., *Development of a fluorescence-based sensor for rapid diagnosis of cyanide exposure.* Analytical chemistry, 2014. **86**(3): p. 1845-1852.
8. Mehta, P.S., et al., *Bhopal tragedy's health effects: a review of methyl isocyanate toxicity.* Jama, 1990. **264**(21): p. 2781-2787.
9. Goswami, H., *Cytogenetic effects of methyl isocyanate exposure in Bhopal.* Human genetics, 1986. **74**(1): p. 81-84.
10. Greskevitch, M., et al., *Respiratory disease in agricultural workers: mortality and morbidity statistics.* Journal of agromedicine, 2008. **12**(3): p. 5-10.
11. Lillienberg, L., et al., *A population-based study on welding exposures at work and respiratory symptoms.* Annals of Occupational Hygiene, 2008. **52**(2): p. 107-115.
12. Rushton, L., *Occupational causes of chronic obstructive pulmonary disease.* Reviews on environmental health, 2007. **22**(3): p. 195-212.
13. Manandhar, E., et al., *Rapid analysis of sulfur mustard oxide in plasma using gas chromatography-chemical ionization-mass spectrometry for diagnosis of sulfur mustard exposure.* Journal of Chromatography A, 2018. **1572**: p. 106-111.
14. Greenfield, R.A., et al., *Microbiological, biological, and chemical weapons of warfare and terrorism.* The American journal of the medical sciences, 2002. **323**(6): p. 326-340.
15. Franz, D.R. and N. Jaax, *Medical aspects of chemical and biological warfare.* Sidell, F., Takafuji, E., Franz, D., Eds, 1997: p. 631À642.
16. Noort, D., H. Benschop, and R. Black, *Biomonitoring of exposure to chemical warfare agents: a review.* Toxicology and applied pharmacology, 2002. **184**(2): p. 116-126.
17. Lehto, S.G., et al., *Selective antagonism of TRPA1 produces limited efficacy in models of inflammatory-and neuropathic-induced mechanical hypersensitivity in rats.* Molecular pain, 2016. **12**: p. 1744806916677761.
18. Bessac, B.F., et al., *TRPA1 is a major oxidant sensor in murine airway sensory neurons.* The Journal of clinical investigation, 2008. **118**(5): p. 1899-1910.

19. Alarie, Y., *Irritating properties of airborne materials to the upper respiratory tract.* Archives of Environmental Health: An International Journal, 1966. **13**(4): p. 433-449.
20. Kuwabara, Y., et al., *Evaluation and application of the RD50 for determining acceptable exposure levels of airborne sensory irritants for the general public.* Environmental Health Perspectives, 2007. **115**(11): p. 1609-1616.
21. McLoud, T.C., *Occupational lung disease.* Radiologic Clinics of North America, 1991. **29**(5): p. 931-941.
22. Nowak, D., *Chemosensory irritation and the lung.* International archives of occupational and environmental health, 2002. **75**(5): p. 326-331.
23. Francis, H.C., et al., *Defining and investigating occupational asthma: a consensus approach.* Occupational and environmental medicine, 2007. **64**(6): p. 361-365.
24. Springer, J., et al., *Neurokinin-1 receptor activation induces reactive oxygen species and epithelial damage in allergic airway inflammation.* Clinical & Experimental Allergy, 2007. **37**(12): p. 1788-1797.
25. Wemmie, J.A., R.J. Taugher, and C.J. Kreple, *Acid-sensing ion channels in pain and disease.* Nature Reviews Neuroscience, 2013. **14**(7): p. 461.
26. Xiong, Z.-G., et al., *Acid-sensing ion channels (ASICs) as pharmacological targets for neurodegenerative diseases.* Current opinion in pharmacology, 2008. **8**(1): p. 25-32.
27. Jaquemar, D., T. Schenker, and B. Trueb, *An ankyrin-like protein with transmembrane domains is specifically lost after oncogenic transformation of human fibroblasts.* Journal of Biological Chemistry, 1999. **274**(11): p. 7325-7333.
28. Clapham, D.E., *TRP channels as cellular sensors.* Nature, 2003. **426**(6966): p. 517-524.
29. Nilius, B. and G. Owsianik, *The transient receptor potential family of ion channels.* Genome biology, 2011. **12**(3): p. 218.
30. Nilius, B., et al., *Transient receptor potential cation channels in disease.* Physiological reviews, 2007. **87**(1): p. 165-217.
31. Nilius, B., G. Owsianik, and T. Voets, *Transient receptor potential channels meet phosphoinositides.* The EMBO journal, 2008. **27**(21): p. 2809-2816.
32. Hinman, A., et al., *TRP channel activation by reversible covalent modification.* Proceedings of the National Academy of Sciences, 2006. **103**(51): p. 19564-19568.
33. Macpherson, L.J., et al., *Noxious compounds activate TRPA1 ion channels through covalent modification of cysteines.* Nature, 2007. **445**(7127): p. 541-545.
34. Baraldi, P.G., et al., *Transient receptor potential ankyrin 1 (TRPA1) channel as emerging target for novel analgesics and anti-inflammatory agents.* Journal of medicinal chemistry, 2010. **53**(14): p. 5085-5107.
35. Inoue, T. and B.P. Bryant, *Multiple cation channels mediate increases in intracellular calcium induced by the volatile irritant, trans-2-pentenal in rat trigeminal neurons.* Cellular and molecular neurobiology, 2010. **30**(1): p. 35-41.
36. Taylor-Clark, T.E., et al., *Transient receptor potential ankyrin 1 mediates toluene diisocyanate–evoked respiratory irritation.* American journal of respiratory cell and molecular biology, 2009. **40**(6): p. 756-762.

37. Andrè, E., et al., *Cigarette smoke–induced neurogenic inflammation is mediated by α, β-unsaturated aldehydes and the TRPA1 receptor in rodents.* The Journal of clinical investigation, 2008. **118**(7): p. 2574-2582.
38. Brone, B., et al., *Tear gasses CN, CR, and CS are potent activators of the human TRPA1 receptor.* Toxicology and applied pharmacology, 2008. **231**(2): p. 150-156.
39. McNamara, C.R., et al., *TRPA1 mediates formalin-induced pain.* Proceedings of the National Academy of Sciences, 2007. **104**(33): p. 13525-13530.
40. Sawada, Y., et al., *Activation of transient receptor potential ankyrin 1 by hydrogen peroxide.* European Journal of Neuroscience, 2008. **27**(5): p. 1131-1142.
41. Caceres, A.I., et al., *A sensory neuronal ion channel essential for airway inflammation and hyperreactivity in asthma.* Proceedings of the National Academy of Sciences, 2009. **106**(22): p. 9099-9104.
42. Julius, D., *TRP channels and pain.* Annual review of cell and developmental biology, 2013. **29**: p. 355-384.
43. Salat, K., A. Moniczewski, and T. Librowski, *Transient receptor potential channels-emerging novel drug targets for the treatment of pain.* Current medicinal chemistry, 2013. **20**(11): p. 1409-1436.
44. Facchinetti, F. and R. Patacchini, *The rising role of TRPA1 in asthma.* The Open Drug Discovery Journal, 2010. **2**(1).
45. Fujita, F., et al., *Intracellular alkalization causes pain sensation through activation of TRPA1 in mice.* The Journal of clinical investigation, 2008. **118**(12): p. 4049-4057.
46. McGaraughty, S., et al., *TRPA1 modulation of spontaneous and mechanically evoked firing of spinal neurons in uninjured, osteoarthritic, and inflamed rats.* Molecular pain, 2010. **6**(1): p. 14.
47. Eid, S.R., et al., *HC-030031, a TRPA1 selective antagonist, attenuates inflammatory-and neuropathy-induced mechanical hypersensitivity.* Molecular pain, 2008. **4**(1): p. 48.
48. Wei, H., et al., *Attenuation of mechanical hypersensitivity by an antagonist of the TRPA1 ion channel in diabetic animals.* Anesthesiology: The Journal of the American Society of Anesthesiologists, 2009. **111**(1): p. 147-154.
49. Chen, J., et al., *Selective blockade of TRPA1 channel attenuates pathological pain without altering noxious cold sensation or body temperature regulation.* Pain, 2011. **152**(5): p. 1165-1172.
50. DeFalco, J., et al., *Oxime derivatives related to AP18: agonists and antagonists of the TRPA1 receptor.* Bioorganic & medicinal chemistry letters, 2010. **20**(1): p. 276-279.
51. Brozmanova, M., et al., *Comparison of TRPA1-versus TRPV1-mediated cough in guinea pigs.* European journal of pharmacology, 2012. **689**(1-3): p. 211-218.
52. Birrell, M.A., et al., *TRPA1 agonists evoke coughing in guinea pig and human volunteers.* American journal of respiratory and critical care medicine, 2009. **180**(11): p. 1042-1047.
53. Xie, Z. and H. Hu, *TRP channels as drug targets to relieve itch.* Pharmaceuticals, 2018. **11**(4): p. 100.

54. Jackson, R. and B.A. Logue, *A review of rapid and field-portable analytical techniques for the diagnosis of cyanide exposure.* Analytica chimica acta, 2017. **960**: p. 18-39.
55. Logue, B.A., et al., *The analysis of cyanide and its breakdown products in biological samples.* Critical Reviews in Analytical Chemistry, 2010. **40**(2): p. 122-147.
56. Baskin, I., and Brewer, TG *Cyanide poisoning.* in Textbook ofMilitary Medicine, Medical Aspects of Chemical and Biological Warfare eds. F. R. Sidell, E. T. Takafuji, and D. R. Franz (Borden

Institute, Washington, DC, , 1997. **Ch. 10**: p. 271–286.
57. Brenner, M., et al., *Comparison of cobinamide to hydroxocobalamin in reversing cyanide physiologic effects in rabbits using diffuse optical spectroscopy monitoring.* Journal of biomedical optics, 2010. **15**(1): p. 017001.
58. Baskin, S.I., et al., *Cyanide poisoning.* Medical aspects of chemical warfare, 2008. **11**: p. 372-410.
59. Sykes, A., *Early studies on the toxicology of cyanide.* Cyanide in Biology, 1981: p. 1-9.
60. Nagasawa, H.T., S.E. Cummings, and S.I. Baskin, *THE STRUCTURE OF "ITCA", A URINARY METABOLITE OF CYANIDE.* Organic preparations and procedures international, 2004. **36**(2): p. 178-182.
61. Alzhrani, E., *Development of a High Performance Liquid Chromatography Method for the Analysis of Next-generation Cyanide Antidote, 3-mercaptopyruvate, in Plasma.* 2018.
62. Stutelberg, M.W., *Liquid Chromatography-tandem Mass Spectrometry of Next-generation Cyanide Antidotes, 3-mercaptopyruvate and Cobinamide, with the Pharmacokinetic Analysis of 3-mercaptopyruvate.* 2015.
63. Weider, B. and J. Fournier, *The death of Napoleon.* The American Journal of Forensic Medicine and Pathology, 2000. **21**(3): p. 303-305.
64. Lang, J., et al., *Is the "protector of lions" losing his touch.* US News & World Report, 1986. **10**: p. 29.
65. Heylin, M., *US decries apparent chemical arms attack.* Chem Eng News, 1988. **66**: p. 23.
66. Ali, J., *Chemical weapons and the Iran-Iraq war: A case study in noncompliance.* The Nonproliferation Review, 2001. **8**(1): p. 43-58.
67. Bacalso, R.T.M., et al., *Effort reallocation of illegal fishing operations: A profitable scenario for the municipal fisheries of Danajon Bank, Central Philippines.* Ecological modelling, 2016. **331**: p. 5-16.
68. Bacalso, R.T.M. and M. Wolff, *Trophic flow structure of the Danajon ecosystem (Central Philippines) and impacts of illegal and destructive fishing practices.* Journal of Marine Systems, 2014. **139**: p. 103-118.
69. Halim, A., *Adoption of cyanide fishing practice in Indonesia.* Ocean & Coastal Management, 2002. **45**(4-5): p. 313-323.
70. Rubec, P.J. *The effects of sodium cyanide on coral reefs and marine fish in the Philippines*. in *The First Asian Fisheries Forum*. 1986. Manila, Philippines: Asian Fisheries Society.

71. Barber, C.V. and V.R. Pratt, *Sullied seas: Strategies for combating cyanide fishing in Southeast Asia and beyond.* 1997.
72. Wabnitz, C., *From ocean to aquarium: the global trade in marine ornamental species*. 2003: UNEP/Earthprint.
73. Barber, C.V. and V.R. Pratt, *Poison and profits: cyanide fishing in the Indo-Pacific.* Environment: Science and Policy for Sustainable Development, 1998. **40**(8): p. 4-9.
74. Dee, L.E., S.S. Horii, and D.J. Thornhill, *Conservation and management of ornamental coral reef wildlife: successes, shortcomings, and future directions.* Biological Conservation, 2014. **169**: p. 225-237.
75. Dzombak, D.A., et al., *Anthropogenic cyanide in the marine environment*, in *Cyanide in Water and Soil*. 2005, CRC Press. p. 221-236.
76. Calado, R., et al., *Caught in the Act: How the US Lacey Act can hamper the fight against cyanide fishing in tropical coral reefs.* Conservation Letters, 2014. **7**(6): p. 561-564.
77. Wood, J.L. and S.L. Cooley, *Detoxication of cyanide by cystine.* J Biol Chem, 1956. **218**(1): p. 449-57.
78. Mous, P., et al., *Cyanide fishing on Indonesian coral reefs for the live food fish market-what is the problem.* Collected essays on the economics of coral reefs. Kalmar, Sweden: CORDIO, Kalmar University, 2000: p. 69-76.
79. Hodgson, G., *A global assessment of human effects on coral reefs.* Marine Pollution Bulletin, 1999. **38**(5): p. 345-355.
80. Rubec, P.J., et al., *Cyanide-free net-caught fish for the marine aquarium trade.* Aquarium Sciences and Conservation, 2001. **3**(1-3): p. 37-51.
81. Cervino, J.M., et al., *Changes in zooxanthellae density, morphology, and mitotic index in hermatypic corals and anemones exposed to cyanide.* Marine Pollution Bulletin, 2003. **46**(5): p. 573-586.
82. Ward, S., P. Harrison, and O. Hoegh-Guldberg. *Coral bleaching reduces reproduction of scleractinian corals and increases susceptibility to future stress*. in *Proceedings of the Ninth International Coral Reef Symposium, Bali, 23-27 October 2000*. 2002.
83. Eyjolfsson, R., *Recent advances in the chemistry of cyanogenic glycosides*, in *Fortschritte der Chemie Organischer Naturstoffe/Progress in the Chemistry of Organic Natural Products*. 1970, Springer. p. 74-108.
84. Peterson, S.C., N.D. Johnson, and J.L. LeGuyader, *Defensive regurgitation of allelochemicals derived from host cyanogenesis by eastern tent caterpillars.* Ecology, 1987. **68**(5): p. 1268-1272.
85. Vetter, J., *Plant cyanogenic glycosides.* Toxicon, 2000. **38**(1): p. 11-36.
86. Wong-Chong, G.M., et al., *Natural sources of cyanide*, in *Cyanide in Water and Soil*. 2005, CRC Press. p. 37-52.
87. Duffey, S., *Cyanide and arthropods.* Cyanide in biology, 1981: p. 385-414.
88. Simeonova, F.P., L. Fishbein, and W.H. Organization, *Hydrogen cyanide and cyanides: human health aspects.* 2004.
89. Bhandari, R.K., et al., *Cyanide toxicokinetics: the behavior of cyanide, thiocyanate and 2-amino-2-thiazoline-4-carboxylic acid in multiple animal models.* J Anal Toxicol, 2014. **38**(4): p. 218-25.

90. Taylor, J., *Toxicological profile for cyanide*. 2006: US Department of Health and Human Services, Public Health Service, Agency ….
91. Lee, S., *Methane and its Derivatives*. Vol. 70. 1996: Crc Press.
92. Andrussow, L., *Über die katalytische Oxydation von Ammoniak-Methan-Gemischen zu Blausäure.* Angewandte Chemie, 1935. **48**(37): p. 593-595.
93. Endter, F., *Die technische Synthese von Cyanwasserstoff aus Methan und Ammoniak ohne Zusatz von Sauerstoff.* Chemie Ingenieur Technik, 1958. **30**(5): p. 305-310.
94. McKetta, J.J., *Inorganic chemicals handbook.* 1993.
95. Way, J.L., *Pharmacologic aspects of cyanide and its antagonism.* Cyanide in biology. Academic Press, New York, 1981: p. 29-40.
96. Lawson-Smith, P., E.C. Jansen, and O. Hyldegaard, *Cyanide intoxication as part of smoke inhalation-a review on diagnosis and treatment from the emergency perspective.* Scandinavian journal of trauma, resuscitation and emergency medicine, 2011. **19**(1): p. 14.
97. Jackson, R.E., *The development of a field sensor for the rapid detection of cyanide exposure.* 2014.
98. Cherian, M. and I. Richmond, *Fatal methane and cyanide poisoning as a result of handling industrial fish: a case report and review of the literature.* Journal of clinical pathology, 2000. **53**(10): p. 794-795.
99. Blackledge, W.C., et al., *New facile method to measure cyanide in blood.* Analytical chemistry, 2010. **82**(10): p. 4216-4221.
100. Hall, A.H., G.E. Isom, and G.A. Rockwood, *Toxicology of cyanides and cyanogens*. 2015: Wiley Online Library.
101. Way, J.L., et al. *The mechanism of cyanide intoxication and its antagonism*. in *Ciba Found Symp*. 1988. Wiley Online Library.
102. Vos, M., P. Verstreken, and C. Klein, *Stimulation of electron transport as potential novel therapy in Parkinson's disease with mitochondrial dysfunction*. 2015, Portland Press Ltd.
103. Berg, J.M., J.L. Tymoczko, and L. Stryer, *Biochemistry/Jeremy M.* Berg, John L. Tymoczko, Lubert Stryer, 2007: p. 524-560.
104. Gracia, R. and G. Shepherd, *Cyanide poisoning and its treatment.* Pharmacotherapy: The Journal of Human Pharmacology and Drug Therapy, 2004. **24**(10): p. 1358-1365.
105. Petrikovics, I., et al., *Past, present and future of cyanide antagonism research: From the early remedies to the current therapies.* World journal of methodology, 2015. **5**(2): p. 88.
106. Lundquist, P., H. Rosling, and B. Sörbo, *Determination of cyanide in whole blood, erythrocytes, and plasma.* Clinical chemistry, 1985. **31**(4): p. 591-595.
107. Frankenberg, L., *Enzyme therapy in cyanide poisoning: effect of rhodanese and sulfur compounds.* Archives of toxicology, 1980. **45**(4): p. 315-323.
108. Stutelberg, M.W., et al., *Determination of 3-mercaptopyruvate in rabbit plasma by high performance liquid chromatography tandem mass spectrometry.* Journal of Chromatography B, 2014. **949**: p. 94-98.

109. Spallarossa, A., et al., *The "rhodanese" fold and catalytic mechanism of 3-mercaptopyruvate sulfurtransferases: crystal structure of SseA from Escherichia coli.* Journal of molecular biology, 2004. **335**(2): p. 583-593.
110. Lundquist, P., et al., *Analysis of the cyanide metabolite 2-aminothiazoline-4-carboxylic acid in urine by high-performance liquid chromatography.* Analytical biochemistry, 1995. **228**(1): p. 27-34.
111. Logue, B.A., et al., *Determination of the cyanide metabolite 2-aminothiazoline-4-carboxylic acid in urine and plasma by gas chromatography–mass spectrometry.* Journal of Chromatography B, 2005. **819**(2): p. 237-244.
112. Mitchell, B.L., G.A. Rockwood, and B.A. Logue, *Quantification of α-ketoglutarate cyanohydrin in swine plasma by ultra-high performance liquid chromatography tandem mass spectrometry.* Journal of Chromatography B, 2013. **934**: p. 60-65.
113. Flora, S., et al., *Pharmacological perspectives of toxic chemicals and their antidotes*. 2004: Springer Science & Business Media.
114. Norris, J.C., W.A. Utley, and A.S. Hume, *Mechanism of antagonizing cyanide-induced lethality by α-ketoglutaric acid.* Toxicology, 1990. **62**(3): p. 275-283.
115. Houeto, P., et al., *Relation of blood cyanide to plasma cyanocobalamin concentration after a fixed dose of hydroxocobalamin in cyanide poisoning.* The lancet, 1995. **346**(8975): p. 605-608.
116. Fasco, M.J., et al., *Cyanide adducts with human plasma proteins: albumin as a potential exposure surrogate.* Chemical research in toxicology, 2007. **20**(4): p. 677-684.
117. Gyamfi, O.A., et al., *Metabolism of cyanide by glutathione to produce the novel cyanide metabolite, 2-aminothiazoline-4-oxoaminoethanoic acid.* Chemical research in toxicology, 2019.
118. Koontz, M.D. and L. Niang, *Respiratory disease in agricultural workers; mortality and morbidity statistics.* 2007.
119. Cortright, D.N. and A. Szallasi, *TRP channels and pain.* Current pharmaceutical design, 2009. **15**(15): p. 1736-1749.
120. Leffler, A., et al., *Activation of TRPA1 by membrane permeable local anesthetics.* Molecular pain, 2011. **7**(1): p. 62.
121. Andersson, D.A., C. Gentry, and S. Bevan, *TRPA1 has a key role in the somatic pro-nociceptive actions of hydrogen sulfide.* PLoS One, 2012. **7**(10): p. e46917.
122. Banzawa, N., et al., *Molecular Basis Determining Inhibition/Activation of Nociceptive Receptor TRPA1 Protein A SINGLE AMINO ACID DICTATES SPECIES-SPECIFIC ACTIONS OF THE MOST POTENT MAMMALIAN TRPA1 ANTAGONIST.* Journal of Biological Chemistry, 2014. **289**(46): p. 31927-31939.
123. De Luca, L., G. Giacomelli, and A. Porcheddu, *Beckmann rearrangement of oximes under very mild conditions.* The Journal of organic chemistry, 2002. **67**(17): p. 6272-6274.
124. Heitmann, G., G. Dahlhoff, and W. Hölderich, *Catalytically active sites for the Beckmann rearrangement of cyclohexanone oxime to ε-caprolactam.* Journal of Catalysis, 1999. **186**(1): p. 12-19.
125. Peng, J. and Y. Deng, *Catalytic Beckmann rearrangement of ketoximes in ionic liquids.* Tetrahedron Letters, 2001. **42**(3): p. 403-405.

126. Shah, V.P., et al., *Bioanalytical method validation—a revisit with a decade of progress.* Pharmaceutical research, 2000. **17**(12): p. 1551-1557.
127. Shabir, G.A., *Validation of high-performance liquid chromatography methods for pharmaceutical analysis: Understanding the differences and similarities between validation requirements of the US Food and Drug Administration, the US Pharmacopeia and the International Conference on Harmonization.* Journal of chromatography A, 2003. **987**(1-2): p. 57-66.
128. Logue, B.A. and E. Manandhar, *Percent residual accuracy for quantifying goodness-of-fit of linear calibration curves.* Talanta, 2018. **189**: p. 527-533.
129. Bhadra, S., et al., *Analysis of potential cyanide antidote, dimethyl trisulfide, in whole blood by dynamic headspace gas chromatography–mass spectroscopy.* Journal of Chromatography A, 2019. **1591**: p. 71-78.
130. Causon, R., *Validation of chromatographic methods in biomedical analysis viewpoint and discussion.* Journal of Chromatography B: Biomedical Sciences and Applications, 1997. **689**(1): p. 175-180.
131. Eminedoki, D., M. Monanu, and E. Anosike, *Thiocyanate levels of mainly dietary origin in serum and urine from a human population sample in Port Harcourt, Nigeria.* Plant Foods for Human Nutrition, 1994. **46**(4): p. 277-285.
132. Murray, S., et al., *Effect of cruciferous vegetable consumption on heterocyclic aromatic amine metabolism in man.* Carcinogenesis, 2001. **22**(9): p. 1413-1420.
133. Schnepp, R., *Cyanide: sources, perceptions, and risks.* Journal of emergency nursing, 2006. **32**(4): p. S3-S7.
134. Wolnik, K.A., et al., *The Tylenol tampering incident-tracing the source.* Analytical chemistry, 1984. **56**(3): p. 466A-474A.
135. Eckstein, M., *Cyanide as a chemical terrorism weapon.* JEMS: a journal of emergency medical services, 2004. **29**(8): p. suppl 22-31.
136. Logue, B.A., et al., *The analysis of 2-amino-2-thiazoline-4-carboxylic acid in the plasma of smokers and non-smokers.* Toxicology Mechanisms and Methods, 2009. **19**(3): p. 202-208.
137. Bhandari, R.K., et al., *Simultaneous high-performance liquid chromatography-tandem mass spectrometry (HPLC-MS-MS) analysis of cyanide and thiocyanate from swine plasma.* Analytical and bioanalytical chemistry, 2014. **406**(3): p. 727-734.
138. Baskin, S., et al., *Insights on cyanide toxicity and methods of treatment.* Pharmacological perspectives of toxic chemicals and their antidotes, 2004: p. 105-146.
139. Ballantyne, B., *Factors in the analysis of whole blood thiocyanate.* Clinical toxicology, 1977. **11**(2): p. 195-210.
140. Sanchez, C., et al., *Perchlorate, thiocyanate, and nitrate in edible cole crops (Brassica sp.) produced in the lower Colorado River region.* Bulletin of environmental contamination and toxicology, 2007. **79**(6): p. 655-659.
141. Heaney, R.K. and G.R. Fenwick, *The analysis of glucosinolates in Brassica species using gas chromatography. Direct determination of the thiocyanate ion precursors, glucobrassicin and neoglucobrassicin.* Journal of the Science of Food and Agriculture, 1980. **31**(6): p. 593-599.

142. Weuffen, W., et al., *Studies on the relationship between 2-iminothiazolidine-4-carboxylic acid and the thiocyanate metabolism in the guinea-pig (author's transl).* Die Pharmazie, 1980. **35**(4): p. 221-223.
143. Petrikovics, I., et al., *Organ-distribution of the metabolite 2-aminothiazoline-4-carboxylic acid in a rat model following cyanide exposure.* Biomarkers, 2011. **16**(8): p. 686-690.
144. Rużycka, M., et al., *Application of 2-Aminothiazoline-4-carboxylic Acid as a Forensic Marker of Cyanide Exposure.* Chemical research in toxicology, 2017. **30**(2): p. 516-523.
145. Luliński, P., et al., *A highly selective molecularly imprinted sorbent for extraction of 2-aminothiazoline-4-carboxylic acid–Synthesis, characterization and application in post-mortem whole blood analysis.* Journal of Chromatography A, 2015. **1420**: p. 16-25.
146. Mitchell, B.L., et al., *Toxicokinetic profiles of α-ketoglutarate cyanohydrin, a cyanide detoxification product, following exposure to potassium cyanide.* Toxicology letters, 2013. **222**(1): p. 83-89.
147. Hall, A.H., R. Dart, and G. Bogdan, *Sodium thiosulfate or hydroxocobalamin for the empiric treatment of cyanide poisoning?* Annals of emergency medicine, 2007. **49**(6): p. 806-813.
148. Borron, S.W., M. Stonerook, and F. Reid, *Efficacy of hydroxocobalamin for the treatment of acute cyanide poisoning in adult beagle dogs.* Clinical Toxicology, 2006. **44**(sup1): p. 5-15.
149. Karmi, O., et al., *Measurement of vitamin B12 concentration: A review on available methods.* IIOAB J, 2011. **2**(2): p. 23-32.
150. Ahmad, I. and W. Hussain, *Stabiliiy of cyanocobalamin solutions insunlight and artificial light.* Pakistan journal of pharmaceutical sciences, 1993. **6**(1): p. 23-28.
151. Youso, S.L., et al., *Determination of cyanide exposure by gas chromatography–mass spectrometry analysis of cyanide-exposed plasma proteins.* Analytica chimica acta, 2010. **677**(1): p. 24-28.
152. Youso, S.L., G.A. Rockwood, and B.A. Logue, *The analysis of protein-bound thiocyanate in plasma of smokers and non-smokers as a marker of cyanide exposure.* Journal of analytical toxicology, 2012. **36**(4): p. 265-269.
153. Turner, P.C., et al., *Detectable levels of serum aflatoxin B1-albumin adducts in the United Kingdom population: implications for aflatoxin-B1 exposure in the United Kingdom.* Cancer Epidemiology and Prevention Biomarkers, 1998. **7**(5): p. 441-447.
154. Pompella, A., et al., *The changing faces of glutathione, a cellular protagonist.* Biochemical Pharmacology, 2003. **66**(8): p. 1499-1503.
155. Pastore, A., et al., *Determination of blood total, reduced, and oxidized glutathione in pediatric subjects.* Clin Chem, 2001. **47**(8): p. 1467-9.
156. Hatch, R., D. Laflamme, and A. Jain, *Effects of various known and potential cyanide antagonists and a glutathione depletor on acute toxicity of cyanide in mice.* Veterinary and human toxicology, 1990. **32**(1): p. 9-16.
157. Okafor, P., et al., *The role of low-protein and cassava-cyanide intake in the aetiology of tropical pancreatitis.* Global Journal of Pharmacology, 2008. **2**(1): p. 6-10.

158. Okafor, P., V. Anyanwu, and H. Onyema, *The effects of cassava cyanide on the antioxidant (Glutathione) status and some clinically important enzymes of rats.* Journal of Pharmacology and Toxicology, 2010. **5**(7): p. 389-395.
159. Catsimpoolas, N. and J.L. Wood, *Specific cleavage of cystine peptides by cyanide.* Journal of Biological Chemistry, 1966. **241**(8): p. 1790-1796.
160. Degani, Y. and A. Patchornik, *Cyanylation of sulfhydryl groups by 2-nitro-5-thiocyanobenzoic acid. High-yield modification and cleavage of peptides at cysteine residues.* Biochemistry, 1974. **13**(1): p. 1-11.
161. Chelius, D., et al., *Formation of pyroglutamic acid from N-terminal glutamic acid in immunoglobulin gamma antibodies.* Analytical chemistry, 2006. **78**(7): p. 2370-2376.
162. Clason, B., W. Langston, and G.-P. Zauke, *Bioaccumulation of trace metals in the amphipod Chaetogammarus marinus (Leach, 1815) from the Avon and Tamar estuaries (UK): comparison of two-compartment and hyperbolic toxicokinetic models.* Marine environmental research, 2004. **57**(3): p. 171-195.
163. Sips, P.Y., et al., *Identification of specific metabolic pathways as druggable targets regulating the sensitivity to cyanide poisoning.* PloS one, 2018. **13**(6): p. e0193889.
164. McAllister, D.E., N.L. Caho, and C. Shih, *Cyanide fisheries: where did they start.* Secretariat of the Pacific Community Live Reef Fish Information Bulletin, 1999. **5**: p. 18-21.
165. Johannes, R.E. and M. Riepen, *Environmental, economic, and social implications of the live reef fish trade in Asia and the Western Pacific.* 1995.
166. Jones, R.J., T. Kildea, and O. Hoegh-Guldberg, *PAM chlorophyll fluorometry: a new in situ technique for stress assessment in scleractinian corals, used to examine the effects of cyanide from cyanide fishing.* Marine Pollution Bulletin, 1999. **38**(10): p. 864-874.
167. Pet-Soede, L. and M. Erdmann, *How fresh is too fresh? The live reef food fish trade in Eastern Indonesia.* SPC Live Reef Fish Information Bulletin, 1997. **3**: p. 41-45.
168. Clark, T.R., et al., *Historical photographs revisited: A case study for dating and characterizing recent loss of coral cover on the inshore Great Barrier Reef.* Scientific reports, 2016. **6**: p. 19285.
169. Jones, R.J. and O. Hoegh-Guldberg, *Effects of cyanide on coral photosynthesis: implications for identifying the cause of coral bleaching and for assessing the environmental effects of cyanide fishing.* Marine Ecology Progress Series, 1999. **177**: p. 83-91.
170. McManus, J.W., R.B. Reyes Jr, and C.L. Nanola Jr, *Effects of some destructive fishing methods on coral cover and potential rates of recovery.* Environmental management, 1997. **21**(1): p. 69-78.
171. King, T.A., *Wild caught ornamental fish: A perspective from the UK ornamental aquatic industry on the sustainability of aquatic organisms and livelihoods.* Journal of fish biology, 2019. **94**(6): p. 925-936.
172. Murray, J.M., et al., *Detecting illegal cyanide fishing: Establishing the evidence base for a reliable, post-collection test.* Marine Pollution Bulletin, 2020. **150**: p. 110770.

173. Madeira, D. and R. Calado, *Defining research priorities to detect live fish illegally collected using cyanide fishing in Indo-Pacific coral reefs.* Ecological Indicators, 2019. **103**: p. 659-664.
174. Bonanno, J.A., et al., *Where does it go? The fate of thiocyanate in the aquarium water and blood plasma of Amphiprion clarkii after exposure to cyanide.* bioRxiv, 2020.
175. Lanno, R.P. and D.G. Dixon, *Chronic toxicity of waterborne thiocyanate to the fathead minnow (pimephales promelas): A partial life-cycle study.* Environmental Toxicology and Chemistry: An International Journal, 1994. **13**(9): p. 1423-1432.
176. Lanno, R.P. and D.G. Dixon, *Chronic toxicity of waterborne thiocyanate to rainbow trout (Oncorhynchus mykiss).* Canadian Journal of Fisheries and Aquatic Sciences, 1996. **53**(9): p. 2137-2146.
177. Lanno, R., *The chronic toxicity of thiocyanate to rainbow trout and fathead minnow.* 1993.
178. Brown, D., et al., *HPLC determination of plasma thiocyanate concentrations in fish blood: application to laboratory pharmacokinetic and field-monitoring studies.* Ecotoxicology and environmental safety, 1995. **30**(3): p. 302-308.
179. Breen, N.E., et al., *On the half-life of thiocyanate in the plasma of the marine fish Amphiprion ocellaris: implications for cyanide detection.* PeerJ, 2019. **7**: p. e6644.
180. Vaz, M.C., et al., *Excreted thiocyanate detects live reef fishes illegally collected using cyanide—a non-invasive and non-destructive testing approach.* PloS one, 2012. **7**(4).
181. Vaz, M.C., V.I. Esteves, and R. Calado, *Live reef fish displaying physiological evidence of cyanide poisoning are still traded in the EU marine aquarium industry.* Scientific reports, 2017. **7**(1): p. 1-5.
182. Rubec, P.J., M. Frant, and M.B. Manipula, *Methods For Detection of Cyanide and Its Metabolites In Marine Fish.* 2008.
183. Moffitt, C.M. and J.A. Schreck, *Accumulation and depletion of orally administered erythromycin thiocyanate in tissues of chinook salmon.* Transactions of the American Fisheries Society, 1988. **117**(4): p. 394-400.
184. Rong, L., L. Lim, and T. Takeuchi, *Determination of iodide and thiocyanate in seawater by liquid chromatography with poly (ethylene glycol) stationary phase.* Chromatographia, 2005. **61**(7-8): p. 371-374.
185. Breen, N.E., et al., *Can excreted thiocyanate be used to detect cyanide exposure in live reef fish?* PloS one, 2018. **13**(5).
186. Herz, N., et al., *High-performance liquid chromatography to detect thiocyanate in reef fish caught with cyanide: A practical field application.* SPC Live Reef Fish Information Bulletin, 2016. **21**: p. 8-16.
187. Mak, K.K., H. Yanase, and R. Renneberg, *Cyanide fishing and cyanide detection in coral reef fish using chemical tests and biosensors.* Biosensors and Bioelectronics, 2005. **20**(12): p. 2581-2593.
188. Bortey-Sam, N., et al., *Diagnosis of cyanide poisoning using an automated, field-portable sensor for rapid analysis of blood cyanide concentrations.* Analytica Chimica Acta, 2020. **1098**: p. 125-132.

189. Ansell, M. and F. Lewis, *A review of cyanide concentrations found in human organs. A survey of literature concerning cyanide metabolism,'normal', non-fatal, and fatal body cyanide levels.* Journal of forensic medicine, 1970. **17**(4): p. 148.
190. Sousa, A.B., et al., *Toxicokinetics of cyanide in rats, pigs and goats after oral dosing with potassium cyanide.* Archives of toxicology, 2003. **77**(6): p. 330-334.
191. Vinnakota, C.V., et al., *Comparison of cyanide exposure markers in the biofluids of smokers and non-smokers.* Biomarkers, 2012. **17**(7): p. 625-633.
192. Bhandari, R.K., *The Toxicokinetic Behavior of Cyanide, Thiocyanate and 2-Amino-2-Thiazoline-4-Carboxylic Acid Following Cyanide Exposure in Multiple Animal Models Utilizing Novel Methods of Detection.* 2013.
193. Tor-Agbidye, J., *Dietary deficiency of cystine and methionine in rats alters thiol homeostasis required for cyanide detoxification.* Journal of Toxicology and Environmental Health Part A, 1998. **55**(8): p. 583-595.
194. Hasuike, Y., et al., *Accumulation of cyanide and thiocyanate in haemodialysis patients.* Nephrology Dialysis Transplantation, 2004. **19**(6): p. 1474-1479.
195. Manzano, H., et al., *Effects of long-term cyanide ingestion by pigs.* Veterinary research communications, 2007. **31**(1): p. 93-104.
196. Leuschner, J., A. Winkler, and F. Leuschner, *Toxicokinetic aspects of chronic cyanide exposure in the rat.* Toxicology letters, 1991. **57**(2): p. 195-201.